

NORTHWESTERN UNIVERSITY

Structural and Conformational Requirements of Membrane Fusion Mediated by the
Parainfluenza Virus 5 Fusion Protein

A DISSERTATION

SUBMITTED TO THE GRADUATE SCHOOL
IN PARTIAL FULFILLMENT OF THE REQUIREMENTS

for the degree

DOCTOR OF PHILOSOPHY

Field of Biochemistry, Molecular Biology, and Cell Biology

By

Mei Lin Zimmerman Bissonnette

EVANSTON, ILLINOIS

December 2008

ABSTRACT

Structural and conformational requirements of membrane fusion mediated by the parainfluenza virus 5 fusion protein

Mei Lin Zimmerman Bissonnette

Fusion of biological membranes is dictated by the interaction between specialized membrane proteins and the lipid bilayer. Parainfluenza virus 5 (PIV5) mediates fusion using two surface glycoproteins: the fusion protein (F) and the attachment protein hemagglutinin-neuraminidase (HN). Activation of membrane fusion of PIV5 typically occurs at neutral pH, and involves binding of HN to sialic acid, interaction of HN with the F protein, insertion of the F fusion peptide into the target membrane, and refolding of the F protein to the final postfusion form that provides the necessary energy for membrane merger.

The F protein contains a hydrophobic fusion peptide, a transmembrane domain (TM), and a cytoplasmic tail (CT). The ectomain and CT of the F protein and their role in fusion have been extensively studied. Different natural isolates of PIV5 have F proteins with CTs of varying length, either a short (20 residues) or long (42 residues). A long tail porcine isolate of PIV5, known as SER, was reported to be an exception to the dogma of paramyxovirus fusion at neutral pH in it requires a low pH step for fusion (S. Seth, A. Vincent, and R.W. Compans, *J. Virol.* 77:

6520-6527, 2003). However, by using multiple assays we could not find a requirement for low pH triggering of PIV5 SER fusion.

Although the contributions of the ectodomain and CT of PIV5 F to membrane fusion have been well studied, little is known about the role of the PIV5 F TM domain in fusion. Alanine scanning mutagenesis determined the TM domain of F is sequence dependent, and hydrophobic string of residues cannot substitute for the TM domain in fusion. Continued substitution revealed residues L486 and I488 play a key role in fusion, where the hydrophobicity of the side chains at these residues affects the interplay of the F protein and the lipid bilayer during membrane merger. Our studies suggest the TM domain is involved in the lipidic steps of fusion, and mutants L486A and I488A are trapped at the lipid stalk intermediate of membrane fusion. Oxidative cross-linking studies of the TM domain indicate the TM regions of the F trimer are in close proximity, and modeling studies suggest the TM domain is α -helical and forms a modified three-helix bundle.

ACKNOWLEDGEMENTS

First and foremost I would like to thank my advisor Dr. Robert A. Lamb; I am fortunate to have been a member of his laboratory. Although my journey for this PhD was not always easy, I believe I am a stronger person and scientist for it. I thank him for pushing me to think critically, inspiring me to work harder and smarter, and instilling in me the desire to do better. In the future I will always be able to get on with it.

I would like to thank Dr. Reay G. Paterson for her wealth of knowledge that spans across many years in the lab. I also thank Olga Rozhok, the Vero cell whisperer, for plating Vero cells for the luciferase assay like I never could, and for purifying the soluble protein for the MAb project. The hybridoma cloning is now in good hands.

I will miss many members of the Lamb lab, especially the members of Fusion League. I thank Dr. Sara Connolly for our discussions on fusion and trying to clear the confusion of the F and HN interaction, for always being available and willing to help out a graduate student, and for fun times in and out of the lab. I will also miss Jessica Robach. We share not only an interest in PIV5 fusion and 3.5% gels, but also a love of Camper shoes, premium denim, and wine from the Rioja. I thank Dr. George Leser for his microscope expertise as well as his thoughts on car repair. My mornings won't quite be the same without the morning chat with Barb St. Cyr around the coffee pot. I will also miss my weekly Thursday run with Dr. Rie Watanabe. Anneli Asikainen always made each day more interesting than the last.

I would also like to thank my thesis committee, Dr. Curt Horvath, Dr. Richard Longnecker, and Dr. Theodore Jardetzky. I greatly appreciate Dr. Jardetzky for remaining on my committee after moving to Stanford University School of Medicine and for his continued insightful comments and suggestions on my research. I would not have had this opportunity without the Medical Scientist Training Program, and I thank Dr. David Engman and Dr. Sandra Lee for their career advice and continued support of me in the program.

I am grateful for the continued love and support of my family. I thank my mother-in-law for her love and support over the years. My parents have always encouraged me and aided me emotionally and financially in all my endeavors. I am grateful for their unending love and their understanding as to why their only child is almost 30 years old and is still in school.

Finally, I thank my husband Chris for knowing the life of a graduate student and accepting that neither one of us has a typical job. Whether it's to rant about experiments that refuse to work, to keep me company during an 11 pm infection, or to listen to my talks and give helpful feedback, he has always supported me completely. We have been through Johns Hopkins, medical school, and then graduate school together. We have aided each other through joyous and stressful times, and I know we will be there for each other as we forge ahead to our future.

LIST OF ABBREVIATIONS

3HB	Three-helix bundle	MAb	Monoclonal antibody
6-CF	6-carboxyfluorescein	MFI	Mean fluorescence intensity
6HB	Six-helix bundle	MOI	Multiplicity of infection
ASLV	Avian sarcoma/leukosis virus	NDV	Newcastle disease virus
BFLA1	Bafilomycin A1	PAb	Polyclonal antibody
BHK	Baby hamster kidney	PAGE	Polyacrylamide gel electrophoresis
CT	Cytoplasmic tail	PBS	Phosphate buffered saline
CuP	Cu(II)(1,10-phenanthroline)₃	pfu	Plaque forming unit
DMEM	Dulbecco's modified Eagle's medium	p.i.	Post infection
F	Fusion protein	PIV5	Parainfluenza virus 5
FP	Fusion peptide	p.t.	Post transfection
HA	Hemagglutinin	R18	Octadecyl rhodamine B chloride
HIV	Human immunodeficiency virus	RBC	Red blood cell
HN	Hemagglutinin-neuraminidase	RNP	Ribonucleocapsid
HRA	Heptad repeat A	SFV	Semliki forest virus
HRB	Heptad repeat B	TBEV	Tick borne encephalitis virus
hPIV3	Human parainfluenza virus 3	TM	Transmembrane
HSV	Herpes simplex virus	VSV	Vesicular stomatitis virus

TABLE OF CONTENTS

ABSTRACT	2
ACKNOWLEDGEMENTS	4
LIST OF ABBREVIATIONS	6
TABLE OF CONTENTS	7
LIST OF FIGURES	11
LIST OF TABLES	13
CHAPTER 1: GENERAL INTRODUCTION	14
CLASSIFICATION AND GENERAL BIOLOGY OF PARAMYXOVIRUSES	14
ENVELOPED VIRUS FUSION.....	16
TRIGGERS OF FUSION	18
Host cell receptor binding.....	18
Low pH	22
Combination and novel triggers of fusion	23
FUSION PROTEINS	24
The F protein, a class I fusion protein	24
The E protein, and class II protein.....	29
The G fusion protein, a class III fusion protein	30

	8
The GP2 fusion protein.....	33
The unifying mechanism of fusion.....	35
REMAINING QUESTIONS IN FUSION.....	40
CHAPTER 2: ANALYSIS OF THE PH-REQUIREMENT FOR MEMBRANE FUSION OF DIFFERENT ISOLATES OF THE PARAMYXOVIRUS PARAINFLUENZA VIRUS 5	43
INTRODUCTION	43
RESULTS	44
PIV5 SER infectious centers detected by immunostaining	44
Syncytia formation caused by PIV5 isolates	45
PIV5 SER and W3A cell-cell fusion using luciferase reporter assay.....	46
Real-time kinetics of virus-erythrocyte ghost fusion.....	46
Bafilomycin A1 treatment does not affect PIV5 SER replication	51
DISCUSSION.....	55
MATERIALS AND METHODS	56
CHAPTER 3: RESIDUES IN THE OUTER LEAFLET OF THE TRANSMEMBRANE DOMAIN OF THE PARAINFLUENZA VIRUS 5 FUSION PROTEIN ARE CRITICAL FOR MEMBRANE FUSION.....	59
INTRODUCTION	59
RESULTS	63
F protein TM domain residues bordering the ectodomain have a key role in fusion	63

F TM domain residues L486 and I488 are key residues involved in fusion.....	66
F TM domain mutants L486A and I488A form the open-stalk and pre-hairpin intermediates of fusion	68
F TM domain mutants 486 and 488 mutants have the same or a closely related conformation as wt F protein that is independent of their ability to cause fusion	72
The addition of a hyperfusogenic mutation can rescue fusion for F TM mutants L486A and I488A	73
Changing the curvature of the membrane rescues fusion of F TM domain mutants L486A and I488A	75
Evidence that the hydrophobicity of the side chains of F TM domain residues 486 and 488 controls fusion activity.....	77
The F protein TM domains are in close proximity and likely form a three-helix bundle	79
DISCUSSION.....	85
MATERIALS AND METHODS.....	92
CHAPTER 4: DISCUSSION AND FUTURE DIRECTIONS.....	99
REFERENCES.....	103
APPENDIX A: MONOCLONAL ANTIBODIES THAT RECOGNIZE THE PRE- AND POSTFUSION CONFORMATIONS OF THE F PROTEIN.....	118
APPENDIX B: A THREE-HELIX BUNDLE ON THE CYTOPLASMIC TAIL OF THE PIV5 FUSION PROTEIN TRAPS THE PRE-HAIRPIN INTERMEDIATE IN FUSION132

CURRICULUM VITA 141

LIST OF FIGURES

Figure 1-1. The PIV5 attachment protein hemagglutinin-neuraminidase.....	17
Figure 1-2. The PIV5 fusion protein F.....	27
Figure 1-3. The dengue virus fusion protein E.....	29
Figure 1-4. The VSV fusion protein G.....	32
Figure 1-5. The Ebola virus fusion protein GP.....	34
Figure 1-6. The unifying mechanism of fusion.....	37
Figure 2-1. Immunostained PIV5 W3A and SER plaques.....	45
Figure 2-2. Low pH does not induce syncytia formation in either cells expressing PIV5 W3A F or SER F or in cells infected with PIV5 W3A or SER viruses.....	48
Figure 2-3. Bafilomycin A1 does not inhibit replication of PIV5 isolates W3A or SER.....	52
Figure 2-4. Antigens of PIV5 W3A, PIV5 SER and other PIV5 isolates were detected in bafilomycin A1 treated cells.....	55
Figure 3-1. Analysis of fusion activity of alanine mutations in the F protein TM domain.....	64
Figure 3-2. Analysis of fusion activity of alanine point mutants for F TM domain residues 485-489.....	67
Figure 3-3. Analysis of the protein conformation of F mutants L486A and I488A and examination of the steps of fusion attained by these mutants.....	70
Figure 3-4. Syncytia formation mediated by F mutants L486A and I488A containing a second destabilizing mutation.....	74

Figure 3-5. Altering the curvature of the lipid membrane can rescue fusion for the F L486A and I488A mutants.....	76
Figure 3-6. Fusion activity of F proteins depends on the hydrophobicity of substituted residues at TM residues L486 and I488.....	78
Figure 3-7. Fusion activity of F TM domain cysteine substitution mutants.....	80
Figure 3-8. F protein TM domain cysteine substitution and disulfide bond formation on oxidation.....	83
Figure 3-9. Model of membrane fusion for F TM domain mutants L486A and I488A.....	90
Figure A-1. Shape of pre- and postfusion F-GCNt in electron microscopy.....	119
Figure A-2. Immunoprecipitation of wt W3A F by select MAb.....	124
Figure A-3. Mean fluorescent intensity of several MAb to the cleavage mutant FR3 F.....	126
Figure B-1. Long tail PIV5 isolates and the extended tail mutants.....	131
Figure B-2. Fusion of F3HBii and F 3HBaa.....	132
Figure B-3. Analysis of the pre-hairpin intermediate.....	134
Figure B-4. Capture of the pre-hairpin intermediate.....	136
Figure B-5. Protease digestions of wt F, F 3HBii, and F 3HBaa proteins.....	137

LIST OF TABLES

Table 1-1: Examples of members of the family <i>Paramyoviridae</i>	13
Table 3-1: Cell surface expression of F mutants.....	66
Table A-1: Mean fluorescence intensity of all candidate MAb to wt W3A F.....	121
Table A-2: Candidate MAb screened by immunofluorescence microscopy.....	123

CHAPTER 1: GENERAL INTRODUCTION

CLASSIFICATION AND GENERAL BIOLOGY OF PARAMYXOVIRUSES

The *Paramyxoviridae* are a family of enveloped, nonsegmented, negative-strand RNA viruses and include some of the most prevalent viruses known, such as parainfluenza viruses and respiratory syncytial virus, and they can cause disease of great social and economical impact, such as measles virus and the recently identified Nipah and Hendra viruses. The *Paramyxoviridae* family is divided into two subfamilies, the *Pneumovirinae* and the *Paramyxovirinae*. The *Pneumovirinae* contain two genera: *Pneumovirus* and *Metapneumovirus*. The *Paramyxovirinae* contain five genera: *Respirovirus*, *Morbillivirus*, *Avulavirus*, *Henipavirus*, and *Rubulavirus*. Examples of viruses in each genera are listed in Table 1-1(69). Parainfluenza virus 5 (PIV5), formally known as SV5, a member of the *Rubulavirus* genera, is one of the viruses studied as a prototype of the *Paramyxoviridae*. PIV5 was originally isolated in 1956 as a contaminant in primary monkey kidney cells during vaccine safety testing (60). It was identified by formation of syncytia, which are large multinucleated giant cells. Syncytia formation is a cytopathic effect resulting from neighboring cells fusing together and is a hallmark of paramyxovirus infection.

Paramyxovirus virions are generally spherical, 150-350 nm in diameter, and have glycoprotein spikes inserted into the lipid envelope extending 8-12 nm from the surface of the membrane.

Table 1-1: Examples of members of the family *Paramyxoviridae*

Family <i>Paramyxoviridae</i>	The viral core contains a
Subfamily <i>Paramyxovirinae</i>	single-stranded negative-sense
Genus <i>Rubulavirus</i>	RNA 15,000-19,000
Mumps virus (MuV)	nucleotides in length that
Parainfluenza virus 5 (PIV5)	serves as a template for viral
Human parainfluenza virus type 2, type 4a and 4b (hPIV2/4a/4b)	mRNA and as a template for
Mapuera virus	the antigenome (positive sense
Porcine rubulavirus	strand). The antigenome then
Genus <i>Avulavirus</i>	acts as the template for further
Newcastle disease virus (NDV)	copies of the negative strand.
Genus <i>Respirovirus</i>	The viral RNA is encapsulated
Sendai virus (mouse parainfluenza virus type 1) (SeV)	by viral proteins and forms the
Human parainfluenza virus type 1, type 3 (hPIV1/3)	infectious ribonucleocapsid
Bovine parainfluenza virus 3 (bPIV3)	(RNP). Each RNP is
Genus <i>Henipaviruses</i>	extremely stable and consists
Hendra virus (HeV)	of about 2,600 nucleocapsid
Nipah virus (NiV)	
Genus <i>Morbillivirus</i>	
Measles virus (MeV)	
Cetacean morbillivirus	
Canine distemper virus (CDV)	
Rinderpest virus	
Subfamily <i>Pneumovirinae</i>	
Genus <i>Pneumovirus</i>	
Human respiratory syncytial virus A2, B1, S2 (hRSV)	
Bovine respiratory syncytial virus (bRSV)	
Pneumovirus of mice (PVM)	
Genus <i>Metapneumovirus</i>	
Human metapneumovirus (hMPV)	
Avian metapneumovirus	

(N), 300 phosphoprotein (P), and 50 large (L) proteins. The N protein and the genome RNA form the nucleocapsid core with the P and L proteins attached (69).

PIV5 encodes eight proteins from seven genes: N, P, the V protein, the matrix protein (M), the fusion protein (F), the small hydrophobic protein (SH), the hemagglutinin-neuraminidase protein

(HN), and L. The P gene contains an editing site and encodes the P and V proteins. The unedited gene encodes the V protein, which plays a role in counteracting the host cell antiviral response. The addition of two non-templated nucleotides by transcriptional editing at the editing site produces an mRNA that encodes the P protein (142), which is essential for vRNA synthesis. The N protein forms the RNase-resistant viral core with the genomic RNA, associates with the P-L polymerase during transcription replication, and likely interacts with the M protein during virus assembly. The L protein forms a complex with P and is considered to be the viral polymerase. The M protein associates with the viral lipid bilayer, the cytoplasmic tails of integral membrane proteins, and the nucleocapsid and is considered to be the driving force of virus budding (69).

Paramyxoviruses contain two or three integral membrane proteins in their lipid envelope. All paramyxoviruses encode a cell attachment protein (HN, H, or G) and a fusion mediating protein (F) (69). The *Rubulavirus* and *Pneumovirus* also possess the SH protein, which for PIV5 is thought to block virus-induced apoptosis (51).

ENVELOPED VIRUS FUSION

All enveloped viruses are presented with a biophysical problem: overcoming the large energy barrier to fuse the viral and host cell lipid bilayers in order to cause infection. Lipids will spontaneously assemble into bilayers, but lipid bilayer membranes do not spontaneously fuse (20). Investment of energy is necessary in order to initiate the restructuring of the lipid

membranes to initiate fusion (140). Lipid bilayers are stabilized against structural changes by their strong hydrophobic interactions and these interactions can be modified by the shape of the lipids (20). Lysophosphatidylcholine (LPC) and its inverted cone-shape induce a positive curvature to the membrane whereas oleic acid (OA) and its cone-shape induce a negative curvature to the membrane, and these lipids inhibit or facilitate fusion, respectively (17). In addition to hydrophobic interactions, a layer of water separates the polar heads of neighboring membranes, and energy must be expended to overcome hydration repulsion (19, 20). The energy for this remodeling is derived from specialized fusion proteins (140).

Recent biochemical and structural studies have enhanced our understanding of how diverse enveloped viruses mediate membrane fusion with various fusion proteins. Enveloped viruses utilize fusion proteins analogous to the SNARE super family of proteins. SNAREs are found in all eukaryotic organisms and are employed in many biological processes, such as neuronal synaptic vesicle fusion, endosomal fusion, and exocytosis (86). All SNARE proteins have a common heptad-repeat that forms four-helix coiled-coil structures. This coiled-coil SNARE complex forms in *trans* to promote fusion of the two membranes in which the SNARE proteins are anchored (149). The enveloped virus fusion proteins and their methods to initiate membrane fusion are diverse, but all share a general common mechanism for lowering the kinetic barrier to membrane fusion.

TRIGGERS OF FUSION

Fusion proteins reside on the virion surface in a native, or metastable, state, where the fusion proteins are primed to refold to the more stable postfusion state and release the requisite energy to fuse the virus-cell membranes (126, 148, 155). To ensure fusion occurs at the right place and at the right time, the fusion protein must be activated by a fusion trigger which promotes the fusion protein to refold and insert itself into the target membrane (69, 148). There are four types of known fusion triggers: receptor binding, low pH, a combination of receptor binding followed by low pH, and the novel mechanism of filoviruses involving proteolytic digestion (148).

Host cell receptor binding

The fusion proteins of many viruses, such as paramyxo-, retro-, and herpes viruses, are activated by binding host cell receptors at neutral pH (33, 69, 148, 150). PIV5 utilizes the attachment protein hemagglutinin-neuraminidase (HN). HN is a type II integral membrane protein that binds virus to sialic acid-containing cell surface molecules, either glycoproteins or glycolipids (Fig. 1-1A). In addition to hemagglutinating, HN has neuraminidase activity that mediates the enzymatic cleavage of sialic acid from the surface of virions and the surface of infected cells. The neuraminidase activity is optimal at acidic pH and acts in the *trans* Golgi network to remove sialic acid from the HN and F carbohydrate chains. This removal most likely prevents self-aggregation of virions at the cell surface, a function similar to that performed by influenza virus neuraminidase (NA) (69).

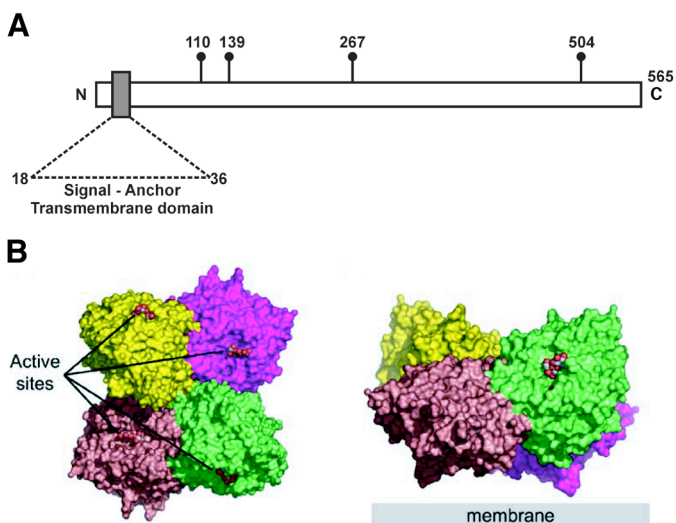


Figure 1-1. The PIV5 attachment protein hemagglutinin-neuraminidase

(A) Schematic diagram of the PIV5 hemagglutinin-neuraminidase (HN). Sites of N-linked carbohydrate addition are indicated. (B) PIV5 tetramers shown from the top (left) or side (right). The four subunits are shown in different colors, and the active sites are indicated (69).

The binding and enzymatic domains reside in the globular HN (106, 128). Like other HN proteins, the PIV5 HN globular head consists of a sialidase fold with six antiparallel β strands and the active site located in the center (156). In PIV5 HN, the hemagglutinin and neuraminidase activities are located at one site, whereas Newcastle Disease virus (NDV) HN has been shown to possess an additional sialic acid binding site (26, 156). When the head domains are expressed alone they are found to be monomeric (26, 72, 156); however expression of the head plus stalk domain forms a homotetramer and thus HN is thought to be a homotetramer (69, 156). Rather than having four-fold rotational symmetry, HN is arranged with two two-fold symmetry axes, and the dimer places the two active sites at ~ 90 degrees to each other (156) (Fig. 1-1B). HN also promotes fusion by interacting with its homologous fusion (F) protein and inducing conformational changes in F that mediate fusion. However, the F protein of the W3A strain of PIV5 can mediate fusion without coexpression of its HN (58). Although not always required, coexpression of F with its homologous HN increases fusion activity (58) (59, 153).

Whereas mutagenesis of many residues in both F and HN affect fusion, the stalk domain in HN seems to play an essential role in fusion (29, 88, 117, 137).

It is unknown how HN tetramers interact with the trimeric F protein. The two proteins are known to interact at the cell surface for some paramyxoviruses the two homotypic F and HN proteins can be immunoprecipitated (1, 28, 137). Currently there are two models of how F is activated. In the first model, the HN-F interaction maintains F in its metastable form and receptor binding causes the two glycoproteins to dissociate, which then unclamps and releases F to initiate fusion (97). In the second model, receptor binding induces a conformational change in HN, which in turn causes a conformational change in F that then initiates fusion (125). It has been difficult to determine if HN prevents a conformational change in F until it is released at the proper time or if HN triggers a conformational change at the proper time to initiate fusion. In the dissociation model, F and HN would interact intracellularly to maintain F in the proper conformation. In the second model, F and HN would interact at the cell surface in the presence of receptor binding. Support for the first dissociation model comes from mutational studies in measles and Nipah F proteins, where an increase in the interaction between the receptor binding protein and the fusion protein correlates with a decrease in fusion (1, 25). In contrast, mutational studies of NDV HN indicate that mutants deficient in receptor binding do not coimmunoprecipitate with F (28, 80). While there have been no definitive experiments supporting one hypothesis over the other, the ability to use increased temperature as a surrogate for PIV5 HN suggests that HN provides the energy needed to convert the F protein from its metastable to its fusogenic form and supports the second model. Increased temperature can also

increase the reactivity of monoclonal antibodies that recognize the postfusion form of F (125, 144, 146). The existence of HN-independent hyperfusogenic F mutants also supports the second model. These hyperfusogenic mutants cause massive fusion independent of HN coexpression, have faster fusion kinetics, and lower temperature requirements for fusion (58, 111, 124, 126). These fusion proteins can be interpreted as highly destabilized such that they no longer require the energy barrier-lowering step of HN receptor binding. The triggering mechanism may differ among paramyxoviruses, with viruses that use a proteinaceous receptor triggering fusion by dissociation and viruses that use the ubiquitous sialic acid receptor triggering by the second mechanism (25).

Like paramyxoviruses, the retrovirus human immunodeficiency virus (HIV) relies on receptor binding to trigger fusion at neutral pH. For HIV, the attachment and fusion protein functions are carried out by a single protein gp160. HIV gp160 is proteolytically cleaved into the fusion subunit gp41 and the outer receptor binding subunit gp120 that are disulfide bonded (35). HIV fusion is activated by sequential interactions of gp120. Gp120 binds the receptor CD4 and also a member of the chemokine family, usually CXCR4 or CCR5 (148). CD4 binding causes large conformational changes in gp120 that expose the binding subunit gp41 and further induces conformational changes in gp41 that initiate fusion (148).

Unlike other enveloped viruses, herpes simplex virus (HSV) requires four glycoproteins for fusion: gD, gB, and the gH/gL heterodimer. gB and the nonessential protein gC mediate an initial binding to cell surface proteoglycans and viral fusion is triggered by gD binding to one of

several receptors, including HVEM, nectin-1, or a modified heparan sulfate (136). It is unclear how the interactions between the proteins trigger fusion, however both gB and the gH/gL complex possess fusion activity (38) and gD binding to receptor can trigger an interaction between gB and the gH/gL complex (3). In addition, a receptor for gB has recently been identified (127). The mode of entry is cell-type dependent. The virus infects some cells at neutral pH by fusing with the plasma membrane (102). In other cell types, the virus requires a low pH trigger for fusion with the endosomal membrane (101). In some neuronal cells, virus fusion is independent of pH but the virus fuses with the endosomal membrane (93).

Low pH

Low pH is the fusion trigger for many viruses, such as orthomyxo-, alpha-, flavi-, and rhabdoviruses, that enter cells by endocytosis and fuse with the endosomal membrane (148). For influenza virus HA, fusion will be triggered by $\text{pH} \leq 5.0$ (30). Fusion proteins are divided by class (described later), and low pH is utilized by all classes of fusion proteins: influenza virus HA (class I), Dengue virus E (class II), and vesicular stomatitis virus (VSV) G (class III). Low pH causes structural changes in the fusion protein to expose the fusion peptide or loop for insertion into the target membrane (148). For class I fusion proteins such as HA, low pH acts to separate the globular head domains and reposition the fusion peptide for membrane insertion (68). For class II E proteins, low pH triggers these proteins to rearrange from dimers with their fusion loops sequestered to trimers with their fusion loops directed away from the virion surface and primed for fusion (50). The class III VSV G protein also utilizes low pH to expose its fusion loop; however, unlike other low pH activated fusion proteins, the effect of low pH on G is

reversible (50). Interestingly, all class II fusion proteins are triggered by low pH, but there appears to be no universal low pH requirement for the other class I proteins such as paramyxovirus F or the class III protein HSV gB (69, 102).

Combination and novel triggers of fusion

The retrovirus avian sarcoma/leukosis virus (ASLV) utilizes a combination of receptor binding and low pH to trigger its fusion protein Env. Upon receptor binding of the Env subunit SU, a conformational change is induced that exposes the fusion peptide of the metastable fusion subunit TM, and TM inserts into the target cell membrane (27, 56). To convert from this extended conformation into the postfusion trimer of hairpins, the pH must be lowered and endocytosis of the pre-hairpin intermediate must occur to place it in an acidic environment (87, 98). The requirement of low pH was not apparent in initial studies, likely due to the high stability of the Env extended intermediate (44, 100).

Similar to above mentioned fusion proteins, the Ebola virus fusion protein GP is proteolytically cleaved in to a receptor binding subunit GP1 and a fusion subunit GP2 that are disulfide linked (148). Ebola virus is thought to enter cells by receptor-mediated endocytosis, although low pH is not sufficient to activate GP in fusion (131). Entry requires the endosomal proteases cathepsins B and L to further cleave GP1. These cathepsins cleave the 130 kD GP1 down to a 19 kD form that still is bound to the GP2 (148). The 19 kD GP1 requires additional undefined cathepsin L activity for GP1 to release GP2 and trigger fusion (148). Cathepsins have also been implicated

in entry for SARS coronavirus and the Nipah and Hendra paramyxoviruses, though the role of cathepsins is not clear (79, 104, 105).

FUSION PROTEINS

High resolution crystal structures of 11 enveloped virus fusion proteins have been solved (7, 9, 16, 42, 52, 76, 96, 119, 120, 122, 154, 155), and these proteins have been classified as class I, class II, or class III fusion proteins based on structural features in their pre- and postfusion forms (50, 148). Although fusion proteins in each class have distinct features, there are unifying characteristics among all the classes. All fusion proteins are trimers at some stage of fusion, all require a trigger (as discussed in the previous section), all form an extended intermediate where the fusion peptides or loops have inserted into the target membrane, and all reach a hairpin postfusion form, where the C-terminal region packs tightly against the N-terminal trimeric core to form a thermodynamically stable structure that brings the fusion peptides/loop and transmembrane (TM) domains into close proximity (148).

The F protein, a class I fusion protein

Class I fusion proteins contain a hydrophobic fusion peptide (FP) that is at or near the N-terminus of the fusion subunit of the fusion protein. Their final postfusion states are characterized by a core α -helical coiled-coil with C-terminal α -helices packing into the grooves of the central three-helix bundle to form the 6HB (148). The paramyxovirus F protein is a class I fusion glycoprotein that is synthesized as type I integral membrane protein that is folded into homotrimers, post-translationally modified by the addition of carbohydrate chains, and then

proteolytically cleaved to become biologically active. Similar processing occurs for other class I fusion proteins, such as influenza virus HA, HIV gp160, retrovirus Env, and Ebola GP (69). The PIV5 F precursor protein (F0) is cleaved by the host cell protease furin in the *trans* Golgi network into the disulfide linked and biologically active membrane-anchored F1 fragment and the smaller N-terminal F2 fragment (Fig. 1-2A); however, these two fragments are not independent protein domains of F (155). F1 contains two hydrophobic regions, the N-terminal fusion peptide (FP), located at the new N-terminus after cleavage, and the TM domain, and two heptad repeat regions, HRA and HRB. HRA is located immediately C-terminal to the FP. HRA and HRB are separated by 250 residues, and HRB is proximal to the TM domain. In the postfusion form of F, HRA and HRB interact to form the 6HB (4, 125). Connected to the TM domain is the cytoplasmic tail that ranges from 20-40 residues depending on the strain of PIV5 (146). Truncation of fusion protein cytoplasmic tail can enhance fusion, suggesting it may form a specific protein structure that impedes F protein conformational changes required for fusion (99, 143, 146).

The pre- and postfusion crystal structures of uncleaved paramyxovirus F proteins have been solved (154, 155). To solve the structure of the prefusion form of PIV5 F, a soluble trimerization domain (GCNt) was added to the C-terminal end of a truncated secreted F protein to act as a surrogate for the TM domain and to stabilize the metastable F protein. The PIV5 F trimer possesses a large globular head attached to a three-helix bundle (3HB) coiled-coil stalk made up of HRB that extends to the GCNt trimer, orienting the head away from the viral membrane (Fig. 1-2C). The globular head of F contains three domains (DI-DIII) that make extensive intersubunit

contacts. DI and DII form the sides of a large cavity present as the base of the head, and DIII covers the top of the cavity and is composed of HRA and the fusion peptide. The C-terminal end of DII contains an extended linker region that extends to HRB and wraps around the outside of the trimer to the center of the base of the head and the beginning of the HRB stalk. In DIII, two sets of six helices seal the top of the head while the HRB 3HB seals the bottom (155). The uncleaved hydrophobic fusion peptide is nestled between the DIII of its own monomer and the DII subunit of the neighboring monomer within the trimer (Fig. 1-2C). The fusion peptide folds back on itself and forms a hydrophobic core. Proteolytic cleavage may cause additional contacts with DII and affect intersubunit interactions (155).

The structure of uncleaved hPIV3 was determined by molecular replacement using the extensively proteolysed NDV F structure (16). The NDV F structure was originally interpreted to be the prefusion structure of F; however, the analysis of the data was complicated because of the proteolysis electron. Like the PIV5 F structure, hPIV3 F forms a trimer with head, neck, and stalk regions (Fig. 1-2D). Some density is missing, including that for the fusion peptide and cleavage site (residues 95-135), but these residues would be draped flexibly on the exterior of the stalk region. This uncleaved F was secreted as a soluble protein by removing the TM domain and CT. The 6HB, which is considered to be the hallmark of the postfusion conformation, is well formed and similar to the 6HB structures of PIV5 and hRSV F previously determined using peptides (4, 160). Cleavage was initially considered to be a requirement for conversion to the postfusion form. However, hPIV3 F was confirmed to be uncleaved, and multiple arguments support that it does not represent the prefusion form. The structure of hPIV3 F representing a

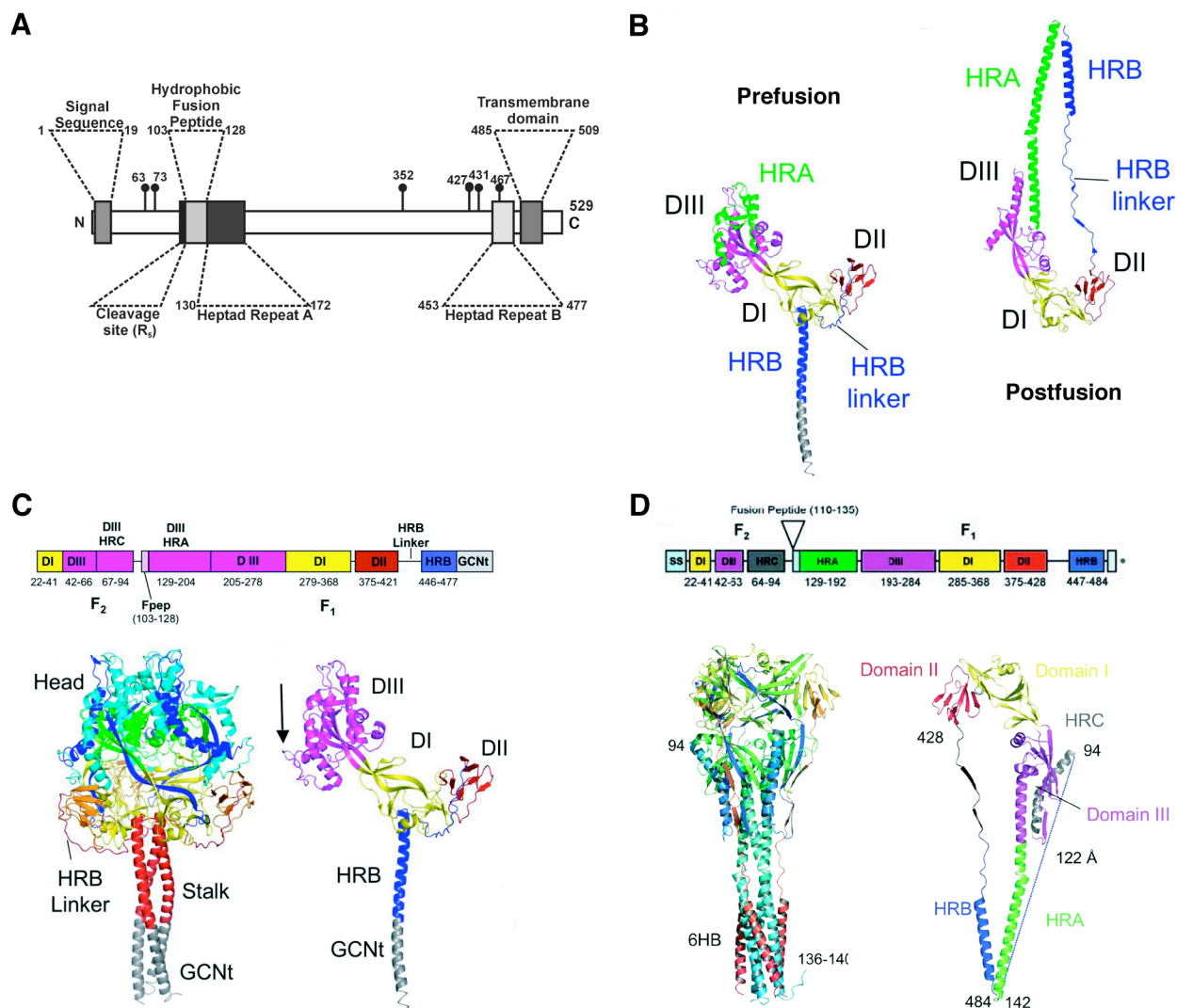


Figure 1-2. The PIV5 fusion protein F

(A) Schematic of the PIV5 F protein domains. Sites of N-linked carbohydrate addition are indicated. (B) Ribbon diagram of single monomers of the PIV5 F-GCNt trimer (prefusion) and the hPIV3 solF0 trimer (postfusion). Homologous domains are indicated. (C) Schematic of the PIV5 F-GCNt domains and ribbon diagrams of the PIV5 F-GCNt trimer and monomer. The trimer is colored in a gradient from N-terminus (blue) to C-terminus (red). The monomer is colored as in the schematic. The cleavage site is indicated by an arrow. (C) Schematic of the hPIV3 solF0 domains and ribbon diagrams of the hPIV3 solF0 trimer and monomer. The trimer is colored in a gradient from N-terminus (blue) to C-terminus (red). The monomer is colored as in the schematic. The direct distance between residue 94 in HRC and 142 at the base of the trimer is 122Å. (69, 96)

prefusion form would be inconsistent with inhibitory peptide data that show HRA and HRB are available at various intermediates of fusion (125). The behavior of destabilizing mutations in F could also not be explained by this structure (125, 126). Cleavage of this structure would likely place the fusion peptide into the same membrane as the TM domain anchor rather than provide a mechanism for the merger of two membranes. The folding of hPIV3 F into the postfusion state is likely due to the lack of a TM domain (154, 155). The TM domain may be necessary for the stability of the metastable prefusion F, where the TM domain provides some of the energy barrier that keeps F in the prefusion state. The TM domain could also be needed for prefusion F to properly fold into the metastable state. PIV5 F was able to remain in the prefusion state due to the addition of the GCNt domain to substitute for the hydrophobic TM domain (155).

Although PIV5 F and hPIV3 F are from different paramyxoviruses, the two conformations are consistent with the transition from the pre- to postfusion forms in fusion. The two structures are related by flipping the stalk domains relative to the head domain (Fig. 1-2B). The head domain of hPIV3 is significantly more compact compared to PIV5 F, but the individual DI and DII domains remain very similar, with root-mean-square (r.m.s.) deviations of 1.97Å and 1.5Å, respectively. The region that undergoes the most conformational change in DIII, where HRA transforms from 11 distinct segments that wrap around the DIII core in the globular head to an extended coil-coil that moves 115Å from its position in the prefusion conformation. For the HRA coiled-coil to form, DIII must rotate and collapse inward, which also compacts the head (155). The transition from pre- to postfusion also requires the opening and repositioning of

HRB. To form the postfusion form, HRB must separate and swing around the head to form the 6HB with the newly formed HRA coiled-coil extending from the head of F (155).

The E protein, and class II protein

The crystal structures of pre-and postfusion proteins of alphaviruses (Semiliki Forest virus E1) and flaviviruses (Dengue virus and tick borne encephalitis virus (TBEV) E) have been solved (9, 43, 96, 119). Unlike class I fusion proteins like PIV5 F and influenza HA (11, 15) that are predominately α -helical, the class II fusion proteins E and E1 consist primarily of β -sheet structures with internal fusion peptides formed as loops at the tips of the β -strands (148). Class

II fusion proteins do not have fusion peptides like class I proteins that are exposed from cleavage by a host cell protease, but instead have shallow fusion loops (148). The prefusion form of

Dengue virus E is an antiparallel homodimer with three domains, Domains I, II, and III,

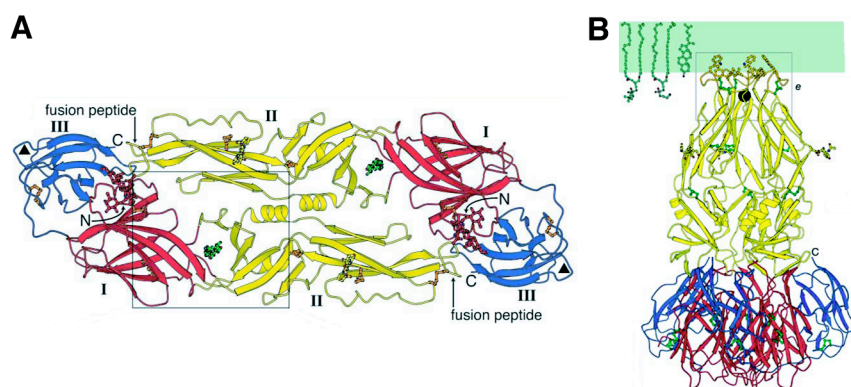


Figure 1-3. The dengue virus fusion protein E.

(A) Structure of the dengue virus E protein dimer, the conformation in the mature virus particle and when above the pH of fusion. Domain I is red, Domain II is yellow, and domain III is blue. The fusion loops are indicated by the arrow. (B) Ribbon diagram of the postfusion trimer. Domains of E are the same color as in (A). The shallow predicted insertion of the fusion loops is shown in comparison to representative membrane lipids drawn to scale. (Adapted from (95)).

that consist primarily of β -sheets. Domain I resides at the N-terminus and Domain III is at the C- the dimer interface (Fig. 1-3A). The domains reorganize and reorient during fusion, but there is limited protein refolding (62). Upon triggering by low pH, the dimers reassociate into trimers on the virus surface (96) (Fig. 1-3B). The dimer contacts between the subunits are broken, and Domain II rotates 20 degrees with respect to Domain I, allowing the E monomers to rearrange laterally into trimers (62, 96). Trimer formation is irreversible and positions the fusion loop in Domain II to point away from the virion toward the target membrane. In this orientation, all domains are involved in forming trimer contacts (96). Three hydrophobic residues in the fusion loop, Trp 101, Leu 107, and Phe 108, are fully exposed, and the fusion loops of the trimer insert into the target cell membrane. It is likely that fusion loops do not insert as deeply into the target membrane as fusion peptides due to the charged residues surrounding the hydrophobic residues (96). The C-terminal stem region not present in the crystal structure is thought to fold back and pack into the channel between the monomers of Domain II, similar to the packing of the 6HB (96).

The G fusion protein, a class III fusion protein

With the recently solved crystal structures of the pre- and postfusion VSV fusion protein G (120, 122) and the presumptive postfusion structure of herpes simplex virus 1 glycoprotein B (gB) (52), a third class of fusion proteins (class III) that shares features with class I and class II fusion proteins has been identified. Like class I fusion proteins, G and gB are trimers and contain central α -helical coiled-coils. However, these fusion proteins contain fusion loops at the tip of

β -strands similar to class II fusion proteins, although G contains two fusion loops per monomer (50, 148).

Unlike the fusion loop in class II fusion proteins, the fusion loops in the pre-fusion structure of VSV G are exposed on the outside of the trimer rather than shielded by a domain interface (122). The prefusion trimer of G is shorter than that of PIV5 F, with the G protein structure resembling a tripod with each leg contains a fusion domain that is set widely apart (Fig. 1-5A). The fusion loops face the viral membrane, positioning the fusion loops and TM domains in close proximity in the prefusion form, which differs greatly from class I and class II fusion proteins (50, 122). When triggered by low pH, the fusion domain is projected toward the target membrane by several conformational changes. The fusion domain (DIII) rotates around a hinge region between DIII and DIV. This rotation involves the reorganization to two segments, and each of these segments contains an unstructured linker and a helical region. During the conformational change, the unstructured region becomes helical and the helical region becomes unstructured. This rearrangement causes a 94° rotation of the fusion domain such that the fusion loops can insert into the target membrane (122, 148).

The C-terminal stem (not present in the crystal structure) is thought to then rearrange to bring the fusion loops and TM domain into close proximity, with the C-terminal stem laying in the channel between the monomers of DIII to form the postfusion form of G (120). The inversion of the stem is facilitated by structural rearrangements in DII. An unstructured loop in DII refolds and extends the central helix found in DII in the prefusion form of G then forms a sharp bend and

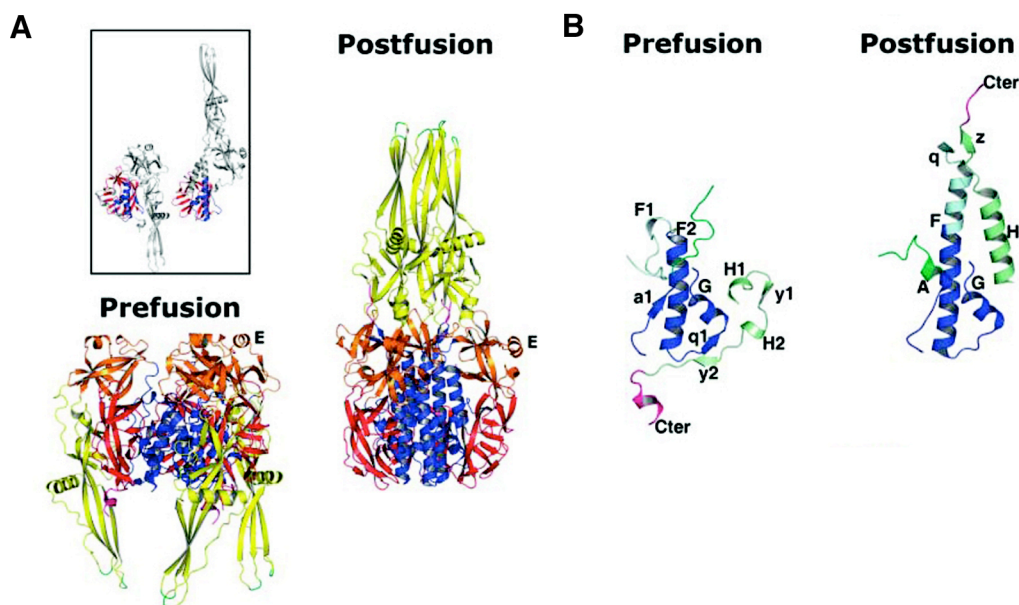


Figure 1-4. The VSV fusion protein G.

(A) Ribbon diagrams of the pre- and postfusion VSV G trimers. Domain I is in red, domain II in blue, domain III in orange, and domain IV in yellow. Fusion loops are at the base of the domain IV in the pre-fusion trimer in cyan. Domain IV, the fusion domain, rotates to insert the fusion loops into the target cell membrane. The invariant parts of domains I and II are highlighted to show how they remain similar in the pre- and post-fusion structures. (B) The refolding of the α -helices in domain II is shown. The F and H regions in pre-fusion G refold into α -helices that form the central coiled-coil in post-fusion G. (Adapted from (122))

another α -helix (helix F) (Fig. 1-5B) (122). Another unstructured region of DII becomes α -helical (helix H), and when the G protein refolds to form the postfusion conformation, this nascent helix packs in an antiparallel orientation to the core structure α -helix, similar to the arrangement in the 6HB of PIV5 F (120, 122). This movement of the helices brings the TM domains and fusion loops together and facilitates membrane fusion (122).

The presumptive HSV-1 gB postfusion crystal structure is similar to the VSV G postfusion structure. This was surprising because HSV-1 is a DNA virus and not a negative-strand RNA virus like VSV, and HSV-1 fusion does not require low pH (50, 102). The gB protein has not been confirmed biochemically to be the fusion protein for HSV-1 and does not have an obvious fusion peptide. However, the structure does show putative fusion loops at the tips of the β -sheets adjacent to the TM domain similar to the postfusion form of VSV G (52), and mutational studies confirm that residues in these loops are integral to gB function (48). The gB protein is a trimer like other fusion proteins, and like the VSV G postfusion structure, the gB domain III contains a long α -helix that forms a central coiled-coil (52).

The GP2 fusion protein

The prefusion structure crystal structure of Ebola virus glycoprotein (GP) has recently been solved (76). GP is cleaved post-translationally by host cell furin into a large receptor binding subunit (GP1) and a fusion subunit (GP2) that are disulfide-linked (148). However, this cleavage does not expose a fusion peptide at the new N-terminus. Rather, GP2 contains an internal fusion loop similar to class II and class III fusion proteins (76). The mucin-like and TM domains of GP were removed prior to crystallization, and GP was complexed with a Fab derived from a human survivor that recognizes a conformational epitope (76). The GP trimer forms a chalice-like shape and consists of three non-covalently linked monomers, with each monomer composed of the disulfide-linked subunits GP1 and GP2. Trimerization is mediated by GP1-GP2 and GP2-GP2 contacts; there are no contacts between GP1 domains (76). The GP1 subunit is composed of three regions: the base, the head, and the glycan cap (Fig. 1-5A). The base region is made up

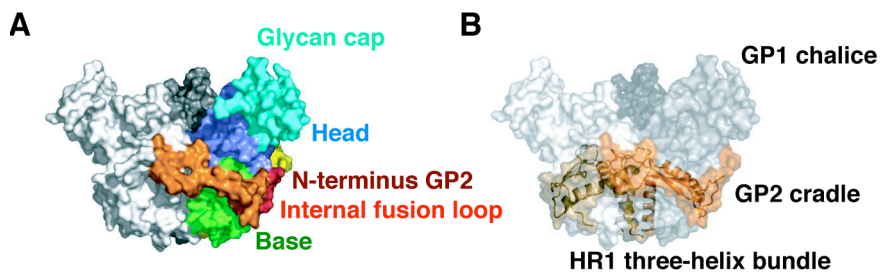


Figure 1-5. The Ebola virus fusion protein GP.

(A) Molecular surface of the GP trimer. Two of the monomer subunits shown in grey and light grey. The domains of the GP monomer are colored in the third monomer. Glycan cap in cyan, head in blue, N-terminus GP2 in red, fusion loop in orange, and the base in green. (B) The three GP1 monomers form the chalice in shades of grey. The GP2 monomers are shown as ribbon diagrams in orange and form the cradle. HR1 curls around GP1. The HR1 three-helix bundle that would extend to the viral membrane is shown. HR2 is not present in the crystal structure. (Adapted from (76))

of β -sheets that forms a semicircular surface that clamps the internal fusion loop and a helix in GP2. GP2 contains an internal fusion peptide that is partly helical and packs in GP1 similar to the packing of the PIV5 FP in its prefusion form (76, 155). GP2, like class I fusion proteins, is made up of two heptad repeats, HR1 and HR2, that are only separated by 25 residues in contrast to the 250 residues that separate PIV5 HRA and HRB (76). The crystal structure of postfusion GP2 fragments have shown that HR1 and HR2 form antiparallel α -helices similar to the HRA and HRB peptides of PIV5 (4, 84). HR2 is disordered and is not present in the solved crystal structure (76). HR1 is α -helical and divided into three segments that curl around GP1. One of these α -helical HR1 segments points toward the viral membrane and is an amphipathic helix that forms a 3HB at the trimer interface, similarly to PIV5 F HRB (Fig. 1-5B) (76, 155). While Ebola virus GP has several commonalities with PIV5 F and other class I fusion proteins, it is

distinct in some of its features. The head arrangement is unique, as is its heptad repeat arrangement, where by analogy, the HR2 region would be predicted to form a trimeric 3HB.

The unifying mechanism of fusion

Enveloped viruses fuse their viral membrane with target cell membranes by analogous mechanisms, though the fusion and attachment proteins differ. These mechanisms have been designated class I (paramyxovirus F, influenza virus HA, HIV gp41), class II (Dengue virus E, TBEV E, SFV E1), and class III (VSV G, HSV-1 gB) fusion. All three classes of fusion proteins possess distinctive attributes. PIV5 F and other class I fusion proteins contain fusion peptides at a new N-terminus that is formed by host cleavage and contain the 6HB coiled-coil structure in the postfusion form. Unlike influenza virus HA or PIV5 F, dengue virus E and other class II fusion proteins initially exist as dimers on the viral surface that reassociate after triggering into trimers, which protrude from the viral surface. Rather than requiring cleavage to expose the fusion peptide at a new N-terminus, class II and III fusion proteins contain internal fusion loops that do not insert deeply into the target membrane. In the prefusion form of VSV G, rather than residing in a protected pocket, the fusion loops reside near the viral membrane but are not inserted (50). The fact that class II shares elements of classes I and II and that recent crystal structures of Ebola GP2 (76) and baculovirus GP64, in press, demonstrate characteristics of several classes, such as possessing the HRA and HRB of class I but the fusion loops of class II and III, may render these distinctions obsolete.

Fusion proteins of these classes are diverse, but all begin the process of fusion as prefusion membrane bound surface glycoproteins whose conformational energy cascade drives the merger of two membrane bilayers (Fig. 1-6A). All fusion proteins require a trigger to start the fusion cascade, and this trigger also varies among fusion proteins. Some viruses, such as paramyxoviruses and herpesviruses, require an additional attachment protein for fusion. In PIV5 F fusion, F0 protein must be cleaved to expose the fusion peptide at the new N-terminus of F1. However, cleavage of PIV5 F is not predicted to be the trigger for F fusion, given that hPIV3 F0 can fold to the postfusion form of F even as an uncleaved protein (154). In addition, cleavage occurs in the *trans* Golgi network; hence some mechanism must regulate the F protein so it remains in its metastable state until it reaches its cell surface. For all paramyxoviruses, HN (or H, G) is required for or improves fusion. The homotypic HN (from the same virus as F) is necessary, and heterotypic HN cannot usually substitute to promote fusion. While class I proteins use a variety of triggers, all characterized class II proteins are activated by low pH. When class II E proteins are exposed to low pH, the dimers dissociate, then associate into trimers, and E rearranges such that the fusion loops extend from the surface of the virion (9, 96). Of the class III proteins, VSV G is activated by low pH, but unlike the E proteins or influenza virus HA, the conformational change induced by low pH is reversible (121). Upon triggering, the domain containing the fusion loop rotates to reorient the fusion loop toward the target cell membrane (120, 122).

Following triggering, all fusion proteins eventually form an extended pre-hairpin intermediate where the fusion protein is anchored by a TM domain in the viral membrane and a fusion

peptide or loop has inserted into the target cell membrane (Fig. 1-6B). In all classes, the pre-hairpin intermediate is homotrimeric (148). For class I proteins such as influenza virus HA and PIV5 F, the pre-hairpin intermediate is characterized by refolding to α -helical structures that extend the fusion protein towards the target membrane. After triggering by HN, the HRB helices in F separate, forming the open-stalk intermediate, which breaks the interactions in head between trimer subunits but leaves HRA in its prefusion conformation. The opening of HRB is consistent with peptide inhibition data from HRA derived peptides, which bind to HRB and inhibit fusion at its early stages (12, 125). The open-stalk intermediate may also affect the intersubunit contacts, which then destabilize the globular head. Following the open-stalk intermediate, DIII refolds and HRA forms the coiled-coil, which causes the translocation of the fusion peptide. The fusion peptide inserts into the target cell membrane, forming the pre-hairpin intermediate that can be inhibited by HRB-derived peptides (Fig. 1-6C) (125).

For class II and III, the domains containing the fusion loops that extend to the target membrane are predominantly composed of β -sheets. Although structurally different, dominant negative domains to the class II trimeric pre-hairpin intermediate have been made by analogy to the class I inhibitory peptides (83). Soluble domain III blocked low pH-induced virus fusion of SFV by binding to a hydrophobic pocket between domains I and II where domain III would usually fold during formation of the final hairpin structure (83). This inhibition suggests that domain III and core trimer binding is an important step in forming the postfusion form and may be the driving force of class II fusion (83). However, stem peptides, which would act similarly to the C1 peptide, have not demonstrated fusion inhibition (83).

This extended intermediate then folds back, or zippers up, to form a compact trimer of hairpins and bring the fusion peptide or loop and TM domain into close proximity and promote membrane merger (Fig. 1-6C) (50). This conversion may occur in steps, but the end result is the postfusion conformation of the fusion protein where the three C-terminal regions of the trimer pack stably against the central N-terminal trimeric core (148). The class I F protein refolds such that HRB binds into the grooves between the HRA monomers and forms the 6HB, bringing the FP and TM domain into juxtaposition within the same membrane (4, 34). The formation of the 6HB and the associated free energy change is tightly linked to the merger of the target and viral membranes (91, 125). The formation of the final trimer-of-hairpins occurs regardless of whether these regions form the 6HB with the predominant α -helical coiled-coil (class I), whether it consists of mainly β -sheet structures (class II), or a combination of both (class III) (148). The postfusion hairpin conformation is thermodynamically stable, and the conversion to this final state is thought to drive merger of the two membranes, which possess a large energy barrier (18).

The fusion proteins not only bring the membranes into close proximity, but also facilitate the local dehydration between the bilayers (140). After initial contact, the fusion stalk forms, where the outer leaflets of each membrane merge while the inner leaflets remain intact (Fig. 1-6B-C). This stalk then expands radially and a single mixed bilayer forms, referred to as the hemifusion diaphragm (Fig. 1-6B-C). Continued expansion leads to the formation of the initial fusion pore, which can flicker open and closed (Fig. 1-6B-C). The final stage is the formation of the larger fusion that allows the aqueous content of the virion to be transferred to the target cell (17, 18).

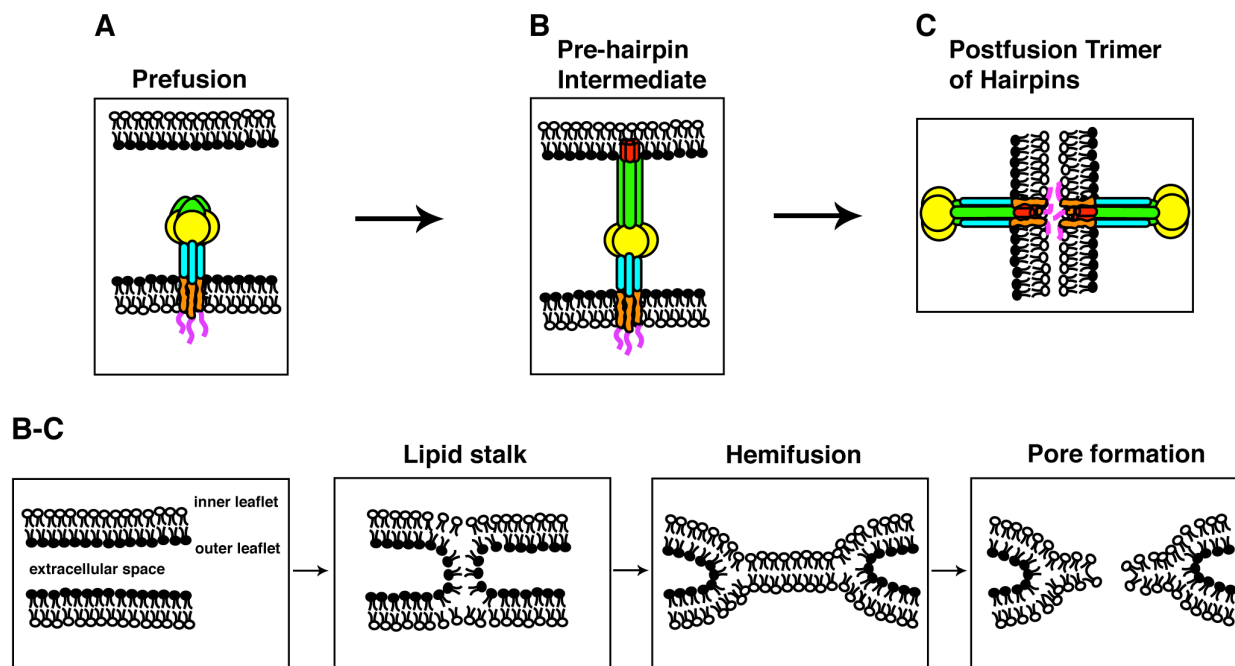


Figure 1-6. The unifying mechanism of fusion.

(A) Fusion proteins of all three classes begin the fusion cascade in the trimeric prefusion form. Class II proteins are initially homodimers on the virion surface until triggered by low pH to reassociate into fusion-ready homotrimers. (B) After the fusion triggering event, either receptor binding, low pH, combination of receptor binding and low pH, or cleavage by cathepsins, all fusion proteins insert their fusion peptides or loops into the target cell membrane to form the pre-hairpin intermediate. In this fusion intermediate, the fusion protein is anchored by the TM domains (orange) in the viral membrane and is now inserted into the target membrane via the fusion peptides or loops (red) with the fusion protein spanning the gap in an extended conformation. (C) The pre-hairpin intermediate then refolds to form a trimer of hairpins, or the postfusion conformation. For class I proteins, the hallmark of the postfusion form is the α -helical coiled-coil, or six-helix bundle (green and blue). Class II and III proteins form analogous structures made up of β -sheets. (B-C) The lipid bilayer intermediates are shown in with the fusion protein removed for clarity. The two bilayers contain an inner and outer leaflet and are separated by the extracellular space. During the process of F refolding to form the postfusion form, water is excluded from the extracellular space and the outer leaflets initially merge to form the lipid stalk intermediate. The inner leaflets then merge to form the hemifusion diaphragm. Continued expansion of the hemifusion diaphragm leads to formation of the fusion pore. Fusion peptide: red; TM domain: orange; CT: pink; head domain: yellow; inner leaflet: white; outer leaflet: black.

REMAINING QUESTIONS IN FUSION

Structural data on the pre- and postfusion forms of numerous fusion proteins and biochemical data on fusion intermediates together have created a general mechanism of protein-mediated membrane fusion, however, many questions remain. The number of trimers needed to cause bilayer fusion is not known. Many pre-hairpin structures may aggregate and cooperate to facilitate the formation of the fusion pore. However, it is not necessary for fusion machinery to surround the fusion stalk or pore because the energy barrier to progress through the fusion stalk could be derived from the refolding of one or two trimers if the interactions driving the refolding were strong enough (50). Some retroviral studies suggest only one trimer is sufficient for fusion (152), but the number of paramyxovirus F trimers necessary for fusion has not been determined. The specifics of the structural changes in the fusion protein during membrane fusion are not known. While biochemical data with inhibitory peptides has shed some light on what domains, such as heptad repeats, are exposed in the various intermediates or what domains may drive the refolding events (36, 83, 125), the structure and conformation of these fusion intermediates, such as the open-stalk and pre-hairpin intermediate, have not been determined.

The extent of fusion protein involvement in lipid bilayer fusion is unknown. The refolding to the final hairpin structure is thought to provide the requisite energy to remove water between the two merging membranes (20, 140), but do the two hydrophobic regions inserted into the opposing membranes, the fusion peptide or loop and the TM domain, contribute to lipid fusion? Does insertion of the fusion peptide or fusion loop into the target membrane contribute to lowering the kinetic barrier of fusion? What, if any, is the interaction between the fusion peptide or loop and

the TM domain after formation of the final hairpin structure? Studies suggest the TM domain of several class I fusion proteins is involved with formation of the fusion pore (2, 64, 92). Is the formation of the pore driven by fusion peptide or loop and TM domain interactions? Structural studies of the influenza virus HA fusion peptide in micelles suggest it is α -helical and kinked, with hydrophobic residues on the inner surface of the kink and glycines on the outer surface (47). The fusion peptide of HIV gp41, however, is mainly α -helical and lacking a kink (81). Structural studies have not examined the TM domain of fusion proteins, though they may prove to be α -helical in nature, similar to the TM domain of ion channels, such as the influenza virus M2 protein (130, 138).

Though their individual fusion proteins may differ, there is a commonality to all enveloped viruses in membrane fusion. They vary in their fusion trigger, requirement for additional proteins, and type of hydrophobic insertion into the target membrane. However, they all begin fusion with metastable fusion proteins, transition through an extended pre-hairpin intermediate that spans the virion and target membrane, collapse to form the postfusion hairpin structure, merge through a hemifusion intermediate, and finally form aqueous pores. Due to the commonalities of all fusion proteins, it is possible to gain greater insight and knowledge of all virus fusion mechanisms by analogy among enveloped viruses. Fusion is necessary for virus infection, and due to the precise conformational changes necessary for fusion, fusion proteins are less likely to undergo large adaptation or mutation than other surface proteins. Therefore, with greater knowledge of the conformational changes in fusion proteins, it is possible to develop new pharmaceuticals to inhibit virus infection and treat or prevent disease. Such innovation has

benefited the treatment of HIV. The inhibitory peptide T20, analogous to the HRB derived inhibitory peptide, is used under the names Fuzeon and Enfuviride (US Pat. 10578013), and was the first anti-fusion anti-viral approved for clinical use (148). Corresponding peptides have been shown to inhibit fusion of hPIV3 (US patent 7371809). Analogous peptides have been shown to inhibit fusion of other class I fusion proteins, and peptides derived from one paramyxovirus fusion protein may even inhibit fusion of another paramyxovirus fusion protein (115). Recent studies suggest that similar strategies may also apply to class II fusion proteins (83), and the possibility of new treatments will likely only grow.

**CHAPTER 2: ANALYSIS OF THE PH-REQUIREMENT FOR MEMBRANE FUSION
OF DIFFERENT ISOLATES OF THE PARAMYXOVIRUS
PARAINFLUENZA VIRUS 5**

INTRODUCTION

Enveloped viruses gain entry into cells by fusing their lipid bilayer with a membrane of the host cell. The viral proteins that mediate membrane fusion may fold into a metastable state that requires activation to undergo a protein refolding event to bring about the coalescence of the viral and cellular membrane. Such a mechanism is known to occur for influenza virus hemagglutinin (HA), paramyxovirus fusion protein (F), human immunodeficiency virus (HIV-1) envelope glycoprotein (gp120/41) and alphavirus E1 glycoprotein (22, 33, 62, 65, 70). Until recently, it was thought that activation of viral fusion occurred through one of two routes (55). The first route is activation at the plasma membrane and this route is used by paramyxoviruses, HIV-1 and herpes viruses among others. The second route involves internalization of the virion and activation of fusion by the low pH environment found in endosomal compartments. Fusion between the viral and intracellular membrane releases the viral genome into the cytoplasm. This pathway is used by influenza viruses, alphaviruses and the rhabdoviruses, vesicular stomatitis virus and rabies virus, among others. Recently, it has been recognized that there are variations on the two major themes with some viruses beginning their entry activation process by receptor binding at the plasma membrane but also requiring internalization and the low pH environment

of the endosomal lumen to complete the activation process: e.g. avian sarcosis/leukosis virus envelope glycoprotein (5, 87, 98).

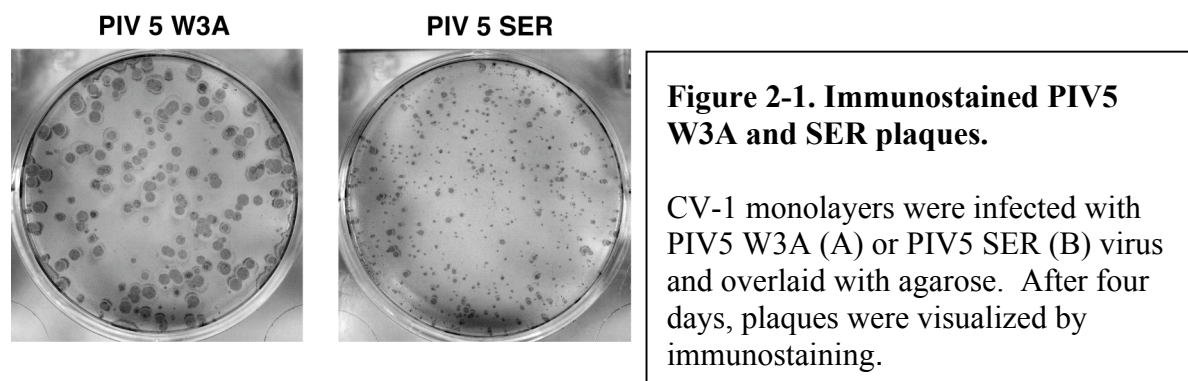
The porcine isolate of the paramyxovirus parainfluenza virus 5 (PIV5), known as SER, unlike the W3A isolate (also called SV5), does not induce readily detectable syncytium formation (143). The SER and W3A F proteins differ by only nine amino acids in their ectodomains, but SER has a 22 residue longer cytoplasmic tail than W3A F due to substitution of a translational stop codon for a serine residue (143). Mutagenesis of specific residues in the SER cytoplasmic tail enhance significantly the ability of SER to cause syncytia (134) and it has been suggested that the SER cytoplasmic tail forms a specific protein structure that inhibits the F protein conformational changes required for fusion activation (146). Recently, it has been reported that SER entry into cells occurs by a low pH-dependent process, suggesting that the conversion to the fusion-active state for SER F protein is triggered by exposure to reduced pH (133). PIV5 isolate SER would be the first paramyxovirus to require a low pH step for fusion. Thus, the fusion requirements of the PIV5 isolate SER required further investigation.

RESULTS

PIV5 SER infectious centers detected by immunostaining

The lack of syncytium formation caused by PIV5 SER has made it difficult to quantify virus titers. However, we observed that PIV5 SER infectious titers could be determined readily by

immunostaining of infectious centers (Fig. 2-1). The small size of the stained infectious centers does suggest limited cell to cell spread of virus, but PIV5 SER grew to similar infectious titers as compared to PIV5 W3A (1×10^8 pfu/ml).



Syncytia formation caused by PIV5 isolates

BHK-21F cells were transfected with plasmids expressing the SER and W3A F protein together with their homotypic and heterotypic receptor binding protein, hemagglutinin-neuraminidase (HN). Cell surface expression levels of the glycoproteins was examined by cell surface biotinylation and found to be essentially equivalent for each protein and to be approximately equivalent to the cell surface expression levels observed in W3A and SER virus-infected cells (data not shown). Transfected cells were treated either without or with a 2 min. low pH incubation (pH 5.3). As a control for low pH-induced fusion, cells expressing influenza virus HA were used (Fig. 2-2A). In a related experiment, BHK-21F cells infected with PIV5 isolates SER or W3A, or influenza virus, were examined for syncytia formation either without or with a low pH treatment (Fig. 2-2B). In the cells expressing W3A F and HN proteins, extensive syncytium formation (Fig. 2-2A) was observed as expected (58, 108). In cells expressing SER F and HN small foci of syncytia of up to 10-14 nuclei could be detected (Fig. 2-2A) but no

syncytia were detected in SER virus-infected cells (Fig. 2-2B). SER HN supported extensive - syncytia formation by the W3A F protein, whereas W3A HN did not enhance the limited syncytia formation detected with coexpression of SER F and SER HN. Low pH treatment of cells expressing HA induced syncytia formation. However, low pH treatment of either cells expressing SER F and HN or SER virus-infected cells did not induce increased syncytia formation over that observed at pH 7.0 (Figs. 2-2A and B). The data shown here are in contrast to data obtained by Seth and coworkers (133) who observed extensive syncytia formation after low pH treatment of cells expressing SER F and HN.

PIV5 SER and W3A cell-cell fusion using luciferase reporter assay

Vero cells expressing F and HN, and as a control cells expressing HA, were incubated with BSR T7/5 cells either without or with low pH treatment. Coexpression of SER F and HN resulted in detectable fusion using the luciferase reporter assay (Fig. 2-2C) and both W3A and SER fusion levels were very similar after pH 7.0 or pH 5.3 treatment. In contrast, influenza virus HA only showed detectable fusion after low pH treatment as expected.

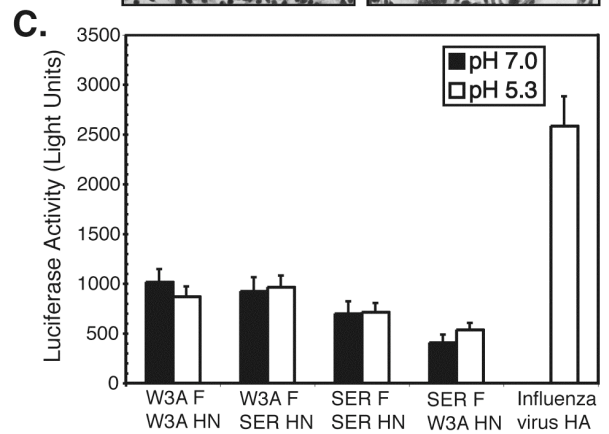
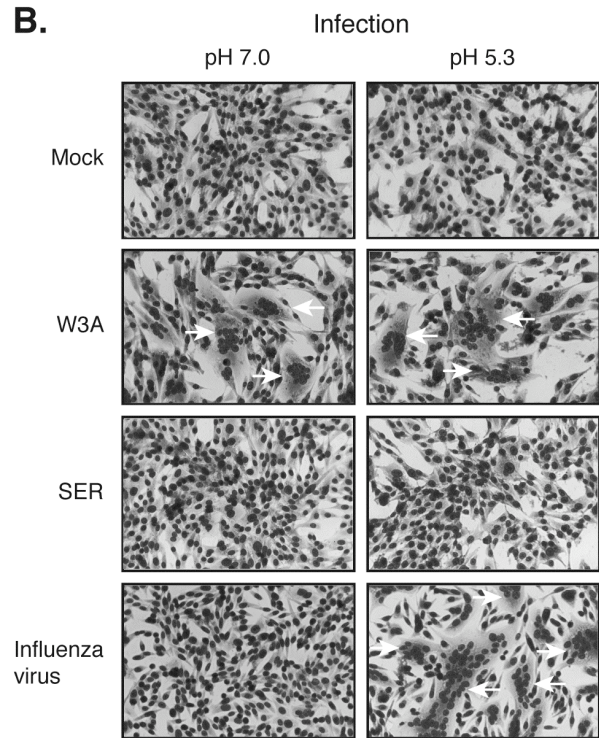
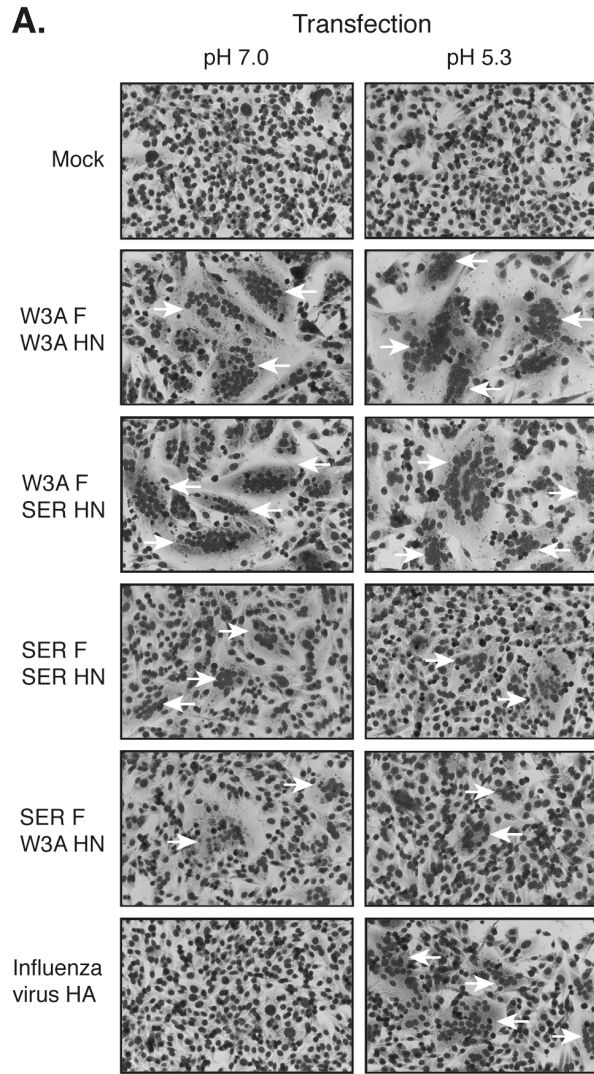
Real-time kinetics of virus-erythrocyte ghost fusion

To examine the kinetics of fusion of PIV5 W3A and SER virus to target membranes, a real time fluorescence dequenching fusion assay was used (23). Purified W3A, SER and influenza virus were labeled with octadecyl rhodamine B (R18), incubated with erythrocyte (RBC) ghosts at 4 °C and fusion initiated by injection of the virus bound to ghosts into pre-warmed (37 °C) PBS+

and fluorescence recording begun. After ~60 seconds, the pH was lowered to pH 5 and the fluorescence recording continued. As a control RBC ghosts were treated with *Vibrio cholera* neuraminidase to block virus binding. Dequenching of R18 (an increase in fluorescence at 590 nm) indicates fusion of the labeled-virions to the RBC ghosts. As shown in Fig. 2-2D influenza virions only showed fusion after lowering the pH to 5.0. In contrast W3A virions showed fusion occurring immediately after injection of the virus/ghosts into the pre-warmed PBS and fusion continued for ~130 seconds before reaching a plateau (Fig. 2-2D). Fusion was only minimally affected by changing to pH 5 after ~60 seconds of initiation of the fusion reaction. SER virions also caused detectable fusion in the real time fluorescence dequenching (Fig. 2-2D). Lowering the pH on SER virus/ghosts to pH 5.0 did not cause a change in the kinetics of fusion over that observed at pH 7.0. The maximum extent of fusion of the pH 5.0 treated sample is slightly higher than the pH 7.0 treated sample but the increased extent was evident at a point prior to changing the pH. For all three virus/ghost preparations the large spikes in OD₅₉₀ at ~20 seconds after recording began is due to light scatter from injection of the virus/ghosts into the cuvette.

Figure 2-2. Low pH does not induce syncytia formation in either cells expressing PIV5 W3A F or SER F or in cells infected with PIV5 W3A or SER viruses.

(A) BHK21 cells were transfected with 1 μ g each of F, HN, or HA. Cells were transfected in the combinations W3A F/W3A HN, SER F/SER HN, SER F/W3A HN, W3A F/SER HN or HA alone. 16 h p.t. phosphate buffered saline at pH 7.0 or pH 5.3 buffered with 10mM HEPES and 10mM MES was added to the cultures for two min. at 37°C. Cells were then incubated in DMEM pH 7 for 4 h. (B) BHK-21F cells were infected with W3A, SER, or influenza virus at MOI of 10 pfu/cell. 16 h p.i. the cells were treated with low pH and incubated in DMEM for 4 h. (C). Luciferase reporter gene assay. Vero cells were co-transfected with cDNA encoding luciferase under the control of the T7 RNA polymerase promoter (Promega, Madison, WI) together with W3A or SER F, W3A or SER HN, or influenza virus HA. At 16 h p.t., BSR T7/5 cells expressing the T7 RNA polymerase were overlaid onto the Vero cells and incubated at 37°C. After 3 h, the pH was lowered as for the syncytia formation assay and further incubated for 3 h at 37°C. The luciferase activity of each cell lysate was quantified using luciferase assay substrate (Promega) and an Lmax luminescence microplate reader (Molecular Devices, Sunnyvale, CA). Error bars represent standard deviations of three experiments each performed in triplicate.



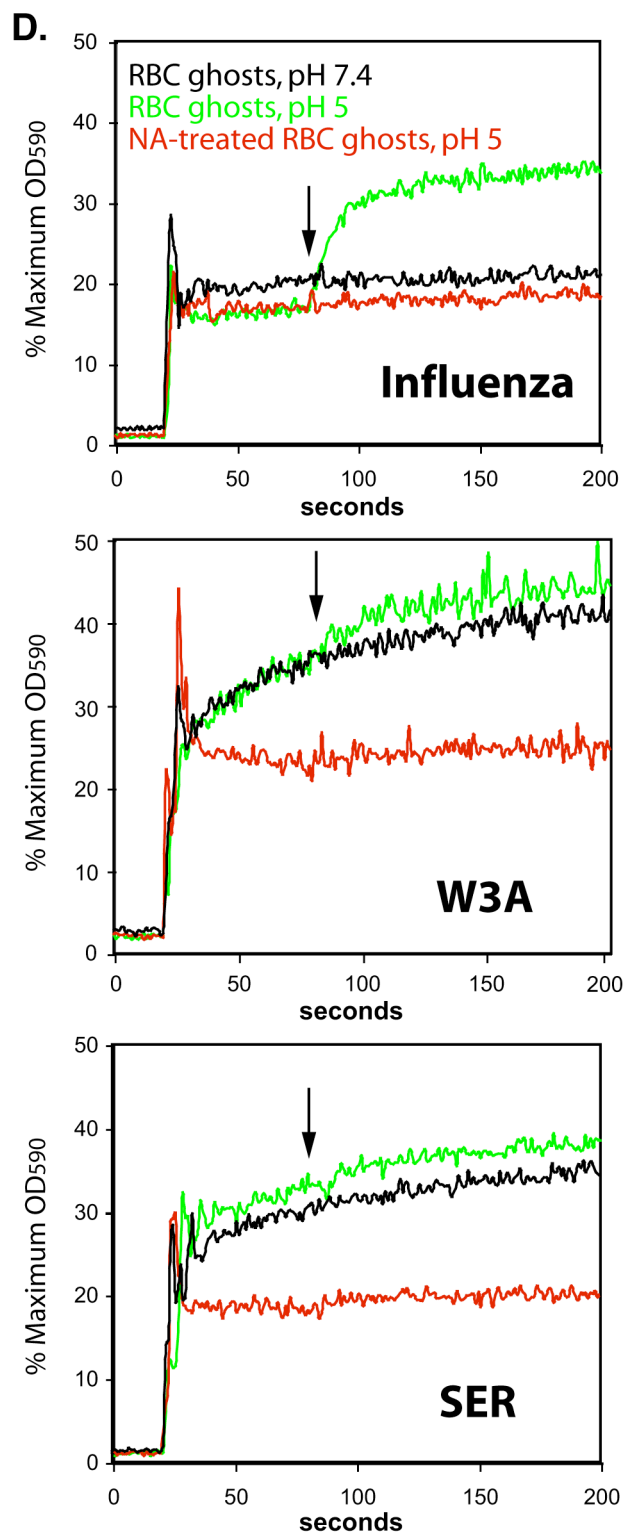


Figure 2-2. Continued.

(D) Real-time fusion assay. Purified R18-labeled viruses were bound to RBC ghosts or neuraminidase-treated (NA) RBC ghosts for 30 min on ice. Fusion was monitored by fluorescence dequenching at 590 nm using a spectrofluorimeter. Twenty seconds after starting readings, ice-cold virus-cell mixtures were injected into cuvettes holding 37°C PBS+ at pH 7.4. For low pH samples, citric acid was injected at 80 seconds to lower the pH to 5 (arrows). To determine the maximum level of dequenching, Triton X-100 was injected at 200 seconds. Data are expressed as a percentage of maximum OD₅₉₀.

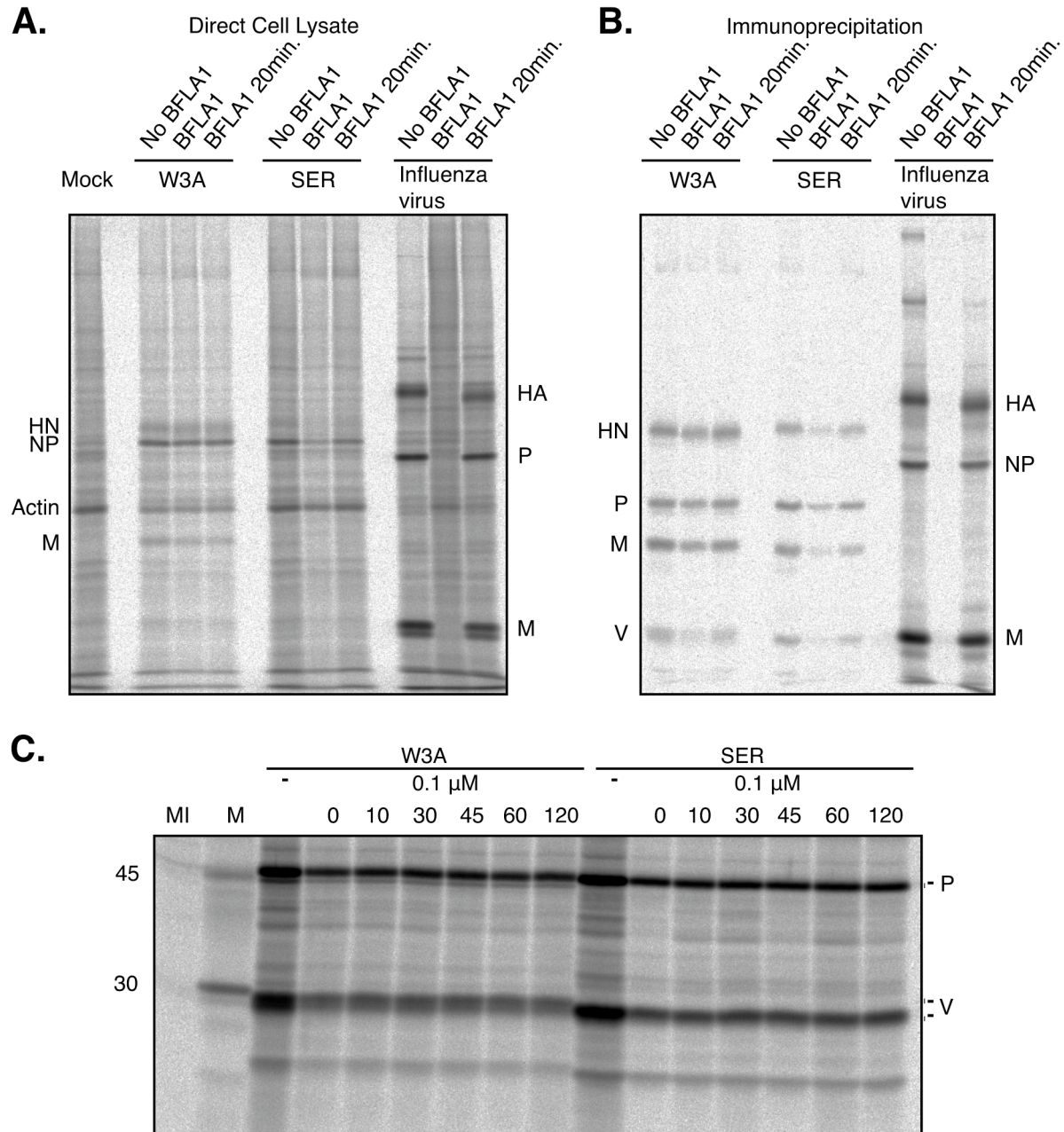
Bafilomycin A1 treatment does not affect PIV5 SER replication

Another approach to studying a possible low pH requirement for SER fusion activation is to use the inhibitor of the vacuolar-type H⁺ ATPase, bafilomycin A1 (BFLA1). This drug blocks the lowering of pH within acidic compartments in the cell, including the endosomal lumen (Drose 1993). CV-1 cells were infected with W3A, SER or influenza virus. The cells were either untreated, treated with BFLA1 (1.0 μM) before, during and after infection, or treated with BFLA1 20 min. after infection and then the drug maintained throughout further incubations. At 16 h p.i. (W3A and SER) or 10 h p.i. (influenza virus) the cells were metabolically labeled and proteins either analyzed directly by SDS-PAGE, or HN, P, M and V proteins were immunoprecipitated with specific MAbs and proteins analyzed by SDS-PAGE. As shown in Fig. 2-3A and B, BFLA1 was highly effective at preventing influenza virus polypeptide synthesis if added to the cells prior to infection. However, if BFLA1 was added to the influenza virus infected cells 20 minutes after infection, then the window of opportunity to prevent influenza virus-specific protein synthesis, due to blocking virus fusion activation, was lost. In contrast BFLA1 treatment before, during and after W3A or SER infection did not block W3A or SER protein synthesis. Decreased protein synthesis was observed for W3A and SER in cells treated with BFLA1 as compared to untreated control cells but a non-specific toxic effect of the drug can be anticipated given that the drug was present on cells for 18 h.

To further examine the effect of BFLA1 on PIV5 protein synthesis, MDBK cells were infected with W3A or SER and BFLA1 added either with the virus inoculum or 10, 30, 45, 60 or 120 min after addition of the virus. After 8 h drug treatment the cells were washed extensively and

Figure 2-3. Bafilomycin A1 does not inhibit replication of PIV5 isolates W3A or SER.

(A and B). PIV5 W3A, PIV5 SER, and influenza virus-infected CV1 cells (MOI of 10 pfu/cell) were either untreated, treated 20 min. before infection and then throughout the infection with 1.0 μ M BFLA1, or treated with 1.0 μ M BFLA1 20 min after the start of infection. At 16 h p.i. (W3A and SER) or 10 h p.i. (influenza virus), cells were labeled metabolically with Pro-mix-L [35 S] for 20 min. and proteins either analyzed directly by SDS-PAGE (A) or (B) proteins immunoprecipitated with antibodies specific for P, V, HN and M (for PIV5) or an anti-influenza virus goat serum. (C). MDBK cells were infected with either W3A or SER viruses at a MOI of 10 pfu/cell. Bafilomycin A1 was added to a final concentration of 0.1 μ M either with the virus inoculum or 10, 30, 45, 60 or 120 min after addition of the virus. At 8 h p.i. the cells were washed with PBS to remove the drug and excess virus. The cells were then incubated in DMEM for a further 16 h. At 24 h p.i. cells were metabolically labeled with Pro-mix-L [35 S] for 1.5 h. Immunoprecipitation was performed using MAb P/k specific for P and V proteins. Polypeptides were analyzed by SDS-PAGE on 15% acrylamide gels and radioactivity analyzed using a Fuji BioImager 1000 and MacBas software (Fuji Medical Systems, Stamford, CT).



incubated in DMEM for a further 16 h prior to metabolic labeling. The P and V proteins were immunoprecipitated and proteins analyzed by SDS-PAGE. As shown in Fig. 2-3C the P and V proteins were readily detected at all times whether the drug was added at the time of infection or up to 2 h p.i.

Another method to examine viral protein synthesis in the continuous presence of BFLA1 is to immunostain the cells for specific viral antigens. MDBK cells were infected with W3A, SER or influenza virus in the presence or absence of BFLA1 and maintained with or without the drug for 10 h prior to immunostaining with antisera specific for the P/V proteins (W3A and SER) or the M2 protein (influenza virus). As shown in Fig. 2-4A no difference in staining pattern could be observed for untreated or BFLA1 treated W3A or SER infected cells. In contrast for influenza virus-infected cells, no M2 protein could be detected in BFLA1 treated cells.

In addition to W3A and SER there are many other isolates of PIV5. Thus, to test if any of these isolates were sensitive to BFLA1, Vero cells were infected a low MOI (0.005–0.5 pfu/cell) with the PIV5 isolates W3A, SER, Mil, Mel, LN, Den and RQ (Chatziandreou 2004) and as a control influenza virus. Cells were either untreated or pretreated with 0.5 μ M BFLA1 and treated cells remained in the presence of the BFLA1 and at 18 h p.i. were immunostained for the P/V protein (for influenza virus antisera specific for HA was used). As shown in Fig. 2-4B the P/V proteins could be stained in both untreated and BFLA1 treated cells indicating that none of the PIV5 isolates required a low pH step during virus entry.

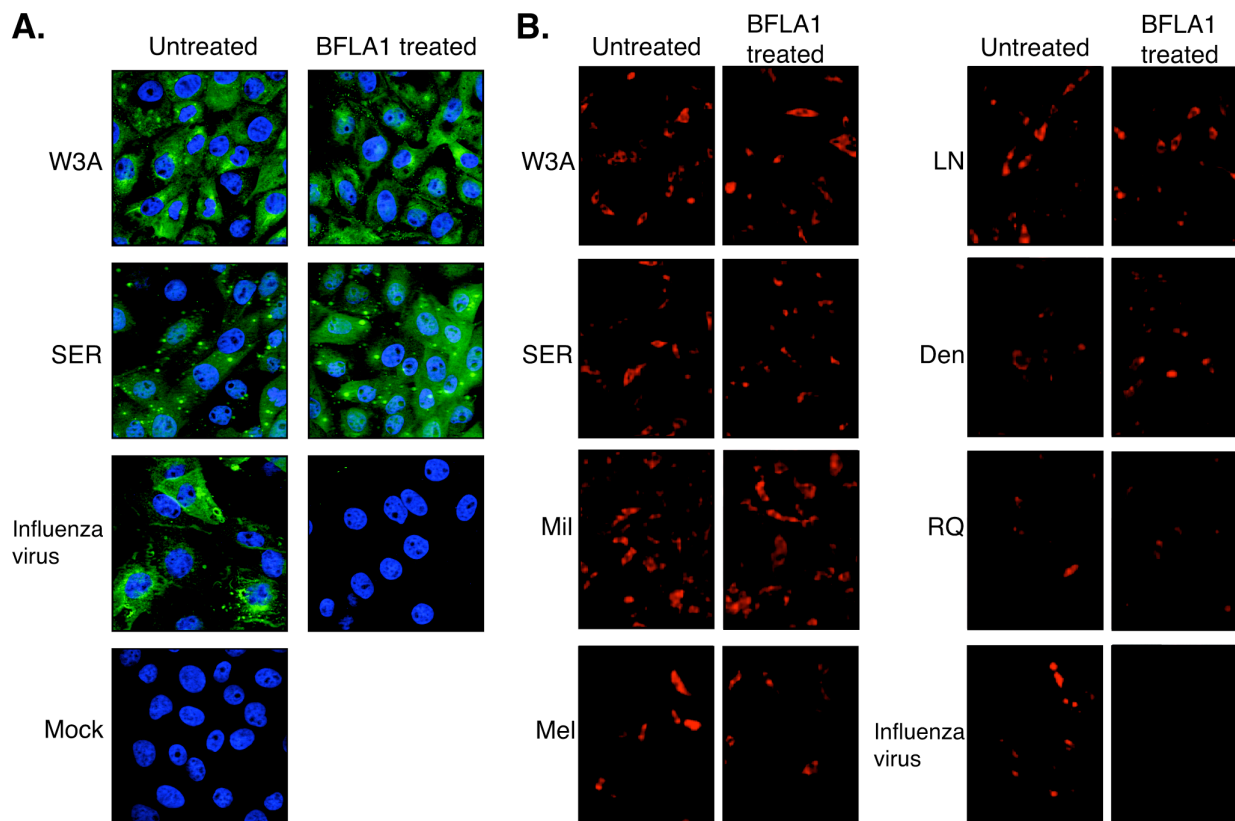


Figure 2-4. Antigens of PIV5 W3A, PIV5 SER and other PIV5 isolates were detected in bafilomycin A1 treated cells.

(A) Influenza virus, W3A, SER, and mock-infected MDBK cells (MOI of 10 pfu/cell) were treated with 1.0 μ M BFLA1 and immunostained with MAb P/k (W3A and SER) or MAb 14C2 (influenza virus) at 10 h p.i. (B) Vero cells were infected with several natural isolates of PIV5 or influenza virus at an MOI between 0.005 and 0.5 pfu/cell. Cells were either untreated or pretreated with 0.5 μ M BFLA1 1 h prior to infection, and treated cells remained in the presence of BFLA1. At 18 h p.i. the cells were fixed and incubated with MAb P/k for PIV5 or an anti-influenza virus goat serum.

DISCUSSION

In summary, using three different assays for fusion (syncytia formation, a luciferase reporter assay for cell-cell fusion and real-time virus-red blood cell ghost fusion) and lowering of pH, no

evidence for low pH-induced fusion by PIV5 SER could be obtained. For each assay influenza virus was used as a control for low pH-induced fusion. Furthermore by using various protocols for BFLA1 treatment of PIV5 SER-infected cells no effect of the drug on PIV5 SER replication was observed. For each assay influenza virus was used as a positive control and in each case influenza virus-specific protein synthesis was inhibited by the drug. Thus, the data could not provide any evidence for a requirement of a low pH step during PIV5 SER entry into cells. We have no explanation for the data obtained by Seth and colleagues (133) who observed low pH-dependent activation of fusion by PIV5 SER. Indeed such an activation mechanism would have greatly facilitated studies on paramyxovirus-mediated membrane fusion, as currently temperature shifts have to be used to activate the F protein. Now that the atomic structures of both the metastable pre-fusion form of F and the post-fusion form of F have been obtained (154, 155) revealing the major F protein refolding event that takes place during fusion, one of the big challenges remains to discover how the paramyxovirus receptor binding protein (HN, H or G) activates the metastable fusion protein to cause membrane fusion at neutral pH.

MATERIALS AND METHODS

Cells, viruses, and plasmids. Madin-Darby bovine kidney (MDBK), CV-1, Vero, BHK-21F and BSR T7/5 cells were grown as described (109). The PIV5 isolates W3A and porcine isolate SER (133, 134, 143) (provided by Richard W. Compans, Emory University School of Medicine, Atlanta, GA) were grown in MDBK cells. pCAGGS plasmids encoding W3A F, W3A HN and

influenza virus HA (A/Udorn/72) have been described previously (118). The cDNAs encoding SER F and SER HN were synthesized by RT-PCR using RNA isolated from SER virus-infected cells and cloned into the eukaryotic expression vector pCAGGS. The nucleotide sequence of the F and HN cDNAs was determined and found to be identical to that obtained previously (143).

Plaque assay. PIV5 isolates W3A and SER were plaqued on CV-1 cells as described and monolayers immunostained using vacF and vacHN rabbit sera (110) as described (14). Virions were purified on 15-60% sucrose gradients as described (109).

Syncytia formation. To examine syncytia formation BHK-21F cells were transfected with 1.0 μ g pCAGGS expressing W3A F, SER F, W3A HN or SER HN, or influenza virus (A/Udorn/72) HA (Russell 2001). Also BHK-21F cells were infected with W3A, SER or influenza virus at a multiplicity of infection (MOI) of 10 pfu/cell. At 16 h post-transfection (p.t.) or post-infection (p.i), PBS pH 7.0 or pH 5.3 (buffered with 10mM HEPES and 10mM MES) was added to the cells for 2 min. at 37°C and the cells further incubated in DMEM at neutral pH. For influenza virus-infected cells and HA-expressing cells HA was cleaved by addition of N-acetyl trypsin (1 μ g/ml, 10 min, 37°C) prior to low pH treatment. After 4 h incubation, cells were fixed, stained and photographed as described (146).

Luciferase reporter gene assay. For quantification of fusion a luciferase reporter assay was used (124). A real-time fusion assay was used to measure virus-cell fusion. Human RBC ghosts (2.5 mg/ml protein) were prepared as described (139). For NA-treated RBC ghosts,

neuraminidase (*Vibrio cholera*) (Sigma Aldrich, St. Louis, MO) was added at 100 mU/ml for 1 h at 37°C. Purified virus (20 µg per sample) was labeled with octadecyl rhodamine B (R18; Invitrogen, Carlsbad, CA) and virus-ghost fusion assays performed essentially as described (139).

Immunoprecipitation. Metabolic labeling, immunoprecipitation and SDS-PAGE were performed as described (109). To detect virus-specific polypeptides synthesized in direct lysates of virus-infected cells, actinomycin D (5 µg/ml) was also added to the cultures from the start of infection (107). Bafilomycin A1 (BFLA1) was obtained from Calbiochem (EMD Biosciences, La Jolla, CA).

Immunofluorescent staining. Immunofluorescent staining of W3A, SER, or influenza virus infected CV-1 cells was done using P/V protein-specific MAb P/k (118) or the influenza virus M2 protein-specific MAb 14C2 (158) and an Alexa-488 conjugated goat anti-mouse secondary antibody. Cells were counter stained with 4'-6-Diamidino-2-phenylindole (DAPI) and fluorescence visualized using a deconvoluting (ApoTome) Axiovert 200 microscope (Zeiss, Thornwood, NY).

CHAPTER 3: RESIDUES IN THE OUTER LEAFLET OF THE TRANSMEMBRANE DOMAIN OF THE PARAINFLUENZA VIRUS 5 FUSION PROTEIN ARE CRITICAL FOR MEMBRANE FUSION

INTRODUCTION

Membrane fusion is a fundamental biological process that occurs in intracellular trafficking, exocytosis, resealing of plasma membranes, protein trafficking, and in the entry of enveloped viruses. This ubiquitous process is mediated and tightly controlled by a combination of specific protein machinery and lipid composition (140). Lipids spontaneously assemble into bilayer structures such as liposomes; however, lipid bilayer membranes do not spontaneously fuse (20). The spontaneous negative or positive curvature of a lipid can enhance or diminish fusion, respectively, but energy must be expended to overcome hydration repulsion between membranes and to disrupt the bilayer structure. The energy for this remodeling may be derived from the thermal fluctuations of the membrane or from specialized fusion proteins (20). Many biological processes, such as neuronal synaptic vesicle fusion, endosomal fusion, and exocytosis, employ the SNARE superfamily proteins (86). SNAREs are found in all eukaryotic organisms. All SNARE proteins have a common heptad-repeat that forms four-helix coiled-coil structures, and this coiled-coil SNARE complex forms in *trans* to promote fusion of the two membranes in which the SNARE proteins are anchored (149). Enveloped viruses use an analogous strategy and mediate fusion with target cells through specialized fusion proteins. The paramyxovirus parainfluenza virus 5 (PIV5) requires two surface glycoproteins for this process: the attachment

protein hemagglutinin-neuraminidase (HN) that binds sialic acid and the fusion protein (F) that physically merges the two membranes. Paramyxovirus fusion occurs at the plasma membrane and does not require the low pH of the endosome to trigger fusion (69).

The paramyxovirus F protein is a class I fusion glycoprotein that is synthesized as a type I integral membrane protein and it folds into homotrimers, is post-translationally modified by the addition of carbohydrate chains, and is proteolytically cleaved to become biologically active. Similar processing occurs for other class I viral fusion proteins, such as influenza virus HA, HIV gp160, retrovirus Env, Ebola GP, and SARS CoV S (69). The paramyxovirus F precursor protein (F0) is cleaved into the membrane-anchored F1 subunit and the smaller N-terminal F2 fragment. F1 contains two hydrophobic regions, the N-terminal fusion peptide (FP), located at the new N-terminus after cleavage, and the transmembrane (TM) domain, and two heptad repeat regions, HRA and HRB. HRA is located immediately C-terminal to the FP, and HRB is proximal to the TM domain (69).

The paramyxovirus F protein folds initially into a metastable prefusion form that upon triggering undergoes a series of large scale conformational rearrangements, proceeding down an energy gradient to form a final irreversible postfusion form. Recently, the crystal structures of both the uncleaved prefusion conformation of the paramyxovirus F protein and the uncleaved postfusion conformation were solved (154, 155). The prefusion form contains a globular head containing three domains (DI-DIII) attached to a trimeric coiled-coil stalk formed by the HRB region. The HRA region in the prefusion form is composed of 11 distinct segments that wrap around the DIII

core in the globular head (155). This is in contrast to the postfusion form of F where HRA is extended into a long α -helix as part of the 6HB. For the postfusion structure an unanticipated finding emerged as the available data indicate the F TM domain and/or cytoplasmic tail are important for the folding of F into the metastable prefusion form of F (154): secreted F lacking a TM domain converts to the postfusion form.

Upon receptor binding, biochemical studies indicate HN induces a conformational change in F and the HRB three-helix stalk separates (125). It is hypothesized that following the melting of the HRB helices and destabilization of the head, HRA refolds to form an extended α -helical coiled-coil, which enables the insertion of the fusion peptide into the target cell membrane and forms the pre-hairpin intermediate (155). The F protein then refolds where HRB binds into the grooves between the HRA monomers and forms the six-helix bundle (6HB), bringing the FP and TM domain into juxtaposition within the same membrane (4, 35, 67, 155). A conceptually related final post-fusion structure is formed for all enveloped virus fusion proteins. The postfusion structure either consists of a α -helical coiled-coil structure like the 6-HB in PIV5 F or β -strand structures in other fusion proteins, like Dengue virus E, Semliki Forest virus E1, and vesicular stomatitis virus (VSV) G (148). In all cases the fusion peptide and TM domain are together in the same membrane. The formation of the 6HB and the associated free energy change is tightly linked to the merger of the target and viral membranes (91, 125). The collapse of the pre-hairpin intermediate distorts the bilayers to possibly form an initial point-like protrusion (50). Whether the insertion of the fusion peptide insertion perturbs the lipid bilayer and lowers the distortion energy is unknown (50). Following the initial bilayer contact, membrane merger

proceeds to the lipid stalk intermediate, where the outer leaflets of each bilayer merges but the inner leaflets remain separate. This stalk then expands to form the hemifusion diaphragm. Continuation of this expansion leads to formation of the fusion pore that allows for the transfer of aqueous contents (17).

The TM domain of PIV5 F is 25 amino acids long and made up mostly of hydrophobic residues (Fig. 3-1A). In addition to aiding in protein folding and stability, the TM domains of many viral envelope fusion proteins have been shown to have a role in fusion (21, 53, 64, 82, 89, 90, 92, 135, 147). When the TM domain of influenza virus HA was replaced with a with a glycosylphosphatidylinositol (GPI) anchor, it resulted in a fusion protein that could mediate hemifusion by allowing the transfer of a lipid but not aqueous fluorescent probe, suggesting a role of the TM domain in pore formation and enlargement. This GPI-anchored HA was embedded only in the outer leaflet of the membrane, and it was proposed that the TM domain, which spans the entire membrane, affects the positive curvature on the inner leaflet that would allow for pore formation (64, 89). In addition, specific residues in the TM domain have been shown to be important for fusion of influenza virus HA (92), VSV G (21), HIV gp41 (53, 103, 135), and baculovirus GP64 (82). However, little is known about the role of the TM domain in paramyxoviruses.

In this study, we investigate the functional role of the PIV5 F TM domain in membrane fusion. We performed alanine-scanning mutagenesis on the TM domain of F and determined that two residues, 486 and 488, are critical for PIV5 F fusion. The aggregate of analysis of the steps of

fusion indicate these mutants do not support hemifusion and are trapped at the lipid stalk stage just prior to formation of the hemifusion diaphragm. By singly substituting each residue of the TM domain with cysteines, we have examined the structure of the TM domain in the lipid membrane. The addition of an oxidative cross-linker and formation of disulfide bonds indicated the monomers within the trimer of F are in close proximity, freely rotate within the membrane, and are predicted to form a three-helix bundle with modified 4-3 helices. Our results indicate a specific amino acid sequence of the TM domain is necessary for completion of fusion. The amino acid side chains at residues 486 and 488, which are predicted to be in the outer leaflet of the F TM domain, are critical for the merger of the two lipid membranes and fusion completion. The block in fusion observed with mutation of F residues 486 and 488 could be overcome by addition of compounds that affect the curvature of the membrane bilayer.

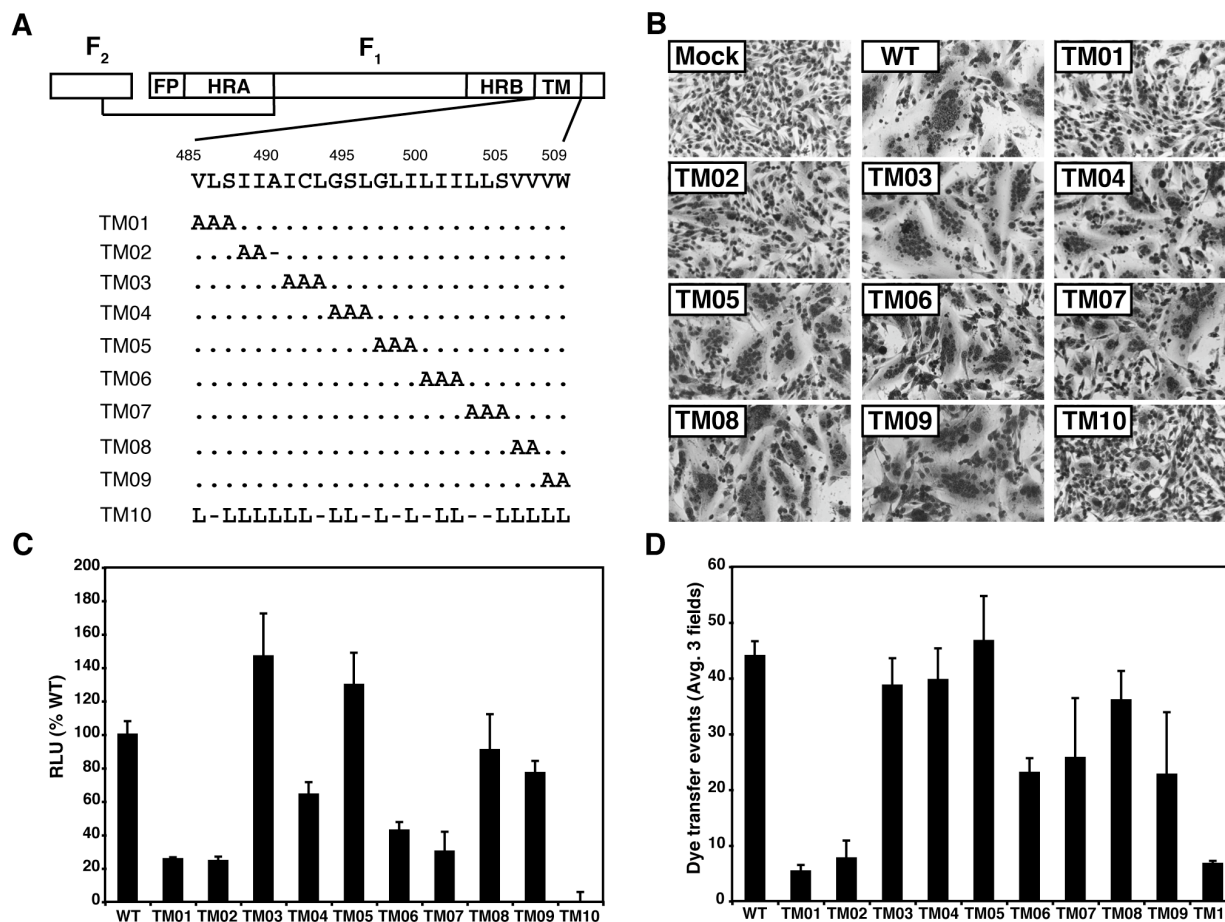
RESULTS

F protein TM domain residues bordering the ectodomain have a key role in fusion

To determine the role of the F protein TM domain in fusion, alanine-scanning mutagenesis was performed in groups of two or three amino acids for the 25 residues of the PIV5 F protein TM domain. Further, the entire TM domain was replaced en bloc with 25 leucine residues (Fig. 3-1A). Cell surface expression of the F protein mutants TM01-TM09 was equivalent to wild type (wt) PIV5 F (Table 3-1). However, mutant TM10 was not expressed at the cell surface and thus F TM10 is likely to be a misfolded protein that is not transported through the exocytic pathway to the cell surface (31). Previously, when the TM domain of PIV5 HN was replaced with leucine

Figure 3-1. Analysis of fusion activity of alanine mutations in the F protein TM domain.

(A) Schematic diagram of the PIV5 F protein. The positions of the fusion peptide (FP), heptad repeat A (HRA), heptad repeat B (HRB), and TM domain are shown. The TM domain is taken as beginning at V485 and ending at W509. The alanine substitutions in the alanine scan for mutants TM01 through TM10 are shown. For mutant TM10, all TM domain residues were replaced with leucine. (B) Representative micrographs of syncytia formed at 20 h p.t. in BHK-21F cells expressing PIV5 HN and either wt F or F containing a TM domain mutation. Mock = expression of HN alone. (C) Luciferase reporter gene assay of cell-cell fusion mediated by the F protein TM domain mutants. Vero cells were cotransfected to express HN, wt F or mutant F protein, and a luciferase reporter construct. Shown is the average of three experiments each performed in triplicate and the data normalized to wt F. (D) Quantification of cell-cell fusion obtained from the dye transfer assay. Effector CV-1 cells were infected with vaccinia virus vTF7-3 and transfected with DNA encoding HN and wt F or F TM domain mutant. RBCs were labeled with the lipidic probe R18 and the aqueous probe 6-CF. Labeled RBCs were bound to CV-1 cells for 1h at 4°C and then incubated at 37°C for 15 min before visualization by confocal microscopy. Cell-cell fusion was observed as the transfer of red R18 and green 6-CF from the target RBCs to the effector CV-1 cells. Shown is the quantification of 6-CF. The means and error bars are from three microscopic fields.



residues, there was no discernable effect on the cell surface expression of HN and no effect on its biological function (78). The ability of the F TM domain alanine scanning mutants to cause cell-cell fusion was determined by using three assays: (1) syncytia formation, (2) a luciferase reporter assay and (3) a dye transfer assay. F TM domain mutants TM03-TM09 formed similar sized syncytia as compared to wt F protein, but mutant F proteins TM01 and TM02 did not cause syncytia formation although these proteins were well expressed at the cell surface (Fig. 3-1B). Whereas several of the TM mutants showed some decrease in fusion in the quantitative

Table 3-1: Cell surface expression of F mutants.

	RMFI (%WT)		RMFI (%WT)
WT	100.00	V485A	102.40
		L486A	81.12
		S487A	99.50
TM01	101.57	I488A	88.75
TM02	98.81	I489A	99.19
TM03	102.75		
TM04	97.80	S443P	113.11
TM05	93.71	S443P/L486A	66.54
TM06	87.30	S443P/I488A	80.74
TM07	90.11	G105A	97.22
TM08	111.46	G105A/L486A	78.21
TM09	97.23	G105A/I488A	85.46
TM10	9.45	G109A	10.29
		G109A/L486A	10.85
		G109A/I488A	8.51

luciferase reporter and dye transfer assays, TM01 and TM02 caused a consistent and major reduction in fusion in all assays used (Fig. 3-1C and D).

F TM domain residues L486 and I488 are key residues involved in fusion

To determine further which residues in mutants TM01 and TM02 are responsible for the greatly reduced fusion activity, the first five residues, 485-489, of the F protein TM domain were changed individually to alanine. All these mutants were expressed at the cell surface at levels similar to wt F (Table 3-1). F TM domain mutants V485A, S487A, and I489A formed syncytia at levels similar to wt F, but F TM domain mutants L486A and I488A did not cause syncytia formation (Fig. 3-2A). These mutants also showed a substantial decrease in fusion in the luciferase reporter and dye transfer assays (Fig. 3-2B, C). In all cases where fusion occurred,

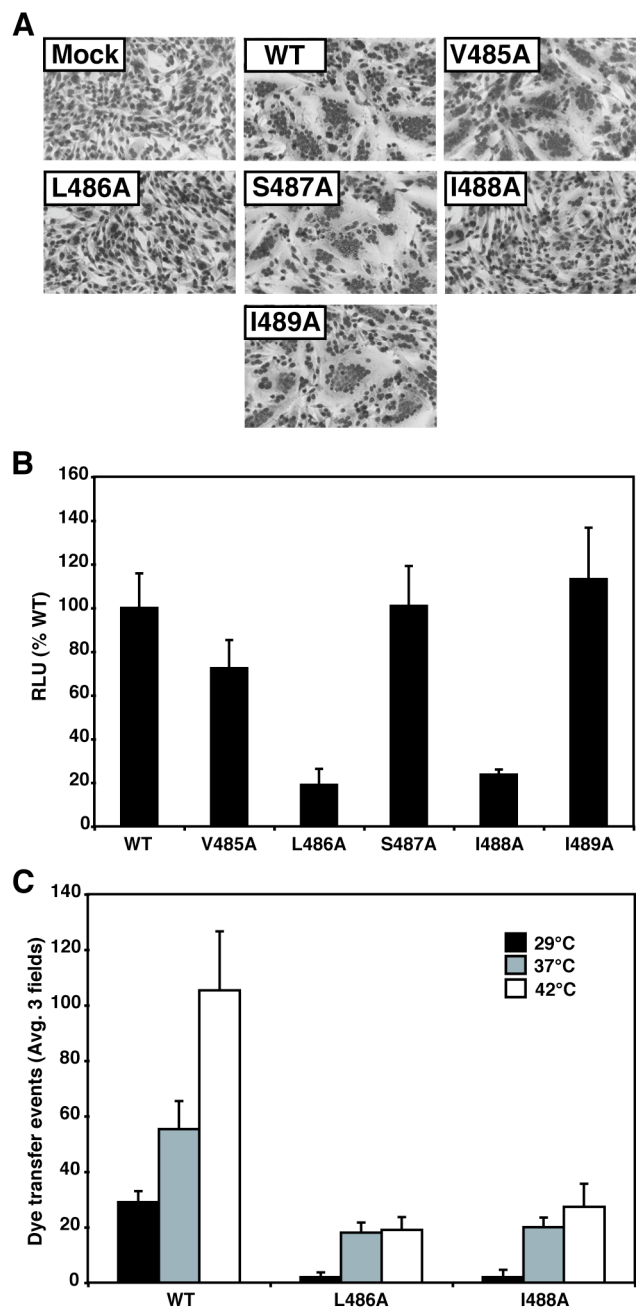


Figure 3-2. Analysis of fusion activity of alanine point mutants for F TM domain residues 485-489.

(A) Representative micrographs of syncytia formed at 20 h p.t. in BHK-21F cells expressing PIV5 HN and either wt F or F containing TM domain point mutations or HN alone (mock). (B) Luciferase reporter gene assay to measure cell-cell fusion mediated by the F point mutants V485A-I489A. Vero cells were cotransfected to express HN, wt F or F point mutant proteins, and a luciferase reporter construct. Shown is the average of three experiments each done in triplicate and normalized to wt F. (C) Cell-cell fusion of F point mutants at different temperatures. After RBCs labeled with 6-CF were bound to CV-1 cells labeled with SYTO-17, the temperature was raised to 29°C, 37°C, or 42°C for 15 min to activate fusion and dye transfer. Shown is the quantification of green 6-CF dye transfer events from three microscopic fields.

both the lipidic dye, R18, and the aqueous content mixing dye, 6-CF, were transferred to the CV-1 cells, whereas F TM domain mutants L486A and I488A did not cause the transfer of R18 or 6-CF. Thus, these mutants do not cause either lipid mixing or contents mixing. Previously, we determined that an increase in temperature can be a surrogate for HN triggering fusion(111, 125).

To examine temperature dependent triggering of the F TM domain mutants RBCs were labeled with 6-CF and bound to effector CV-1 cells expressing HN and F proteins and labeled with SYTO-17 at 4°C. The target-effector complexes were then incubated at 29°C, 37°C, or 42°C for 15 min, and the number of fusion events was measured by confocal microscopy (Fig. 3-2C). For wt F, the number of dye transfer events increased with increasing temperature. The amount of fusion mediated by F TM domain mutants L486A and I488A increased between 29°C and 37°C, but increasing the temperature beyond 37°C did not enhance fusion. The mutants L486A and I488A did not exhibit a hemifusion phenotype, i.e. transfer of the lipidic dye R18 to target cells in the absence of transfer of the aqueous dye 6-CF. It is possible that these mutations either stabilize the F protein and prevent F protein from attaining its lowest energy postfusion conformation or affect protein/membrane interactions that stabilize an intermediate in the fusion pathway. For example, these mutant F proteins may be trapped at a folding/fusion intermediate that cannot be overcome by an increase in temperature.

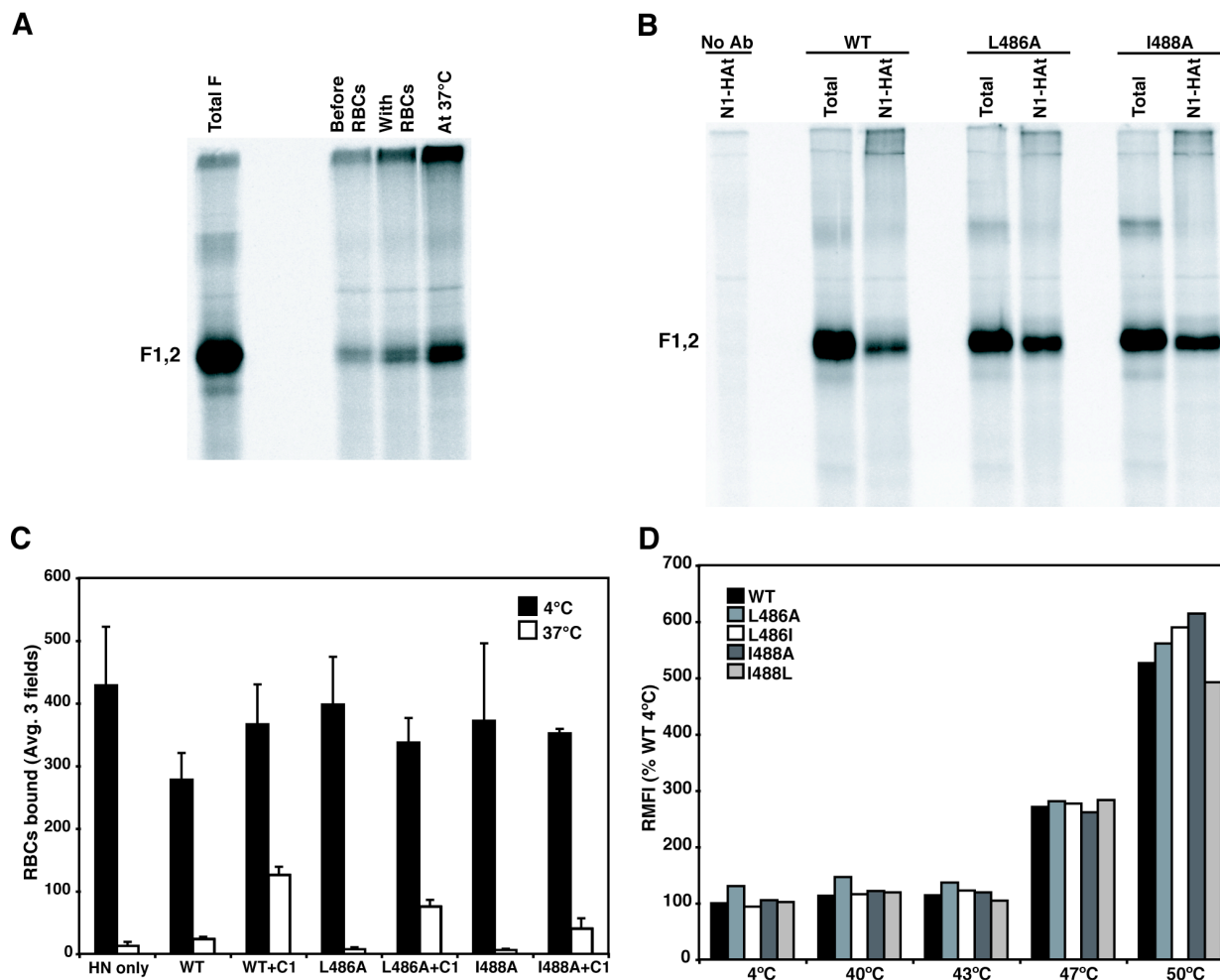
F TM domain mutants L486A and I488A form the open-stalk and pre-hairpin intermediates of fusion

For PIV5 entry into cells by fusion, HN binds to its ligand, sialic acid, and by a process unknown begins the activation of F. The earliest stage of fusion that has been determined was inferred from properties of the N-1 peptide (which is derived from the HRA region of F). N-1 peptide can bind to the HRB region of F after HN has bound to target cells at 4°C and inhibits fusion (125). Based on the atomic structure of prefusion F this step in fusion has been called the open-stalk conformation with the HRB helices melting and breaking the interactions at the base of the

head but leaving the head domain largely intact (155). To determine if F TM domain mutants L486A and I488A can attain the F open-stalk conformation, a modified N1 peptide, N1-HAt, was synthesized that contains an 11 residue HA tag (YPYDVDPDYASL) at the C-terminus of N1. Peptide binding was determined by the ability of the HA tag MAb to immunoprecipitate wt F protein. It was found that the N1-HAt bound to F at 4°C when target RBCs containing the HN receptor sialic acid were present but N1-HAt did not bind to F in the absence of target RBCs. (Fig. 3-3A). To test if F TM domain mutants L486A and I488A reached the open-stalk stage of fusion, N1-HAt peptide was incubated with cells expressing HN and one of the mutant F proteins at 4°C in the presence of 0.5% hematocrit target RBCs (Fig. 3-3B). The HA tag MAb 12CA5 was used to immunoprecipitate the F protein containing bound peptide, and the total F in the lysate was immunoprecipitated with a polyclonal antibody specific for F protein. N1-HAt bound to wt F and F TM domain mutants L486A, and I488A, indicating the HRB region was accessible in all F proteins and thus the alanine substitutions in the TM domain did not prevent the formation of the open-stalk conformation of F protein. The second known step in the F protein refolding event after formation of the open stalk intermediate is thought to be that HRA refolds and the fusion peptide is inserted into the target cell membrane to form the pre-hairpin intermediate (125, 155). At this stage of fusion, the C1 peptide, derived from the HRB region of F, specifically inhibits PIV5 F-mediated fusion (63) by binding in the grooves on the outside of the HRA coiled-coil (4). To capture the pre-hairpin conformation the C1 peptide was used in an RBC retention assay (125). To examine the F TM domain mutants for pre-hairpin formation, target RBCs labeled with 6-CF were bound at 4°C to CV-1 cells that co-expressed F and HN and were labeled with STYO 17. When the RBCs that have bound at 4°C to the CV-1 cell are

Figure 3-3. Analysis of the protein conformation of F mutants L486A and I488A and examination of the steps of fusion attained by these mutants.

(A) HA-tagged N1 peptide binds to the open stalk intermediate of wt F in the presence of HN and target cells (RBCs). HeLa CD4 LTR β gal cells expressing HN and wt F were metabolically labeled with 400 μ Ci of 35 S-Promix. Lane 1, wt F was immunoprecipitated with a polyclonal antibody specific for F (PAb vacF) to indicate the total amount of wt F. Cells were incubated with 0.5% of RBCs. HA-tagged N1 peptide was added either before the RBC incubation, during the RBC incubation, or during the 37°C incubation used to initiate fusion. The F protein was then immunoprecipitated using the HA tag specific antibody 12CA5. Only a significant amount of F was immunoprecipitated when the N1-HAt peptide was added with RBCs or during the 37°C incubation when the open-stalk intermediate has formed. (B) Immunoprecipitation of the open-stalk intermediate for F mutants L486A and I488A. HeLa CD4 LTR β gal cells expressing HN and wt F, F L486A, or F I488A were metabolically labeled with 400 μ Ci of 35 S-Promix. Lane 1: wt F plus N1-HAt peptide with no antibody added. Lanes 2, 4, 6: HN and wt F, L486A, or I488A expressing cells were incubated with 0.5% of RBCs at 4°C in the absence of N1-HAt peptide and were immunoprecipitated using PAb vac F (represents total F). Lanes 3, 5, 7: the N1-HAt peptide was added during the RBC incubation at 4°C. The F protein was co-immunoprecipitated with MAb 12CA5. The polypeptides were analyzed by SDS-PAGE under non-reducing conditions on 15% acrylamide gels. (C) Quantification of RBC binding for HN only or HN plus wt F, F L486A, and F I488A expressing CV-1 cells. CV-1 cells labeled with SYTO 17 were incubated with RBCs labeled with 6-CF for 1h at 4°C. C1 peptide was also added to some samples expressing wt F, F L486A, and F I488A during the 37°C incubation for 15 min to capture the pre-hairpin intermediate. Black bars represent number of RBCs bound at 4°C, and white bars represent the number of RBCs bound after the 15 min 37°C incubation. Means and error bars shown are from three microscopic fields. (D) The conformation of wt F, F L486A, F L486I, F I488A, and F I488L mutant F on the surface of cells. This was determined by reactivity with postfusion specific MAb 6-7 at 4°C, 40°C, 43°C, 47°C, or 50°C. HeLa CD4 LTR β gal cells expressing wt F, F L486A, F L486I, F I488A, or F I488L F protein were heated to 4°C, 40°C, 43°C, 47°C, or 50°C for 10 min before binding MAb 6-7 at 4°C for 30 min. Antibody reactivity was measured by flow cytometry. All data is normalized to wt F at 4°C.



warmed to 37°C, the majority of RBCs either fuse or are released due to the neuraminidase activity of HN that is active at 37°C but not at 4°C (116, 125). In the presence of C1 peptide the F protein forms the pre-hairpin intermediate and the RBCs remain bound to the CV-1 cells because the fusion peptide has inserted into the RBC membrane but further refolding is blocked and fusion is inhibited (125). Addition of C1 peptide did not affect the number of RBCs bound at 4°C (Fig. 3-3C). However, when cells expressing F TM domain mutants L486A and I488A with bound RBCs were warmed to 37°C in the absence of C1 peptide, there was a near complete loss of bound RBCs, suggesting that these mutants are not trapped at the pre-hairpin intermediate

(Fig. 3-3C). To determine if these mutants reached the pre-hairpin intermediate or are unable to transition between the open-stalk conformation and the pre-hairpin intermediate, 40 μ M C1 peptide was added. At 37°C there was an increase in the number of RBCs retained compared to L486A and I488A at 37°C without the addition of peptide, although the number was not as large as for wt F (Fig. 3-3D). Nonetheless the data do suggest these F TM domain mutants do form the pre-hairpin intermediate.

F TM domain mutants 486 and 488 mutants have the same or a closely related conformation as wt F protein that is independent of their ability to cause fusion

MAB 6-7 only recognizes the postfusion conformation of the F protein and not the prefusion conformation of the F protein (24, 111, 125). Thus, MAB 6-7 can be used to determine if F TM mutants L486A and I488A undergo the F protein refolding event that accompanies membrane fusion. It was found that although F TM domain mutants L486A and I488A cause greatly decreased fusion as compared to wt F and TM domain mutants L486I and I488L, all five of these F proteins exhibited the same MAB 6-7 reactivity at 4°C, 40°C, 43°C, 47°C, and 50°C as determined by flow cytometry, supporting the notion that the F protein TM domain mutants can proceed through the known intermediates of fusion and that they have a conformation closely related to postfusion F, even though L486A and L488A are essentially fusion inactive (Fig. 3-3D).

The addition of a hyperfusogenic mutation can rescue fusion for F TM mutants L486A and I488A

It has been shown previously that a mutant of the W3A isolate of PIV5, S443P, demonstrates a lower temperature requirement for fusion activation, faster fusion kinetics, and independence of HN activation (111). Because for F S443P extensive syncytia formation occurs at room temperature in the absence of HN co-expression, F S443P and related mutants (126) have been termed hyperfusogenic. It is thought that F mutation S443P destabilizes the interactions between the top of the HRB three-helix bundle and the linker to the IgG-like Domain II (155) hence lowering the energy barrier for conversion to the open stalk conformation. Two other hyperfusogenic mutants that lower the temperature requirement for fusion and enable HN-independent fusion are Gly to Ala mutations in the fusion peptide G105A (previously referred to as G3A) and G109A (G7A) (57, 124). Both mutations are highly destabilizing: the G109A not only destabilizes the F protein on cell surface expression but also inactivates the F protein relatively quickly and inactivates F for fusion if target cells are not present (124).

It seemed possible that if F TM domain mutants are blocked in causing fusion at a stage beyond the pre-hairpin intermediate then incorporation of a hyperfusogenic mutation into the TM domain mutants might overcome the fusion block, probably due to the increased kinetics of fusion that is thought to be caused by triggering a greater number of F trimers at any one time. The L486A and I488A mutations were introduced into three hyperfusogenic backgrounds, S443P, G105A, and G109A F, to create the double mutants S443P/L486A, S443P/I488A, G105A/L486A, G105A/I488A, G109A/L486A, and G109A/I488A (Fig. 3-4). The F double

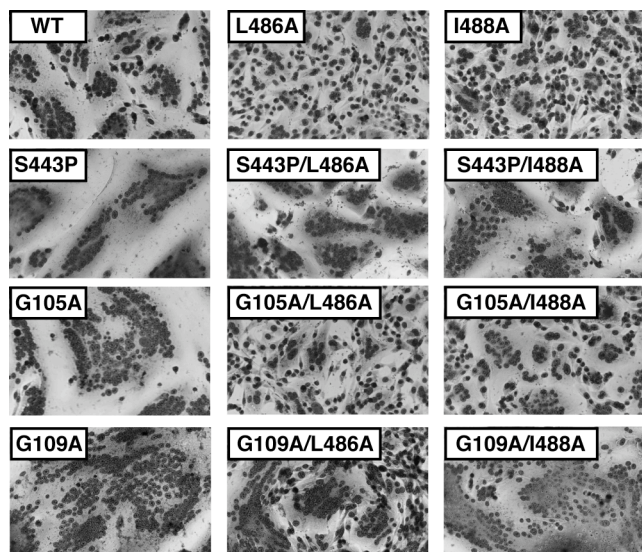


Figure 3-4. Syncytia formation mediated by F mutants L486A and I488A containing a second destabilizing mutation.

Representative micrographs of syncytia formed in BHK-21F cells 20 h p.t. Cells were co-transfected with pCAGGS HN DNA and pCAGGS DNA encoding wt F, F L486A, or F I488A, the hyperfusogenic mutants F S443P, F G105A, or F G109A, or the double mutants containing a hyperfusogenic mutation and also F L486A or F I488A.

mutants were expressed in HeLa CD4 LTR β gal cells and cell surface abundance determined by flow cytometry. S443P/L486A, S443P/I488A, G105A/L486A and G105A/I488A were surface expressed similarly to wt F whereas the surface expression of G109A, G109A/L486A, and G109A/I488A was only 10% of wt F (Table 3-1). Expression in BHK-21F cells showed that F mutants S443P/L486A, S443P/I488A, G109A/L486A, and G109A/I488A exhibited extensive syncytia formation (hyperfusogenic) and syncytia formation was independent of HN expression (data not shown). F G105A/L486A and F G105A/I488A showed higher levels of syncytia formation than F L486A and F I488A but less F G109A protein consistent with earlier data for F mutant G105A (124). Thus, whereas F TM mutants L486A and I488A cannot cause fusion, the addition of the hyperfusogenic mutants to create double mutants lowers the energy barrier to fusion and overcoming the block to fusion caused by the L486A and I488A mutations. These data indicate that the F TM domain mutations L486A and I488A have not caused the F proteins to convert to an inactive “spent” conformation and the F TM mutant proteins have not veered off the fusion pathway. It may be that increasing the number of active

F molecules increases the probability of a successful fusion event as compare to wt – perhaps the membrane state and the number of active F molecules are parameters that interact in a manner unknown to determine a successful outcome. Alternatively, the “lifetime” of the prehairpin intermediate may be different between mutant and wt, and the presence of a greater number of active F molecules could enhance the probability of successful fusion. This second explanation is also consistent with the peptide-pulldown results.

Changing the curvature of the membrane rescues fusion of F TM domain mutants L486A and I488A

In addition to the F protein conformational intermediates of fusion, the changes occurring in the lipid bilayers can be broken down into several intermediates. It is thought that formation of the F protein 6HB brings the membranes of the virus and the target cell together (4, 125) and exclusion of water molecules permits formation of the hemifusion stalk. This stalk is an initial lipid connection between the proximal membrane leaflets (18). The stalk then expands to form the hemifusion diaphragm, which is a single bilayer segment, before the fusion pore forms (18). Lipids can affect membrane fusion based on their molecular shape. The cone shaped lipid stearyl-lysophosphatidylcholine (LPC) has a positive spontaneous curvature, which is predicted to hinder the transition to hemifusion when present in the outer bilayer. The cone shaped lipid oleic acid (OA) has a negative spontaneous curvature, which favors hemifusion when present in the outer bilayer (19). The addition of LPC and OA to cells expressing HN and F proteins has been shown previously to inhibit and favor an increase in fusion, respectively (125). To examine whether addition of cone shaped lipids would overcome the block in fusion of F TM domain

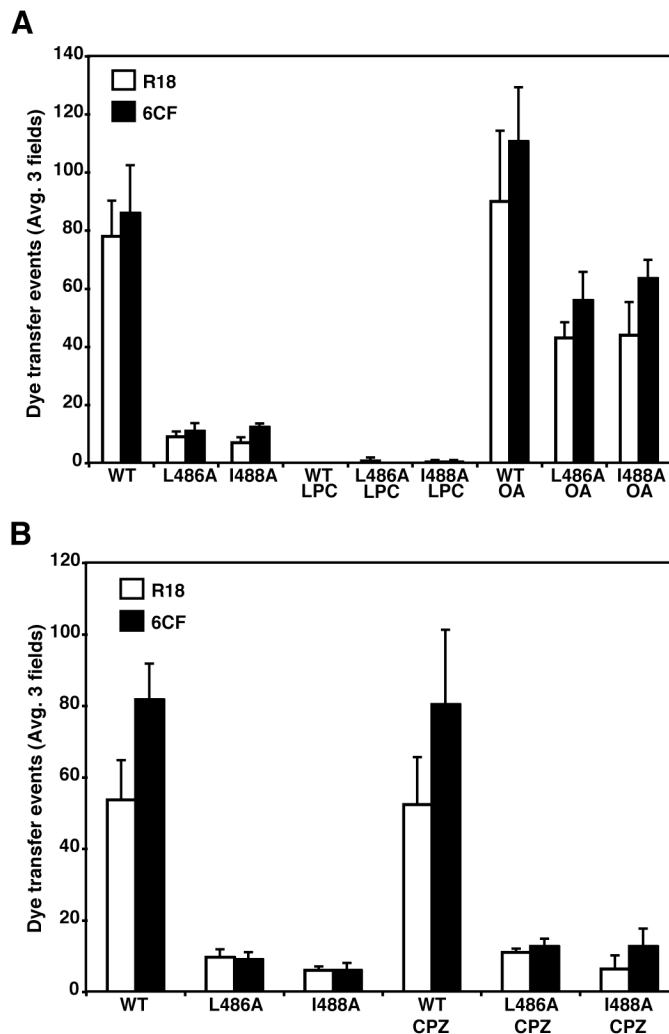


Figure 3-5. Altering the curvature of the lipid membrane can rescue fusion for the F L486A and I488A mutants.

(A) Quantification of cell-cell fusion in the dye transfer assay. Effector CV-1 cells were infected with vaccinia virus vTF7-3 and transfected with HN and wt F or mutant F DNA. RBCs were dually labeled with R18 (open bars) and the 6-CF (black bars). Labeled RBCs were bound to CV-1 cells for 1 h at 4°C and then incubated at 37°C for 15 min before visualization by confocal microscopy. Prior to incubation at 37°C, 10 μM LPC or 10 μM OA was added for 15 min at 4°C. 10 μM LPC or 10 μM OA was also present when the temperature was raised to 37°C. The means and error bars are from three microscopic fields. (B) Quantification of dye transfer with dually labeled RBCs as above, but with 0.5 mM CPZ was added for 1 min at room temperature and then washed out prior raising the temperature to 37°C to trigger fusion.

mutants LPC was added to CV-1 cells expressing

HN and wt F, F L486A, or F I488A prior to and during binding of R18- and 6-CF-labeled RBCs at 4°C. On warming to 37°C neither lipid mixing (R18 transfer) nor cytoplasmic content mixing (6-CF transfer) occurred between the RBCs and the CV-1 effector cells (Fig. 3-5A). In contrast, addition of OA to the effector cells not only increased wt F fusion, but also caused a significant increase in lipid and contents fusion for F TM mutants L486A and I488A (Fig. 3-5A).

Chlorpromazine (CPZ) a drug that causes positive curvature of the lipid bilayer, ruptures the

hemifusion diaphragm and causes pore formation (19). The addition of CPZ to effector cells did not cause an increase in lipid or contents fusion for F TM domain mutants L486A or I488A (Fig. 3-5B). Thus, these data suggest that the block in fusion of F TM domain mutants L486A and I488A occurs during the lipid intermediate stages of fusion rather than the F protein intermediate stages of fusion. It is not known at which stage of the lipid intermediates the F protein attains its final postfusion form, although it is usually considered that refolding of the pre-hairpin intermediate to the postfusion form occurs across the stages of the lipid intermediates. The augmenting of fusion by OA that confers negative curvature to the membrane suggests that the F TM domain mutants are delayed/arrested at the lipid stalk intermediate and do not reach the hemifusion diaphragm or fusion pore stages of fusion.

Evidence that the hydrophobicity of the side chains of F TM domain residues 486 and 488 controls fusion activity

Further substitutions were made at F TM domain residues 486 and 488 to test the notion that the hydrophobicity of the amino acid side chain may affect fusion activity. L486 and I488 were each substituted with I/L, V, F, C, A, G, T, W, Y (Fig. 3-6) and the fusion activity of each of the mutants expressed in Vero cells was determined using a luciferase gene reporter assay. Fusion activity was severely decreased (less than 50% of wt F) for residue 486 or 488 substitutions A, G, T, W, and Y. Substitution for C yielded ~80% fusion, and substitutions for I/L, V, and F showed no difference in fusion activity as compared to wt F protein (Fig. 3-6A). When the fusion activity was plotted against the hydrophobicity index of each residue (66), those amino

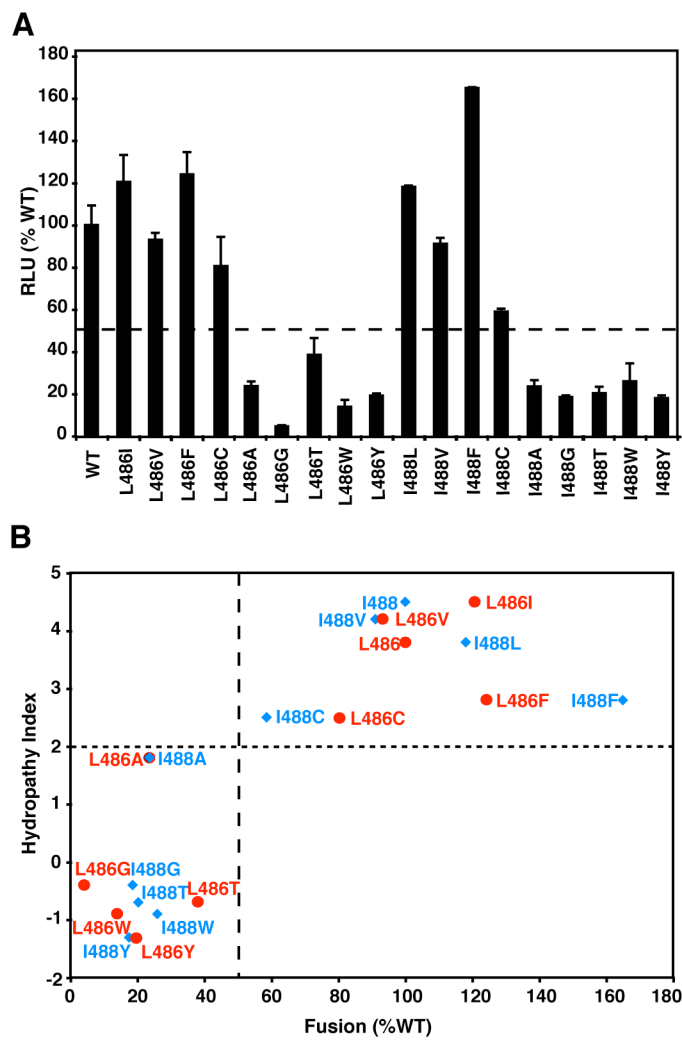


Figure 3-6. Fusion activity of F proteins depends on the hydrophobicity of substituted residues at TM residues L486 and I488.

(A) Cell-cell fusion of substitutions made at residues 486 and 488 were quantified using the luciferase reporter gene assay. Vero cells were cotransfected to express HN, and wt F or mutant F proteins, and a luciferase reporter construct. At 16 h p.t. BSR T7/5 cells were overlaid on the Vero cells, and 6 h post overlay, the luciferase activity of each sampled was read. Dashed line indicates 50% of wt F fusion. Shown is the average of three experiments each done in triplicate and normalized to wt F. (B) Plot of fusion from (A) versus the Kyte and Doolittle hydrophathy index for each substituted residue. Substitutions at 486 are shown in red and substitutions at 488 are shown in blue. Wt F is denoted as L486 or I488. Long dashed line indicates 50% of wt F fusion, and short dashed line indicates hydrophathy index of substitutions producing less than 50% of F fusion. All substitutions in lower left quadrant are deficient in fusion.

acid residues with a hydrophobicity index below 2

(A, G, T, W and Y) show decreased fusion

whereas those amino acid residues with a higher hydrophobicity index exhibited wt F protein

fusion activity (Fig. 3-6B). Thus, the correlation of fusion activity and the hydrophobicity of the

amino acid side chain of residues 486 and 488 suggest that when the hydrophobicity of the side

chain for these residues decreases, fusion becomes arrested at the lipid stalk intermediate.

The F protein TM domains are in close proximity and likely form a three-helix bundle

The TM domain is not part of the solved crystal structure of either the prefusion form of PIV5 F (155) or the postfusion form of hPIV3 F (154). Although it is thought likely that the TM domain of F would be α -helical because the hydrophobic packing of an α -helix would aid in spanning a lipid bilayer, this has not been determined. It is also unknown if the TM domains of the PIV5 F monomer interact to form a trimer. It has been shown recently that TM peptides of influenza virus HA tightly associate with each other in a lipid-free system (13). In prefusion F, HRB forms a three helix bundle (3HB) and HRB is separated from the TM domain by only seven residues. Therefore, it seems likely that the F TM domains monomers would be in close proximity in the membrane if not in a 3HB. To understand better the role that F TM domain residues 486 and 488 play in fusion, it would be useful to know how the side chains of these residues are ordered within the TM domain structure. We used oxidative disulfide cross-linking to examine the structure of the F TM domain. This method has been used to investigate the arrangement of TM domains for several membrane proteins, such as the *Escherichia coli* chemoreceptor (73-75), the aspartate receptor (37), the influenza virus M2 ion channel (6), and CD39 (45, 46).

The PIV5 F protein contains 10 disulfide-bonded cysteine residues in the ectodomain and one free cysteine residue in the TM domain. This latter cysteine at residue 492 was mutated to serine, and single cysteine substitutions were made in the TM domain in this pseudo-wt cys-background. All mutants in the cys- background were expressed at the cell surface equivalently to pseudo wt F (data not shown). The fusion activity of these mutants was determined by using

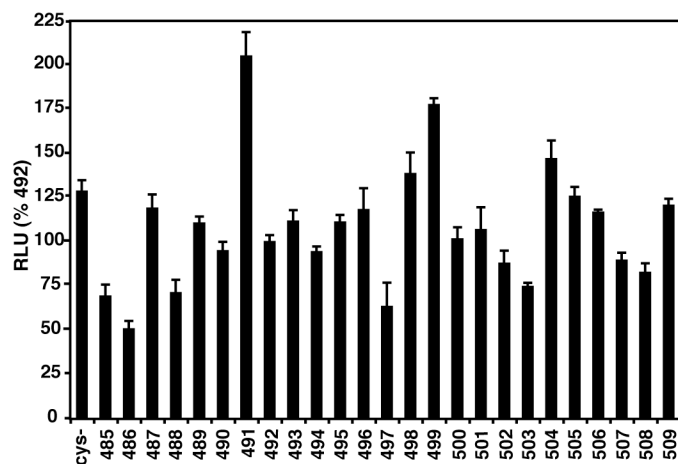


Figure 3-7. Fusion activity of F TM domain cysteine substitution mutants.

Each residue of the F protein TM domain was substituted with cysteine in a background in which the naturally occurring cysteine residue 492 was mutated to serine. The luciferase reporter gene assay was used to measure cell-cell fusion mediated by the single cysteine mutants in the cys-background (pseudo wt). Vero cells were cotransfected to express HN, pseudo wt F or mutant F protein, and a luciferase reporter construct. Shown is the average of three experiments each done in triplicate and normalized to pseudo wt cys- F.

the luciferase reporter gene assay (Fig. 3-7). Most mutants showed fusion activity similar to pseudo wt (cys -, C492S) and wt F protein (denoted as 492). Mutants 485, 486, 488, 497, 503 exhibited

some decrease in fusion activity but never below 50% wt activity (see Fig. 3-6). Mutations in the TM domain of influenza virus HA have been shown to affect raft association (139).

However, none of the cysteine substitutions affected raft association of the F protein (data not shown).

We examined the effect of oxidative cross-linking of these F TM domain single cysteine substitutions. For each mutant, there are three available cysteines in each trimer. If these cysteines are oriented toward each other in the membrane and are within disulfide bond-forming distance, two will form a disulfide bond and leave the third cysteine unbonded (unless it was in very close proximity to a second trimer and then higher oligomers should be observed). In Fig. 3-8A are shown untreated F mutants analyzed under non-reducing conditions on a 3.5% SDS-

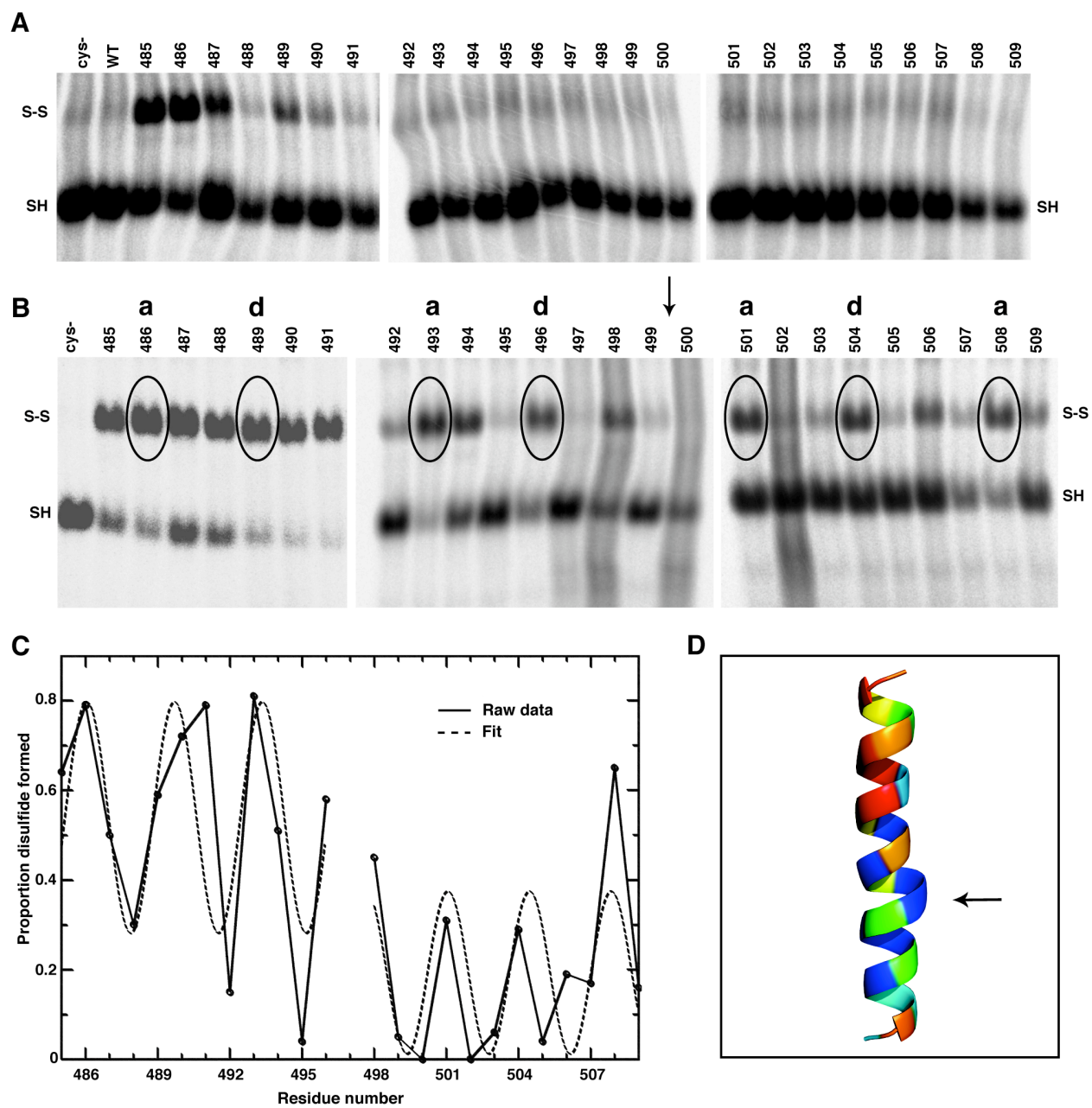
PAGE gel. The majority of the mutants do not form disulfide bonds. However, cysteine residues in the outer leaflet of the bilayer at positions 485, 486, 487, and 489 did form disulfide bonds, indicating the individual F TM domains are in close proximity to themselves. When the F TM mutants were treated with 3 mM (final concentration) of Cu(II)(1,10-phenanthroline)₃ (CuP) for 10 min at 37°C, more extensive disulfide cross-linking was observed (Fig. 3-8B). F TM mutants 485-491, 493, 494, 496, 498, 501, 504, 506, and 508 all showed disulfide bond formation. As some of these residues in the outer leaflet of the bilayers map to all faces of a potential α -helix and under the conditions used disulfide bond formation is essentially irreversible, it is likely there is rotational movement of the TM domain membrane. Interestingly, the native cysteine at 492 showed very little disulfide bond formation, indicating not every residue of the TM domain rotates within the membrane. 3 mM CuP was also added at 4°C, 10°C, and 22°C for 10 min (data not shown). All residues near the ectodomain (485-491, 493, 494) formed disulfide bonds at all temperatures, even 4°C. Mutants that formed disulfide bonds after treatment with 3 mM CuP for 10 min at 37°C also formed disulfide bonds when 3 mM CuP treatment was for 1 or 5 min (data not shown). The affect of cross-linking on fusion could not be determined due to the toxicity of the CuP on live cells that were necessary for the fusion assays (data not shown).

The presumed rotation of the F TM domain within the membrane and multiple disulfide cross-links required quantification of the extent of disulfide cross-linking to examine for evidence of a helical periodicity within the F TM domain. The raw CuP cross-linking data was normalized by dividing the amount of disulfide formed by the total amount of protein (disulfide linked plus not

linked). Because cross-linking was stronger in the outer leaflet of the bilayer, the 4°C CuP data was used for residue positions 485-491 to keep cross linking of the two regions on the same scale (and to maintain linearity of the image plate response to radioactivity). The CuP data at 37°C was used for the remaining residue positions 492-509. A sine wave was fit to the normalized data. This type of approach was previously used to model the structure of the TM domain of the influenza virus M2 protein (114). An initial fit of the F TM domain data was poor ($r = 0.4$), particularly at F TM residue G497. Given the unusual characteristics of glycine residues and their propensity to cause helix distortions, this residue 497 was removed from the calculation and separate fits made to the data before and after this residue. Improved fits were found after this modification ($r = 0.72$ for positions 485-496, $r = 0.68$ for positions 498-509) (Fig. 3-8C). These results point to a TM helical interface with *a* positions at residues 486, 493, 501, and 508 and *d* positions at residues 489, 496, and 504 with a helical distortion between residues 497 and 500 (Fig. 3-6B). To model a structure of a homotrimeric helix interface, existing TM protein database structures were searched for helix interactions that place the highest cross-linking data at the interface. Matching interfaces contained a common feature: a pi bulge near the position equivalent to G497. Because the cross-linking data point to interfaces at both ends of the helix, a straight helix that contains a pi bulge at the position equivalent to G497 was selected as a model for the F TM helix. The helix was found in the Na-dependent aspartate transporter structure (pdb 2nwl, 2.96 Å, (8)). To visualize the cross-linking data, the modeled F TM domain helix was colored by the normalized cross-linking data (Fig. 3-6D). Blue positions demonstrate the least cross-linking, while red positions demonstrate the most cross-linking. The pi bulge allows both the interfaces above and below the bulge to occur on the same face of the helix.

Figure 3-8. F protein TM domain cysteine substitution and disulfide bond formation on oxidation.

(A) F protein TM domain cysteine mutants in a pseudo wt background (cys-, C492S) were expressed in HeLa CD4 LTR β gal cells, and 18 h p.t. cells were labeled with 50 μ Ci of 35 S-Promix, Dounce homogenized, solubilized, and immunoprecipitated with an anti-F2 PAb. Polypeptides were analyzed by SDS-PAGE on a 3.5% acrylamide gel under non-reducing conditions. (B) Cells were transfected and labeled as above, Dounce homogenized, and treated with 3 mM CuP for 10 min at 37°C. Samples were then solubilized, immunoprecipitated with an anti-F2 PAb, and polypeptides analyzed by SDS-PAGE on a 3.5% acrylamide gel under non-reducing conditions. Circled residues indicates *a* and *d* residues in the predicted helix. Arrow indicates the break in the predicted helix. (C) Periodicity of the predicted TM domain helix. The raw CuP cross-linking data in (B) was normalized by dividing the amount of disulfide formed by the total amount of protein. Also shown is the sine wave fit of the data. The data obtained with oxidation occurring at 4°C was used for residue positions 485-491, and the data obtained with oxidation occurring at 37°C data was used for the remaining positions (492-509). This was done to maintain the signal on the image plate used to detect radioactivity within the linear range. (D) The predicted structure of the TM domain helix. Based on the cross-linking data, the TM domain is predicted to form a helix with a pi bulge at residues 497-500 (arrow). Blue indicates less cross-linking and red indicates more cross-linking.



DISCUSSION

For ion channel proteins that have multiple TM spanning domains, atomic structure determinations have enabled a distinction between those TM α -helices that serve architectural structural roles and those that act as the aqueous pore/ionic selectivity filter (145). For the homotetrameric influenza virus M2 proton-selective ion channel protein each polypeptide chain only spans the membrane once and the single hydrophobic domain found in each polypeptide chain has to act as the endoplasmic reticulum membrane insertion sequence, the membrane anchoring sequence and the pore and gate of the channel (6, 71, 114, 130, 138). However, for the majority of integral membrane proteins that span a membrane once, the role of the TM domain besides being a membrane anchorage domain is largely unknown.

For many viral proteins that mediate membrane fusion mutagenesis studies on the TM domain have yield a wide variety of results. However, the preponderance of data indicates that the TM domain of these fusion proteins is not simply a string of hydrophobic amino acids that spans a lipid bilayer but there is amino acid sequence specificity to the TM domain, implying specific roles of TM domain amino acid residues in fusion protein function. Specificity of amino acid residue implies specific structural features or interactions of these TM domain residues with the lipid bilayers and thus a direct role of amino acid side chains in the process of membrane fusion, and further implying that membrane fusion is not simply a solely lipidic event.

Studies with viral membrane fusion proteins such as influenza virus hemagglutinin (HA), baculovirus gp64, VSV G protein and HIV Env glycoprotein have indicated that switching TM domains among various viral fusion proteins or making point mutants can yield, but not always, non-functional fusion proteins (21, 82, 89, 92, 94, 103). Of considerable interest has been the role of glycine residues in the TM domain, particularly in the motif GXXXG, as it has been suggested that such glycine residues may allow deformation of the TM domain and thus a glycine “hinge” has been proposed to destabilize the lipid intermediates and allow fusion pore formation. Mutagenesis of the glycine residues for VSV G severely reduced fusion activity (21), whereas for other viral fusion proteins mutagenesis of the glycine residues have no effect on biological activity e.g. HA (2), HIV Env (94) and PIV5 F (M.L.B and R.A.L. unpublished observations).

Removal of the HA TM domain and substitution with a glycosylphosphatidyinositol (GPI) membrane anchor than spans only the outer leaflet of the lipid bilayers permitted hemifusion but not pore formation and aqueous content mixing (64, 92). Thus, these data suggest the TM residues play an important role in pore formation. The length of the amino acids comprising the HA TM domain is also important for fusion (2) and it is known that the specific residues in the HA TM domain that reside in the outer leaflet of the bilayers are required for the association of HA with cholesterol/sphingomyelin rich lipid microdomains (the viral budzone) required for influenza virus budding from the plasma membrane (129, 139).

To study the features of the paramyxovirus PIV5 F protein TM domain for membrane fusion activity alanine-scanning mutagenesis was used rather than the construction of chimeric molecules. The F protein TM domain was found to exhibit sequence dependence for fusion activity as a block of 20 leucine residues could not substitute for the entire PIV5 F TM domain. Upon further substitution, residues L486 and I488 were found to play a key role in fusion, where altering the hydrophobicity of the side chain at these residues profoundly affected fusion activity (Fig. 3-6). Although F mutants L486A and I488A were deficient for fusion, biological activity could be rescued by the addition of the destabilizing mutations F S443P, F G105A, or F G109A (Fig. 3-4), indicating F L486A and I488A were not trapped in an intermediate conformation nor had the mutant F proteins veered irreversibly off the fusion pathway. It is generally thought that F-mediated membrane fusion requires the action of several trimers and the hyperfusion phenotype of destabilizing mutants may be due to more synchronous F activation events in an otherwise stochastic process. Thus, addition of a destabilizing mutation to F proteins that are trapped for fusion may simply decrease the lifetime of the trapped intermediates, driving the fusion process by mass action. Detailed analysis indicated F L486A and F I488A form the prefusion conformation of F, the open-stalk intermediate, the pre-hairpin intermediate, and F can be converted to a conformation that is close to, or at the post-fusion form (Fig. 3-9 A-D). As discussed above, the precise timing of the conversion of the pre-hairpin conformation to the postfusion form with the formation of the lipid intermediates is not known, but refolding of F may occur across all the lipid intermediate stages. Evidence from studies of HIV gp120/gp41 suggest some 6HB formation occurs after a pore has formed (85, 91).

Thus, it seemed likely that the block in fusion would for the F L486A and F I488A proteins corresponds to their inability to complete the lipidic stages of fusion (Fig. 3-9 C-D). The data obtained using OA to confer negative spontaneous curvature of the membrane and concomitantly causing a large increase in fusion activity of F L486A and F I488A indicates that fusion is delayed/arrested at the lipid stalk intermediate (Fig. 3-9 C-D).

Our studies and those of others suggest that the TM domain is involved in the lipidic steps in fusion, including pore formation (64, 89, 90, 92). In fusion, the formation of the 6HB and the postfusion form of F brings together the TM domain and the FP, which excludes water between the membranes, and this local dehydration allows for membrane contact (20). There is a high-energy requirement for the presumptive next stage, the lipid stalk (151). The energy necessary to form the lipid stalk may be derived from the fusion protein, which may generate bilayer stresses that are relaxed by forming the stalk intermediate (20). For PIV5 F protein, the outer leaflet residues L486 and I488 may facilitate the negative curvature of the outer lipid leaflet that is necessary to merge the two bilayers, and residues with higher hydrophobicity may provide a more negative curvature (Fig. 3-9 C-D). However, in the case of influenza virus HA, the atomic structure of the FP in the membrane is not compatible with bending bilayers toward a more negative curvature (140). Instead it has been proposed that the FP and TM domain of HA promote lipid flipping between bilayers, which facilitates formation of the fusion pore (140, 141).

The available atomic structures of ion channel proteins indicate that the multiple TM domains are mostly α -helical (145) and for the very few known viral proteins, the structures of the TM domains of integral membrane proteins are α -helical (130, 138, 159). Even less is known as to whether the TM α -helices are together in the membrane forming helical bundles or whether each α -helix is separate from the others. Clearly for the influenza virus M2 ion channel the TM domains form a four-helix bundle (130, 138). CryoEM studies on the human immunodeficiency virus fusion protein (Env) differ as some reports indicate the TM domains of the fusion protein are apart, like the legs of a tripod (39, 161), whereas other studies indicate the TM domains are together and form one helical bundle (157).

The substitution of F TM domain residues with cysteine and cross-linking on oxidation with CuP indicates the TM domains in the F trimer are in close proximity. Further, the quite extensive cross-linking of residues in the outer leaflet of the bilayer suggests some rotational flexibility in the TM domain (Fig. 3-8B). Because higher order oligomeric structures with gel mobilities consistent with hexamers were found in very low abundance (data not shown), the disulfide bond formation observed is thought to be inter-subunit within an F trimer. Quantification of the extent of disulfide bond formation and modeling studies indicate that the data fit best a model in which the F TM domain forms a 3HB within the membrane with a pi bulge at residues 497-500 (Fig. 3-8 B-D). The PIV5 TM domain contains glycines at residues 494 and 497 (GXXG), but as discussed above substituting both these glycines with alanine does not affect fusion activity and a glycine hinge architecture does not fit the available data. Residue L486 when plotted on a helical wheel is predicted to be at an *a* position within the 3HB even though the fusion data

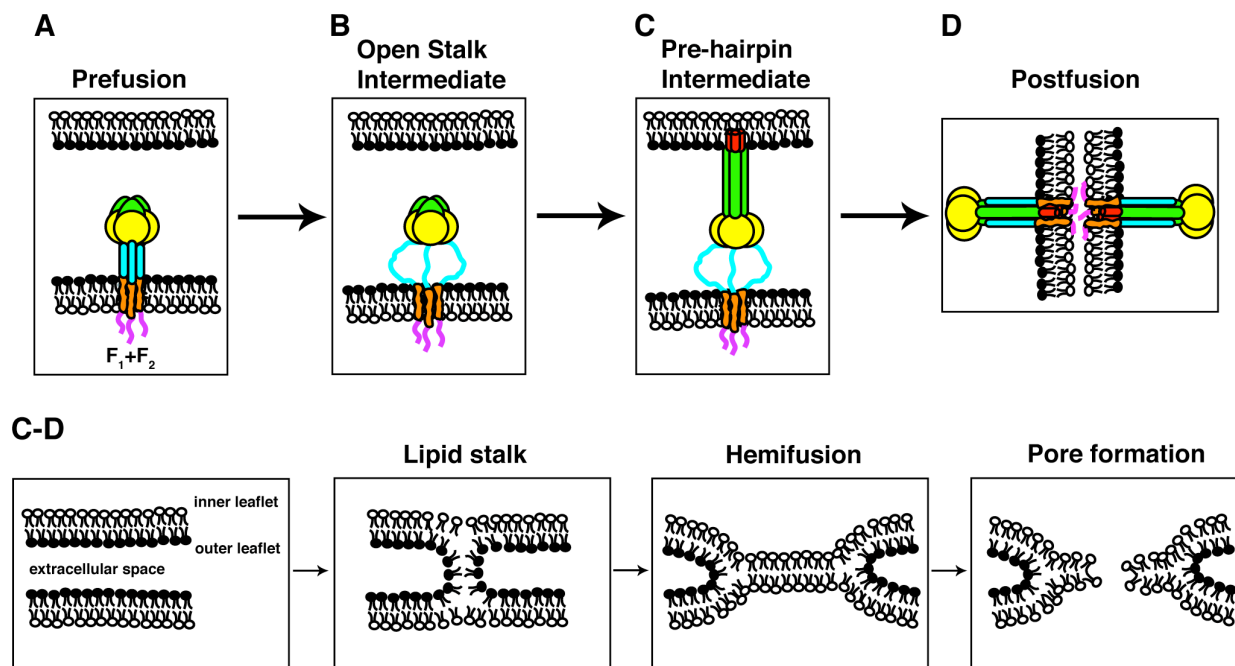


Figure 3-9. Model of membrane fusion for F TM domain mutants L486A and I488A.

(A) The prefusion form of F contains a globular head with the HRA region in 11 distinct sections and the HRB region is in a three-helix bundle. The F TM domain is also represented as a three-helix bundle, consistent with the oxidative cross-linking data. (B) Upon HN binding to target cells, F is activated for fusion, and the HRB region separates, forming the open-stalk conformation where N1 peptide can bind to HRB. At this open-stalk stage, the TM domain is still thought to be in a three-helix bundle because N1-HAT can still bind to HRB after the addition of the oxidative-crosslinker. (C) After formation of the open-stalk conformation, HRA rearranges to form the extended α -helical bundle, and the FP is inserted into the target cell membrane (the pre-hairpin intermediate). Although the mutant F proteins L486A and I488A do not cause fusion, the available data suggests the mutants do refold to some extent from the pre-hairpin intermediate. HN is not shown for clarity. (C-D) Lipid intermediates in fusion with the F protein removed for clarity. The two bilayers contain an inner and outer leaflet and are separated by the extracellular space. During the process of F refolding to form the postfusion form, water is excluded from the extracellular space and the outer leaflets initially merge to form the lipid stalk intermediate. The available data suggests L486A and I488A are likely blocked for fusion at this intermediate. The lipids of the bilayers mix, forming the hemifusion intermediate, and then the fusion pore forms. F domains: FP (red), HRA (green), globular head (yellow), HRB (blue), TM domain (orange), cytoplasmic tail (pink).

indicate this residue is likely to interact with the lipids of the bilayer. Presumably, the rotational mobility that enables the residues close to the ectodomain to form disulfide bonds also enables residue L486 to face the interior of the predicted 3HB but also interact with the lipid bilayer.

It is possible that as the last stage in the F protein refolding event the TM domain interacts with the FP and forms another 6HB. The process of converting prehairpin F to the postfusion form of F may provide the necessary energy to exclude the water between the membranes and form the lipid intermediates (Fig. 3-9 C-D). At the first stage of fusion, the outer leaflets of the two bilayers have just merged but have not mixed (hemifusion). The TM domain and FP may still be segregated in separate bilayers, and the interaction between the TM domain and FP could drive the formation of the hemifusion intermediate. Hyperfusogenic mutants G105A and G109A are located within the FP. These two mutants rescue fusion of L486A and I488A (Fig. 3-4).

Although hypothesized previously that these destabilizing mutants G105A and G109A may cause hyperfusion by lowering the energy necessary to drive the various fusion intermediates (124) it is also possible that these FP mutants affect the potential interaction with the TM domain and destabilize and lower the energy requirement to mix the bilayers and drive the hemifusion intermediate and form the fusion pore (Fig. 9C-D).

MATERIALS AND METHODS

Cells, virus, and plasmids. BHK-21F, Vero, BSR T7/5, CV-1, and HeLa CD4 LTR β gal cells were grown in Dulbecco's modified Eagle's Medium (DMEM) supplemented with 10% fetal bovine serum (FBS). BHK-21F cells were grown in DMEM supplemented with 10% tryptose phosphate broth, and HeLa CD4 LTR β gal cells were grown in DMEM supplemented with 200 β g/ml geneticin, 100 μ g/ml hygromycin B, and 20 mM HEPES pH 7.4. The recombinant vaccinia virus (vTF7-3) that expresses T7 RNA polymerase was grown in CV-1 cells as described previously (40). pCAGGS and pGEM2X plasmids encoding PIV5 F, PIV5 HN, and PIV5 S443P F have been described previously (111). pCAGGS plasmids encoding PIV5 G105A and G107A F have also been previously described (57, 124). PIV5 F proteins containing TM domain amino acid residue substitutions were made by four-primer PCR with *Tgo* DNA polymerase and then by cloning into pCAGGS PIV5 F and pGEM2X PIV5 F. Plasmids encoding the double substitutions were made by subcloning pCAGGS L486A and I488A F into pCAGGS plasmids encoding S443P, G105A, or G107A F. Mutations were confirmed by nucleotide sequencing using an Applied Biosystems 3100-Avant automated DNA sequencer.

Expression of F and HN glycoproteins. PIV5 F and HN cDNAs cloned in the pCAGGS vector were expressed in BHK-21F, Vero, and HeLa CD4 LTR β gal cells by transient transfection using the Lipofectamine Plus expression system (Invitrogen, Carlsbad, CA) according to the manufacturer's protocol. Transfected Vero cells were incubated for 4 h at 37°C (23) before the addition of DMEM containing 2% FBS and incubated a further 18 h at 37°C. PIV5 F and HN

cDNAs in the pGEM2X vector were expressed using the recombinant vaccinia virus-T7 RNA polymerase transient expression system (vac T7) (40). CV-1 cells in 6-well dishes containing glass coverslides were infected at a multiplicity of infection (MOI) of 10 plaque forming units (pfu) of with vTF7-3 for 1 h at 37°C. The cells were then transfected with 1.0 µg each of pGEM2X F and HN DNA using liposomes prepared as previously described (123). After 4 h at 37°C, DMEM with 10% FBS was added and cells were incubated at 33°C overnight.

Syncytia formation. Monolayers of BHK-21F cells in 6-well plates were transfected with 1.0 µg each of pCAGGS PIV5 F and HN DNA as described above. At 20 h post-transfection (p.t.), cells were fixed and stained using a Hema 3 stain (Fisher Scientific, Pittsburgh, PA) according to manufacturer's instructions, and photographs were taken using a with a digital camera (DCS 760, Kodak, Rochester, NY) attached to an inverted phase-contrast microscope (Diaphot, Nikon, Melville, NY).

Luciferase reporter gene assay. To quantify cell-cell fusion, a luciferase reporter gene assay was performed as previously described (126). Briefly, Vero cell monolayers in 6-well plates were transfected with 1.0 µg each of three plasmids, luciferase control DNA expressing the T7 promoter (Promega, Madison, WI), pCAGGS PIV5 F, and pCAGGS PIV HN. At 16 h p.t., BSR T7/5 cells expressing the T7 RNA polymerase were overlaid onto the Vero cells and incubated at 37°C for 6 h. The monolayers were then washed, lysed, and clarified by centrifugation per the manufacturer's instructions (Promega). For each sample, 150 µl of lysate was loaded into a 96-well plate. The luciferase activity of each lysate was quantified using 150 µl luciferase assay

substrate (Promega) and an Lmax luminescence microplate reader (Molecular Devices, Sunnyvale, CA).

Dye transfer assays. Human red blood cells (RBCs) were singly labeled with the aqueous dye 6-carboxyfluorescein (CF, Invitrogen) or dual labeled with 6-CF and the lipid probe octadecyl rhodamine B chloride (R18, Invitrogen). CV-1 cells grown on glass cover slides and F and HN expressed using the vac T7 expression system. To visualize effector cells when using singly labeled RBCs, CV-1 cells were labeled with 1 μ M SYTO-17 nucleic acid dye (Invitrogen) for 1 h at 37°C. Analysis of lipid and aqueous dye transfer was performed as previously described (126). Fusion was quantified by counting positive cells by using a scanning confocal microscopy (LSM 5 Pascal, Carl Zeis MicroImaging, Inc., Thornwood, NY) and averaging the fusion events obtained from three separate fields. For HN-independent retention of RBCs, SYTO-17 CV-1 cells were incubated with 0.1% hematocrit 6-CF labeled RBCs. Following incubation with RBCs, cells were either incubated at 4°C or 37°C for 15 min. During this warming stage, 40 μ M C1 peptide was added to some of the samples. C1 peptide was expressed in bacteria and purified as previously described (63). For the temperature dependence of dye transfer, samples were incubated at 29°C, 37°C, and 42°C for 15 min after the binding of target RBCs. For dye transfer experiments using the addition of lipids, fresh solutions of 10 μ M lysophosphatidylcholine (LPC) (Avanti Polar Lipids, Birmingham, AL) or 10 μ M oleic acid (OA) (Sigma-Aldrich, St. Louis, MO) in PBS were made. After binding R18/6-CF dual labeled RBCs as above, CV-1 cells were incubated in cold LPC and OA solutions for 15 min at 4°C. The temperature was then shifted to 37°C by changing the bathing solution with new PBS

containing LPC or OA prewarmed to 37°C and plates were incubated at 37°C for 15 min as above. For dye transfer experiments with chlorpromazine (CPZ) (Sigma), cells were prepared and R18/6-CF RBCs were bound as above. After raising the temperature to 37°C for 15 min., 0.5 mM CPZ in PBS was added to the CV-1 cells for 1 min. Cells were extensively washed with PBS without drug.

Flow cytometry. To quantify cell surface expression and to determine the protein conformation of the F protein, monolayers of HeLa CD4 LTR β gal cells in 6-well plates were transfected with 1.0 μ g of pCAGGS PIV5 F DNA as described above and flow cytometry was performed as previously described using FITC-labeled secondary antibody (146). For surface expression, the monoclonal antibody (mAb) F1a (118) was used at 1:100 dilution. To examine conformational rearrangements in the F protein, mAb 6-7 (144) was used at 1:30 dilution. Prior to the addition of mAb 6-7, warmed PBS was added to the samples and the plates were incubated at 40°C, 43°C, 47°C or 50°C for 10 min and washed with cold PBS. The fluorescence intensity of 10,000 cells was measured by using a FACSCalibur flow cytometer (Becton Dickinson, Franklin Lakes, NJ).

Capture of open stalk intermediate. Monolayers of HeLa CD4 LTR β gal cells in 6 cm dishes were transfected with 2.0 μ g each of pCAGGS PIV5 F and HN DNA as described above. At 18 h p.t., cells were starved with cysteine (Cys)- and methionine (Met)-deficient DMEM for 30 min. The cells were labeled with 400 μ Ci of 35 S-Promix (GE Healthcare Bio-Sciences, Piscataway, NJ) in 1 ml of Cys- and Met-deficient DMEM for 1 h. To allow for newly synthesized F

proteins to reach the cell surface, the samples were chased with DMEM without serum for 2 h. The cells were washed with PBS and incubated with 1 ml of 0.5% hematocrit RBCs with or without 80 μ g of N1-HAt peptide for 1 h at 4°C. N1-HAt peptide was expressed in bacteria and purified as previously described (63). After washing at least five times with PBS to remove any unbound RBCs, the samples were incubated with 1 ml DMEM without serum containing 60 μ g of anti-HA monoclonal antibody 12CA5 for 3 h at 4°C. After washing another five times with PBS, the cells were lysed with cold RIPA buffer containing protease inhibitors and 50 mM iodoacetamide (109). Clarified lysates were incubated with 40 μ l protein A-Sepharose beads overnight at 4°C. The samples were washed three times with RIPA buffer containing 0.3 M NaCl, three times with RIPA buffer containing 0.15 M NaCl, once with 50 mM Tris buffer (0.25 mM EDTA, 0.15 M NaCl [pH 7.4]), and polypeptides analyzed by SDS-PAGE on 15% acrylamide gels under non-reducing conditions in the absence of dithiothreitol (DTT).

Oxidative cross-linking. Monolayers of HeLa CD4 LTR β gal cells in 6-well plates were transfected with 1.0 μ g each of pCAGGS PIV5 F and HN DNA as described above. At 18 h p.t., cells were starved with Cys- and Met-deficient DMEM for 30 min. The cells were then labeled with 50 μ Ci of 35 S-Promix (GE Healthcare Bio-Sciences) in 1 ml of Cys- and Met-deficient DMEM for 1 h. Cells were Dounce homogenized in cold RSB buffer (10 mM Tris, pH 7.4, 10 mM KCl, and 15 mM MgCl₂), and 3 mM Cu(II)(1,10-phenanthroline)₃ (final concentration, freshly made) was added for 10 min at 37°C or 4°C. The reaction was stopped with 10 mM EDTA and 10 mM *N*-ethylmaleimide (NEM) to chelate the copper and block free sulfhydryl groups. Samples were solubilized by adding 2X RIPA buffer plus 100 mM iodoacetamine and

protease inhibitors as previously described (109), and were clarified by centrifugation for 10 min at 55,000 rpm in a Beckman TLA100 rotor. Samples were incubated for 2 h at 4°C with 10 µl of rabbit polyclonal anti-F2 peptide antiserum, and then incubated with 40 µl protein A-Sepharose beads overnight at 4°C. Samples were washed with RIPA buffer as above and polypeptides analyzed by SDS-PAGE on 3.5% borate-acetate gels (41) under non-reducing conditions in the absence of DTT.

Modeling of the TM domain. To determine the periodicity of the F protein TM domain helix, the raw radioactivity values from the CuP cross-linking data were normalized by dividing the amount of disulfide formed by the total amount of protein (disulfide linked plus not linked). Cross-linking is stronger towards the outside of the membrane, therefore to prevent saturation of image plates on a Fuji Image Analyzer (Valhalla, NY) data obtained using CuP at low temperature (4°C) was used for residue positions 485-491 (towards the outside of the membrane) to put cross-linking of the two regions on the same scale. CuP data at 37°C was used for positions 492-509. Given the normalized data, a sine wave was fit according to the following formula:

$$y = a \cdot \sin((x+b) \cdot 2 \cdot \pi / c) + d$$

where x is the residue number, y is the normalized degree of cross-linking, a is the amplitude of the sine wave, b is the phase offset, c is the α -helical periodicity, and d is the y offset of the sine wave. Values were fit by non-linear regression. To visualize the cross-linking data, the helix was

colored by the normalized cross-linking data in PyMOL in place of the standard B-factor coloring. Blue positions correspond to the least cross-linking, while red positions correspond to the most cross-linking.

CHAPTER 4: DISCUSSION AND FUTURE DIRECTIONS

Enveloped viruses are the cause of numerous significant human diseases, such as mumps, measles, AIDS, Nipah encephalitis, and other encephalitic diseases, and agricultural diseases that have great impact on the economy, such as Newcastle disease and avian influenza.

Parainfluenza virus 5 (PIV5), though not a source of morbidity and mortality, can serve as model enveloped virus, and understanding the mechanism of fusion of PIV5 can provide insight into analogous mechanisms of other more pathogenic viruses. Although enveloped virus fusion proteins may vary in structure and be denoted as class I, class II, or class III, all share common fusion mechanisms. Studying the PIV5 fusion protein F can enhance understanding other fusion proteins that can lead to methods to inhibit virus infection, such as the fusion inhibitor drug Fuzeon (Enfuviride) used to treat HIV-1.

The studies presented in this work have focused on the structural elements of the PIV5 F protein that contribute to and the conformational changes in PIV5 F that occur in membrane fusion. It was shown that for the PIV5 porcine isolate SER, low pH is not the trigger for fusion.

Specifically, by lowering the pH exogenously, SER F did not induce fusion by syncytium formation or by the luciferase reporter gene assay. The endocytic pathway did not play a role in SER fusion; treatment with the inhibitor of the vacuolar-type H⁺ ATPase bafilomycin A1 (BFLA1), which blocks the lowering of pH within acidic compartments in the cell including the endosomal lumen, did not inhibit SER virus infection. Although paramyxovirus fusion is

classified as occurring at neutral pH and at the plasma cell membrane, the pneumovirus human metapneumovirus (hMPV) has been reported to be triggered by low pH (132). However, the most recent study of the pH requirement of several isolates of hMPV suggests the low pH requirement is strain specific (54).

This work also demonstrated the role of the TM domain of PIV5 F in fusion. Alanine scanning mutagenesis determined that fusion is dependent on the sequence of the TM domain, and a string of hydrophobic residues cannot substitute for the F TM domain. Single residue substitutions identified two residues in the TM domain, L486 and I488, that mediate the interaction of F protein and lipid bilayer during fusion. Specifically, the hydrophobicity of the amino acids at these residues affects lipid bilayer fusion by arresting it at the lipid stalk intermediate. The TM domain is hypothesized to be α -helical, though it has not been confirmed. It is also unknown if the TM domains of the PIV5 F monomer interact to form a trimer. By substituting each TM residue with cysteines and cross-linking with an oxidative cross-linker, the TM domains of the F monomers were determined to be in close proximity within the trimer. Quantification of the disulfide bond formation and modeling studies indicate the TM domain forms a 3HB within the membrane with a pi bulge at residues 497-500.

Many questions about the role of the PIV5 F TM domain in fusion remain. The double TM domain and FP mutant F protein data suggest there may be interplay between these two domains after the formation of the 6HB that facilitates the formation of the hemifusion diaphragm or fusion pore. The FP of PIV5 F has an alanine-coil-like sequence, suggesting the possibility of a

TM and FP coiled-coil similar to that of the 6HB (4). To determine the possibility of an interaction, the TM domain and FP have been modeled together (William DeGrado, University of Pennsylvania, unpublished observation). Modeling studies suggest residue S495 in the TM domain and residue Q120 in the FP may form key interchain interactions. Mutations in F to perturb this interaction, such as double alanine substitutions, could be examined in fusion to test this hypothesis. The ability of these mutants to form the lipid stalk, the hemifusion diaphragm, and the fusion pore for contents mixing would be tested. Interchain interactions could also be perturbed by altering the pi bulge modeled in the TM domain. To disrupt the bulge of the TM domain helices, bulky or polar residues could be substituted at residue G497. The potential interaction between the TM domain and FP could be stabilized by the oxidative cross-linking of double cysteine substitutions, one in the TM domain and one in the FP in the cys- background used previously. The oxidative agent $\text{Cu(II)(1,10-phenanthroline)}_3$ (CuP) would cause facing cysteines within disulfide bond-forming distance to form a disulfide bond between the TM domain and FP. The addition of CuP has been shown to disulfide bond many of the residues in the TM domain; however, S495 did not form disulfide bonds between monomers of the F protein trimer (Fig. 3-8B).

Questions also remain about the role of the FP in the later steps of lipid bilayer fusion. The FP in solution has been modeled (Yao Zhang, William DeGrado's lab, unpublished observations), and the soluble fusion peptides form hexamers in solution. The biological relevance must be determined, but it is hypothesized the FP of two F trimers may play a role in the formation of the fusion pore. Studies of the influenza virus HA FP in micelles suggest that it is α -helical and

kinked, causing its insertion to be shallow (47). Further studies of the PIV5 F FP in micelles is necessary to determine if the soluble peptides form the hexamer structure when inserted into lipids.

The conformational changes of F in fusion intermediates such as the open-stalk intermediate and the pre-hairpin intermediate are not known. There are no currently well-characterized MAb to the pre- and postfusion forms of F; it is currently difficult to determine if F mutants are in the pre- or postfusion conformation. Therefore, antibodies were made to pre- and postfusion soluble F protein. Work still remains with screening and characterizing of the potential pre- and postfusion conformational MAb to the F protein. The hybridomas of potential conformational MAb will be cloned (Olga Rozhok). To determine if any of the candidate antibodies are neutralizing, a 96-well format entry assay will be used (Sarah Connolly). EGFP expressing PIV5 W3A virus (made by reverse genetics by Jessica Robach) will be bound to CV1 monolayers in 96-well plates in the presence of an increasing amount of candidate MAb supernatant. Infection and entry can then be determined by reading the fluorescence of the CV1 cells. PIV5 W3A virus can then be grown in the presence of any neutralizing antibodies and sequenced to determine their epitope. The exposure of this epitope can be tracked through the open-stalk and pre-hairpin intermediates with the inhibitory peptides N1 and C1, respectively, and by testing antibody reactivity in flow cytometry or immunoprecipitation under mild detergent conditions. If none are neutralizing, the changes in binding to fusion intermediates can be determined by similar methods, and this data could be combined with structural data to develop a comprehensive of the conformational changes in the F protein during fusion.

REFERENCES

1. **Aguilar, H. C., K. A. Matreyek, C. M. Filone, S. T. Hashimi, E. L. Levroney, O. A. Negrete, A. Bertolotti-Ciarlet, D. Y. Choi, I. McHardy, J. A. Fulcher, S. V. Su, M. C. Wolf, L. Kohatsu, L. G. Baum, and B. Lee.** 2006. N-glycans on Nipah virus fusion protein protect against neutralization but reduce membrane fusion and viral entry. *J Virol* **80**:4878-4889.
2. **Armstrong, R. T., A. S. Kushnir, and J. M. White.** 2000. The transmembrane domain of influenza hemagglutinin exhibits a stringent length requirement to support the hemifusion to fusion transition. *J Cell Biol* **151**:425-437.
3. **Atanasiu, D., J. C. Whitbeck, T. M. Cairns, B. Reilly, G. H. Cohen, and R. J. Eisenberg.** 2007. Bimolecular complementation reveals that glycoproteins gB and gH/gL of herpes simplex virus interact with each other during cell fusion. *Proc Natl Acad Sci U S A* **104**:18718-18723.
4. **Baker, K. A., R. E. Dutch, R. A. Lamb, and T. S. Jardetzky.** 1999. Structural basis for paramyxovirus-mediated membrane fusion. *Mol Cell* **3**:309-319.
5. **Barnard, R. J., D. Elleder, and J. A. Young.** 2006. Avian sarcoma and leukosis virus-receptor interactions: from classical genetics to novel insights into virus-cell membrane fusion. *Virology* **344**: 25-29.
6. **Bauer, C. M., L. H. Pinto, T. A. Cross, and R. A. Lamb.** 1999. The influenza virus M₂ ion channel protein: probing the structure of the transmembrane domain in intact cells by using engineered disulfide cross-linking. *Virology* **254**:196-209.
7. **Bizebard, T., B. Gigant, P. Rigolet, B. Rasmussen, O. Diat, P. Bosecke, S. A. Wharton, J. J. Skehel, and M. Knossow.** 1995. Structure of influenza virus haemagglutinin complexed with a neutralizing antibody. *Nature* **376**:92-94.
8. **Boudker, O., R. M. Ryan, D. Yernool, K. Shimamoto, and E. Gouaux.** 2007. Coupling substrate and ion binding to extracellular gate of a sodium-dependent aspartate transporter. *Nature* **445**:387-393.
9. **Bressanelli, S., K. Stiasny, S. L. Allison, E. A. Stura, S. Duquerroy, J. Lescar, F. X. Heinz, and F. A. Rey.** 2004. Structure of a flavivirus envelope glycoprotein in its low-pH-induced membrane fusion conformation. *EMBO J* **23**:728-738.

10. **Brody, B. A., S. S. Rhee, and E. Hunter.** 1994. Postassembly cleavage of a retroviral glycoprotein cytoplasmic domain removes a necessary incorporation signal and activates fusion activity. *J Virol* **68**:4620-4627.
11. **Bullough, P. A., F. M. Hughson, J. J. Skehel, and D. C. Wiley.** 1994. Structure of influenza haemagglutinin at the pH of membrane fusion. *Nature* **371**:37-43.
12. **Chan, D. C., D. Fass, J. M. Berger, and P. S. Kim.** 1997. Core structure of gp41 from the HIV envelope glycoprotein. *Cell* **89**:263-273.
13. **Chang, D. K., S. F. Cheng, E. A. B. Kantchev, C. H. Lin, and Y. T. Liu.** 2008. Membrane interaction and structure of the transmembrane domain of influenza hemagglutinin and its fusion peptide complex. *BMC Biol* **6**.
14. **Chen, B. J., M. Takeda, and R. A. Lamb.** 2005. Influenza virus hemagglutinin (H3 subtype) requires palmitoylation of its cytoplasmic tail for assembly: M1 proteins of two subtypes differ in their ability to support assembly. *J Virol* **79**:13673-13684.
15. **Chen, J., K. H. Lee, D. A. Steinhauer, D. J. Stevens, J. J. Skehel, and D. C. Wiley.** 1998. Structure of the hemagglutinin precursor cleavage site, a determinant of influenza pathogenicity and the origin of the labile conformation. *Cell* **95**:409-417.
16. **Chen, L., J. J. Gorman, J. McKimm-Breschkin, L. J. Lawrence, P. A. Tulloch, B. J. Smith, P. M. Colman, and M. C. Lawrence.** 2001. The structure of the fusion glycoprotein of Newcastle disease virus suggests a novel paradigm for the molecular mechanism of membrane fusion. *Structure* **9**:255-266.
17. **Chernomordik, L. V., and M. M. Kozlov.** 2008. Mechanics of membrane fusion. *Nat Struct Mol Biol* **15**:675-683.
18. **Chernomordik, L. V., and M. M. Kozlov.** 2005. Membrane hemifusion: crossing a chasm in two leaps. *Cell* **123**:375-382.
19. **Chernomordik, L. V., and M. M. Kozlov.** 2006. Membranes of the world unite! *J Cell Biol* **175**:201-207.
20. **Chernomordik, L. V., and M. M. Kozlov.** 2003. Protein-lipid interplay in fusion and fusion of biological membranes. *Annu Rev Biochem* **72**:175-207.
21. **Cleverley, D. Z., and J. Lenard.** 1998. The transmembrane domain in viral fusion: essential role for a conserved glycine residue in vesicular stomatitis virus G protein. *Proc Natl Acad Sci U S A* **95**:3425-3430.

22. **Colman, P. M., and M. C. Lawrence.** 2003. The structural biology of type I viral membrane fusion. *Nat Rev Mol Cell Biol* **4**:309-319.
23. **Connolly, S. A., and R. A. Lamb.** 2006. Paramyxovirus fusion: real-time measurement of parainfluenza virus 5 virus-cell fusion. *Virology* **355**:203-212.
24. **Connolly, S. A., G. P. Leser, H. S. Yin, T. S. Jardetzky, and R. A. Lamb.** 2006. Refolding of a paramyxovirus F protein from prefusion to postfusion conformations observed by liposome binding and electron microscopy. *Proc Natl Acad Sci U S A* **103**:17903-17908.
25. **Corey, E. A., and R. M. Iorio.** 2007. Mutations in the stalk of the measles virus hemagglutinin protein decrease fusion but do not interfere with virus-specific interaction with the homologous fusion protein. *J Virol* **81**:9900-9910.
26. **Crennell, S., T. Takimoto, A. Portner, and G. Taylor.** 2000. Crystal structure of the multifunctional paramyxovirus hemagglutinin-neuraminidase. *Nat Struct Biol* **7**:1068-1074.
27. **Delos, S. E., J. A. Godby, and J. M. White.** 2005. Receptor-induced conformational changes in the SU subunit of the avian sarcoma/leukosis virus A envelope protein: implications for fusion activation. *J Virol* **79**:3488-3499.
28. **Deng, R., Z. Wang, P. J. Mahon, M. Marinello, A. Mirza, and R. M. Iorio.** 1999. Mutations in the Newcastle disease virus hemagglutinin-neuraminidase protein that interfere with its ability to interact with the homologous F protein in the promotion of fusion. *Virology* **253**:43-54.
29. **Deng, R., Z. Wang, A. M. Mirza, and R. M. Iorio.** 1995. Localization of a domain on the paramyxovirus attachment protein required for the promotion of cellular fusion by its homologous fusion protein spike. *Virology* **209**:457-469.
30. **Doms, R. W., A. Helenius, and J. White.** 1985. Membrane fusion activity of the influenza virus hemagglutinin. The low pH-induced conformational change. *J Biol Chem* **260**:2973-2981.
31. **Doms, R. W., and S. C. Peiper.** 1997. Unwelcomed guests with master keys: how HIV uses chemokine receptors for cellular entry. *Virology* **235**:179-90.
32. **Dutch, R. E., R. N. Hagglund, M. A. Nagel, R. G. Paterson, and R. A. Lamb.** 2001. Paramyxovirus fusion (F) protein: a conformational change on cleavage activation. *Virology* **281**:138-150.

33. **Earp, L. J., S. E. Delos, H. E. Park, and J. M. White.** 2005. The many mechanisms of viral membrane fusion proteins. *Curr Top Microbiol Immunol* **285**:25-66.
34. **Eckert, D. M., and P. S. Kim.** 2001. Design of potent inhibitors of HIV-1 entry from the gp41 N-peptide region. *Proc Natl Acad Sci USA* **98**:11187-11192.
35. **Eckert, D. M., and P. S. Kim.** 2001. Mechanisms of viral membrane fusion and its inhibition. *Annu. Rev. Biochem* **70**:777-810.
36. **Eckert, D. M., V. N. Malashkevich, L. H. Hong, P. A. Carr, and P. S. Kim.** 1999. Inhibiting HIV-1 entry: discovery of D-peptide inhibitors that target the gp41 coiled-coil pocket. *Cell* **99**:103-115.
37. **Falke, J. J., and D. E. Koshland, Jr.** 1987. Global flexibility in a sensory receptor: A site-directed cross-linking approach. *Science* **237**:1596-1600.
38. **Farnsworth, A., T. W. Wisner, M. Webb, R. Roller, G. Cohen, R. J. Eisenberg, and D. C. Johnson.** 2007. Herpes simplex virus glycoproteins gB and gH function in fusion between the virion envelope and the outer nuclear membrane. *Proc Natl Acad Sci U S A* **104**:10264-10269.
39. **Forster, F., O. Medalia, N. Zauberman, W. Baumeister, and D. Fass.** 2005. Retrovirus envelope protein complex structure *in situ* studied by cryo-electron tomography. *Proc Natl Acad Sci U S A* **102**:4729-4734.
40. **Fuerst, T. R., E. G. Nilis, F. W. Studier, and B. Moss.** 1986. Eukaryotic transient-expression system based on recombinant vaccinia virus that synthesizes bacteriophage T₇ RNA polymerase. *Proc Natl Acad Sci USA* **83**:8122-8126.
41. **Gething, M.-J., K. McCammon, and F. Sambrook.** 1989. Protein folding and intracellular transport. Evaluation of conformational changes in nascent exocytotic proteins. *Methods Cell Biol* **32**:185-206.
42. **Gibbons, D. L., A. Ahn, P. K. Chatterjee, and M. Kielian.** 2000. Formation and characterization of the trimeric form of the fusion protein of Semliki Forest Virus. *J Virol* **74**:7772-7780.
43. **Gibbons, D. L., M. C. Vaney, A. Roussel, A. Vigouroux, B. Reilly, J. Lepault, M. Kielian, and F. A. Rey.** 2004. Conformational change and protein-protein interactions of the fusion protein of Semliki Forest virus. *Nature* **427**:320-325.
44. **Gilbert, J. M., D. Mason, and J. M. White.** 1990. Fusion of Rous sarcoma virus with host cells does not require exposure to low pH. *J Virol* **64**:5106-5113.

45. **Grinthal, A., and G. Guidotti.** 2007. Bilayer mechanical properties regulate the transmembrane helix mobility and enzymatic state of CD39. *Biochemistry* **46**:279-290.
46. **Grinthal, A., and G. Guidotti.** 2004. Dynamic motions of CD39 transmembrane domains regulate and are regulated by the enzymatic active site. *Biochemistry* **43**:13849-13858.
47. **Han, X., J. H. Bushweller, D. S. Cafiso, and L. K. Tamm.** 2001. Membrane structure and fusion-triggering conformational change of the fusion domain from influenza hemagglutinin. *Nat Struct Biol* **8**:715-720.
48. **Hannah, B. P., E. E. Heldwein, F. C. Bender, G. H. Cohen, and R. J. Eisenberg.** 2007. Mutational evidence of internal fusion loops in herpes simplex virus glycoprotein B. *J Virol* **81**:4858-4865.
49. **Harbury, P. B., T. Zhang, P. S. Kim, and T. Alber.** 1993. A switch between two-, three-, and four-stranded coiled coils in GCN4 leucine zipper mutants. *Science* **262**:1401-1407.
50. **Harrison, S. C.** 2008. Viral membrane fusion. *Nat Struct Mol Biol* **15**:690-698.
51. **He, B., G. Y. Lin, J. E. Durbin, R. K. Durbin, and R. A. Lamb.** 2001. The SH integral membrane protein of the paramyxovirus simian virus 5 is required to block apoptosis in MDBK cells. *J Virol* **75**:4068-4079.
52. **Heldwein, E. E., H. Lou, F. C. Bender, G. H. Cohen, R. Eisenberg, and S. C. Harrison.** 2006. Crystal structure of glycoprotein B from herpes simplex virus 1. *Science* **313**:217-220.
53. **Helseth, E., U. Olshevsky, D. Gabuzda, B. Ardman, W. Haseltine, and J. Sodroski.** 1990. Changes in the transmembrane region of the human immunodeficiency virus type 1 gp41 envelope glycoprotein affect membrane fusion. *J Virol* **64**:6314-6318.
54. **Herfst, S., V. Mas, L. S. Ver, R. J. Wierda, A. D. M. E. Osterhaus, R. A. M. Fouchier, and J. A. Melero.** 2008. Low-pH induced membrane fusion mediated by human metapneumovirus F protein is a rare, strain-dependent phenomenon. *J Virol* **82**:8891-8895.
55. **Hernandez, L. D., L. R. Hoffman, T. G. Wolfsberg, and J. M. White.** 1996. Virus-cell and cell-cell fusion. *Annu Rev Cell Develop Biol* **12**:627-661.
56. **Hernandez, L. D., R. J. Peters, S. E. Delos, J. A. T. Young, D. A. Agard, and J. M. White.** 1997. Activation of a retroviral membrane fusion protein: Soluble receptor-

- induced liposome binding of the ALSV envelope glycoprotein. *J Cell Biol* **139**:1455-1464.
57. **Horvath, C. M., and R. A. Lamb.** 1992. Studies on the fusion peptide of a paramyxovirus fusion glycoprotein: roles of conserved residues in cell fusion. *J Virol* **66**:2443-2455.
58. **Horvath, C. M., R. G. Paterson, M. A. Shaughnessy, R. Wood, and R. A. Lamb.** 1992. Biological activity of paramyxovirus fusion proteins: factors influencing formation of syncytia. *J Virol* **66**:4564-4569.
59. **Hu, X., R. Ray, and R. W. Compans.** 1992. Functional interactions between the fusion protein and hemagglutinin-neuraminidase of human parainfluenza viruses. *J Virol* **66**:1528-1534.
60. **Hull, R. N., J. R. Minner, and J. W. Smith.** 1956. New viral agents recovered from tissue cultures of monkey kidney cells. 1. Origin and properties of cytopathic agents S.V.₁, S.V.₂, S.V.₄, S.V.₅, S.V.₆, S.V.₁₁, S.V.₁₂, and S.V.₁₅. *Am J Hyg* **63**:204-215.
61. **Ito, M., M. Nishio, H. Komada, Y. Ito, and M. Tsurudome.** 2000. An amino acid in the heptad repeat 1 domain is important for the haemagglutinin-neuraminidase-independent fusing activity of simian virus 5 fusion protein. *J Gen Virol* **81**:719-727.
62. **Jardetzky, T. S., and R. A. Lamb.** 2004. Virology: a class act. *Nature* **427**:307-308.
63. **Joshi, S. B., R. E. Dutch, and R. A. Lamb.** 1998. A core trimer of the paramyxovirus fusion protein: parallels to influenza virus hemagglutinin and HIV-1 gp41. *Virology* **248**:20-34.
64. **Kemble, G. W., T. Danieli, and J. M. White.** 1994. Lipid-anchored influenza hemagglutinin promotes hemifusion, not complete fusion. *Cell* **76**:383-391.
65. **Kielian, M.** 2006. Class II virus membrane fusion proteins. *Virology* **344**:38-47.
66. **Kyte, J., and R. F. Doolittle.** 1982. A simple method for displaying the hydrophobic character of a protein. *J Mol Biol* **157**:105-132.
67. **Lamb, R. A., and T. S. Jardetzky.** 2007. Structural basis of viral invasion: lessons from paramyxovirus F. *Curr Opin Struct Biol* **17**:427-436.
68. **Lamb, R. A., and R. M. Krug.** 2001. *Orthomyxoviridae*: the viruses and their replication, p. 1487-1531. *In* D. M. Knipe and P. M. Howley (ed.), *Fields Virology* (Fourth Edition). Lippincott, Williams and Wilkins, Philadelphia.

69. **Lamb, R. A., and G. D. Parks.** 2007. *Paramyxoviridae: The viruses and their replication*, p. 1449-1496. In D. M. Knipe and P. M. Howley (ed.), *Fields Virology* (Fifth Edition). Wolters Kluwer/Lippincott Williams & Wilkins, Philadelphia.
70. **Lamb, R. A., R. G. Paterson, and T. S. Jardetzky.** 2006. Paramyxovirus membrane fusion: lessons from the F and HN atomic structures. *Virology* **344**:30-37.
71. **Lamb, R. A., S. L. Zebedee, and C. D. Richardson.** 1985. Influenza virus M₂ protein is an integral membrane protein expressed on the infected-cell surface. *Cell* **40**:627-633.
72. **Lawrence, M. C., N. A. Borg, V. A. Streltsov, P. A. Pilling, V. C. Epa, J. N. Varghese, J. L. McKimm-Breschkin, and P. M. Colman.** 2004. Structure of the haemagglutinin-neuraminidase from human parainfluenza virus type III. *J Mol Biol* **335**:1343-1357.
73. **Lee, G. F., G. G. Burrows, M. R. Lebert, D. P. Dutton, and G. L. Hazelbauer.** 1994. Deducing the organization of a transmembrane domain by disulfide cross-linking. *J Biol Chem* **269**:29920-29927.
74. **Lee, G. F., D. P. Dutton, and G. L. Hazelbauer.** 1995. Identification of functionally important helical faces in transmembrane segments by scanning mutagenesis. *Proc Natl Acad Sci USA* **92**:5416-5420.
75. **Lee, G. F., M. R. Lebert, A. A. Lilly, and G. L. Hazelbauer.** 1995. Transmembrane signalling characterized in bacterial chemoreceptors by using sulfhydryl cross-linking *in vivo*. *Proc Natl Acad Sci USA* **92**:3391-3395.
76. **Lee, J. E., M. L. Fusco, A. J. Hessel, W. B. Oswald, D. R. Burton, and E. O. Saphire.** 2008. Structure of the Ebola virus glycoprotein bound to an antibody from a human survivor. *Nature* **454**:177-182.
77. **Lehr, R. V., L. C. Elefante, K. K. Kikly, S. P. O'Brien, and R. B. Kirkpatrick.** 2000. A modified metal-ion affinity chromatography procedure for the purification of histidine-tagged recombinant proteins expressed in *Drosophila* S2 cells. *Protein Expr Purif* **19**:362-368.
78. **Leser, G. P., K. J. Ector, D. T. Ng, M. A. Shaughnessy, and R. A. Lamb.** 1999. The signal for clathrin-mediated endocytosis of the paramyxovirus SV5 HN protein resides at the transmembrane domain-ectodomain boundary region. *Virology* **262**:79-92.
79. **Li, F., M. Berardi, W. Li, M. Farzan, P. R. Dormitzer, and S. C. Harrison.** 2006. Conformational states of the severe acute respiratory syndrome coronavirus spike protein ectodomain. *J Virol* **80**:6794-6800.

80. **Li, V., V. R. Melanson, A. M. Mirza, and R. M. Iorio.** 2005. Decreased dependence on receptor recognition for the fusion promotion activity of L289A-mutated Newcastle disease virus fusion protein correlates with a monoclonal antibody-detected conformational change. *J Virol* **79**:1180-1190.
81. **Li, Y., and L. K. Tamm.** 2007. Structure and plasticity of the human immunodeficiency virus gp41 fusion domain in lipid micelles and bilayers. *Biophys J* **93**:876-885.
82. **Li, Z., and G. W. Blissard.** 2008. Functional Analysis of the Transmembrane (TM) Domain of the *Autographa californica* Multicapsid Nucleopolyhedrovirus GP64 Protein: Substitution of Heterologous TM Domains. *J Virol* **82**:3329-3341.
83. **Liao, M., and M. Kielian.** 2005. Domain III from class II fusion proteins as a dominant-negative inhibitor of virus membrane fusion. *J Cell Biol* **171**:111-120.
84. **Malashkevich, V. N., B. J. Schneider, M. L. McNally, M. A. Milhollen, J. X. Pang, and P. S. Kim.** 1999. Core structure of the envelope glycoprotein GP2 from Ebola virus at 1.9-Å resolution. *Proc Natl Acad Sci USA* **96**:2662-2667.
85. **Markosyan, R. M., F. S. Cohen, and G. B. Melikyan.** 2003. HIV-1 envelope proteins complete their folding into six-helix bundles immediately after fusion pore formation. *Mol Biol Cell* **14**:926-938.
86. **Martens, S., and H. T. McMahon.** 2008. Mechanisms of membrane fusion: disparate players and common principles. *Nat Rev Mol Cell Biol* **9**:543-556.
87. **Matsuyama, S., S. E. Delos, and J. M. White.** 2004. Sequential roles of receptor binding and low pH in forming prehairpin and hairpin conformations of a retroviral envelope glycoprotein. *J Virol* **78**:8201-8209.
88. **Melanson, V. R., and R. M. Iorio.** 2006. Addition of N-glycans in the stalk of the Newcastle disease virus HN protein blocks its interaction with the F protein and prevents fusion. *J Virol* **80**:623-633.
89. **Melikyan, G. B., S. A. Greener, D. C. Ok, and F. S. Cohen.** 1997. Inner but not outer membrane leaflets control the transition from glycosylphosphatidylinositol-anchored influenza hemagglutinin-induced hemifusion to full fusion. *J Cell Biol* **136**:995-1005.
90. **Melikyan, G. B., S. Lin, M. G. Roth, and F. S. Cohen.** 1999. Amino acid sequence requirements of the transmembrane and cytoplasmic domains of influenza virus hemagglutinin for viable membrane fusion. *Mol Biol Cell* **10**:1821-1836.

91. **Melikyan, G. B., R. M. Markosyan, H. Hemmati, M. K. Delmedico, D. M. Lambert, and F. S. Cohen.** 2000. Evidence that the transition of HIV-1 gp41 into a six-helix bundle, not the bundle configuration, induces membrane fusion. *J Cell Biol* **151**:413-423.
92. **Melikyan, G. B., R. M. Markosyan, M. G. Roth, and F. S. Cohen.** 2000. A point mutation in the transmembrane domain of the hemagglutinin of influenza virus stabilizes a hemifusion intermediate that can transit to fusion. *Mol Biol Cell* **11**:1143-1152.
93. **Milne, R. S., A. V. Nicola, J. C. Whitbeck, R. J. Eisenberg, and G. H. Cohen.** 2005. Glycoprotein D receptor-dependent, low-pH-independent endocytic entry of herpes simplex virus type 1. *J Virol* **79**:6655-6663.
94. **Miyauchi, K., J. Komano, Y. Yokomaku, W. Sugiura, N. Yamamoto, and Z. Matsuda.** 2005. Role of the specific amino acid sequence of the membrane-spanning domain of human immunodeficiency virus type 1 in membrane fusion. *J Virol* **79**:4720-4729.
95. **Modis, Y., S. Ogata, D. Clements, and S. C. Harrison.** 2003. A ligand-binding pocket in the dengue virus envelope glycoprotein. *Proc Natl Acad Sci U S A* **100**:6986-6991.
96. **Modis, Y., S. Ogata, D. Clements, and S. C. Harrison.** 2004. Structure of the dengue virus envelope protein after membrane fusion. *Nature* **427**:313-319.
97. **Morrison, T. G.** 2003. Structure and function of a paramyxovirus fusion protein. *Biochim Biophys Acta* **1614**:73-84.
98. **Mothes, W., A. L. Boerger, S. Narayan, J. M. Cunningham, and J. A. Young.** 2000. Retroviral entry mediated by receptor priming and low pH triggering of an envelope glycoprotein. *Cell* **103**:679-689.
99. **Murakami, T., S. Ablan, E. O. Freed, and Y. Tanaka.** 2004. Regulation of human immunodeficiency virus type 1 Env-mediated membrane fusion by viral protease activity. *J Virol* **78**:1026-1031.
100. **Narayan, S., R. J. Barnard, and J. A. Young.** 2003. Two retroviral entry pathways distinguished by lipid raft association of the viral receptor and differences in viral infectivity. *J Virol* **77**:1977-1983.
101. **Nicola, A. V., J. Hou, E. O. Major, and S. E. Straus.** 2005. Herpes simplex virus type 1 enters human epidermal keratinocytes, but not neurons, via a pH-dependent endocytic pathway. *J Virol* **79**:7609-7616.

102. **Nicola, A. V., A. M. McEvoy, and S. E. Straus.** 2003. Roles for endocytosis and low pH in herpes simplex virus entry into HeLa and Chinese hamster ovary cells. *J Virol* **77**:5324-5332.
103. **Owens, R. J., C. Burke, and J. K. Rose.** 1994. Mutations in the membrane-spanning domain of the human immunodeficiency envelope glycoprotein that affect fusion activity. *J Virol* **68**:570-574.
104. **Pager, C. T., W. W. J. Craft, J. Patch, and R. E. Dutch.** 2006. A mature and fusogenic form of the Nipah virus fusion protein requires proteolytic processing by cathepsin L. *Virol J* **346**:251-357.
105. **Pager, C. T., and R. E. Dutch.** 2005. Cathepsin L is involved in proteolytic processing of the Hendra virus fusion protein. *J Virol* **79**:12714-12720.
106. **Parks, G. D., and R. A. Lamb.** 1990. Folding and oligomerization properties of a soluble and secreted form of the paramyxovirus hemagglutinin-neuraminidase glycoprotein. *Virology* **178**:498-508.
107. **Paterson, R. G., T. J. R. Harris, and R. A. Lamb.** 1984. Analysis and gene assignment of mRNAs of a paramyxovirus, simian virus 5. *Virology* **138**:310-323.
108. **Paterson, R. G., S. W. Hiebert, and R. A. Lamb.** 1985. Expression at the cell surface of biologically active fusion and hemagglutinin-neuraminidase proteins of the paramyxovirus simian virus 5 from cloned cDNA. *Proc Natl Acad Sci USA* **82**:7520-7524.
109. **Paterson, R. G., and R. A. Lamb.** 1993. The molecular biology of influenza viruses and paramyxoviruses, p. 35-73. *In* A. Davidson and R. M. Elliott (ed.), *Molecular Virology: A Practical Approach*. IRL Oxford University Press, Oxford.
110. **Paterson, R. G., R. A. Lamb, B. Moss, and B. R. Murphy.** 1987. Comparison of the relative roles of the F and HN surface glycoproteins of the paramyxovirus simian virus 5 in inducing protective immunity. *J Virol* **61**:1972-1977.
111. **Paterson, R. G., C. J. Russell, and R. A. Lamb.** 2000. Fusion protein of the paramyxovirus SV5: destabilizing and stabilizing mutants of fusion activation. *Virology* **270**:17-30.
112. **Paterson, R. G., M. A. Shaughnessy, and R. A. Lamb.** 1989. Analysis of the relationship between cleavability of a paramyxovirus fusion protein and length of the connecting peptide. *J Virol* **63**:1293-1301.

113. **Paterson, R. G., M. Takeda, Y. Ohigashi, L. H. Pinto, and R. A. Lamb.** 2003. Influenza B virus BM2 protein is an oligomeric integral membrane protein expressed at the cell surface. *Virology* **306**:7-17.
114. **Pinto, L. H., G. R. Dieckmann, C. S. Gandhi, C. G. Papworth, J. Braman, M. A. Shaughnessy, J. D. Lear, R. A. Lamb, and W. F. DeGrado.** 1997. A functionally defined model for the M₂ proton channel of influenza A virus suggests a mechanism for its ion selectivity. *Proc Natl Acad Sci USA* **94**:11301-11306.
115. **Porotto, M., L. Doctor, P. Carta, M. Fornabaio, O. Greengard, G. E. Kellogg, and A. Moscona.** 2006. Inhibition of hendra virus fusion. *J Virol* **80**:9837-9849.
116. **Porotto, M., M. Murrell, O. Greengard, L. Doctor, and A. Moscona.** 2005. Influence of the human parainfluenza virus 3 attachment protein's neuraminidase activity on its capacity to activate the fusion protein. *J Virol* **79**:2383-2392.
117. **Porotto, M., M. Murrell, O. Greengard, and A. Moscona.** 2003. Triggering of human parainfluenza virus 3 fusion protein (F) by the hemagglutinin-neuraminidase (HN) protein: an HN mutation diminishes the rate of F activation and fusion. *J Virol* **77**:3647-54.
118. **Randall, R. E., D. F. Young, K. K. A. Goswami, and W. C. Russell.** 1987. Isolation and characterization of monoclonal antibodies to simian virus 5 and their use in revealing antigenic differences between human, canine and simian isolates. *J Gen Virol* **68**:2769-2780.
119. **Rey, F. A., F. X. Heinz, C. Mandl, C. Kunz, and S. C. Harrison.** 1995. The envelope glycoprotein from tick-borne encephalitis virus at 2 Å resolution. *Nature* **375**:291-298.
120. **Roche, S., S. Bressanelli, F. A. Rey, and Y. Gaudin.** 2006. Crystal structure of the low-pH form of the vesicular stomatitis virus glycoprotein G. *Science* **313**:187-191.
121. **Roche, S., and Y. Gaudin.** 2002. Characterization of the equilibrium between the native and fusion-inactive conformation of rabies virus glycoprotein indicates that the fusion complex is made of several trimers. *J Virol* **297**:128-135.
122. **Roche, S., F. A. Rey, Y. Gaudin, and S. Bressanelli.** 2007. Structure of the prefusion form of the vesicular stomatitis virus glycoprotein G. *Science* **315**:843-848.
123. **Rose, J. K., L. Buonocore, and M. A. Whitt.** 1991. A new cationic liposome reagent mediating nearly quantitative transfection of animal cells. *BioTechniques* **10**:520-525.

124. **Russell, C. J., T. S. Jardetzky, and R. A. Lamb.** 2004. Conserved glycine residues in the fusion peptide of the paramyxovirus fusion protein regulate activation of the native state. *J Virol* **78**:13727-13742.
125. **Russell, C. J., T. S. Jardetzky, and R. A. Lamb.** 2001. Membrane fusion machines of paramyxoviruses: capture of intermediates of fusion. *EMBO J.* **20**:4024-4034.
126. **Russell, C. J., K. L. Kantor, T. S. Jardetzky, and R. A. Lamb.** 2003. A dual-functional paramyxovirus F protein regulatory switch segment: activation and membrane fusion. *J Cell Biol* **163**:363-374.
127. **Satoh, T., J. Arai, T. Suenaga, J. Wang, A. Kogure, J. Uehori, N. Arase, I. Shirator, S. Tanaka, Y. Kawaguchi, P. G. Spear, L. L. Lanier, and H. Arase.** 2008. PILPalph is a herpes simplex virus -1 entry coreceptor that associates with glycoprotein B. *Cell* **32**:935-944.
128. **Scheid, A., L. A. Caliguri, R. W. Compans, and P. W. Choppin.** 1972. Isolation of paramyxovirus glycoproteins. Association of both hemagglutinating and neuraminidase activities with the larger SV5 glycoprotein. *Virology* **50**:640-652.
129. **Scheiffele, P., M. G. Roth, and K. Simons.** 1997. Interaction of influenza virus haemagglutinin with sphingolipid-cholesterol membrane domains via its transmembrane domain. *EMBO J.* **16**:5501-5508.
130. **Schnell, J. R., and J. J. Chou.** 2008. Structure and mechanism of the M2 proton channel of influenza A virus. *Nature* **451**:591-595.
131. **Schorner, K., S. Matsuyama, K. Kabsch, S. E. Delos, A. Bouton, and J. M. White.** 2006. Role of endosomal cathepsins in entry mediated by the Ebola virus glycoprotein. *J Virol* **80**:4174-4178.
132. **Schowalter, R. M., S. E. Smith, and R. E. Dutch.** 2006. Characterization of human metapneumovirus F protein-promoted membrane fusion: critical roles for proteolytic processing and low pH. *J Virol* **80**:10931-10941.
133. **Seth, S., A. Vincent, and R. W. Compans.** 2003. Activation of fusion by the SER virus F protein: a low-pH-dependent paramyxovirus entry process. *J Virol* **77**:6520-6527.
134. **Seth, S., A. Vincent, and R. W. Compans.** 2003. Mutations in the cytoplasmic domain of a paramyxovirus fusion glycoprotein rescue syncytium formation and eliminate the hemagglutinin-neuraminidase protein requirement for membrane fusion. *J Virol* **77**:167-178.

135. **Shang, L., L. Yue, and E. Hunter.** 2008. Role of the membrane-spanning domain of human immunodeficiency virus type 1 envelope glycoprotein in cell-cell fusion and virus infection. *J Virol* **82**:5417-5428.
136. **Spear, P. G.** 2004. Herpes simplex virus: receptors and ligands for cell entry. *Cell Microbiol* **6**:401-410.
137. **Stone-Hulslander, J., and T. G. Morrison.** 1997. Detection of an interaction between the HN and F proteins in Newcastle disease virus-infected cells. *J Virol* **71**:6287-6295.
138. **Stouffer, A. L., R. Acharya, D. Salom, A. S. Levine, L. Di Costanzo, C. S. Soto, V. Tereshko, V. Nanda, S. Stayrook, and W. F. DeGrado.** 2008. Structural basis for the function and inhibition of an influenza virus proton channel. *Nature* **451**:596-599.
139. **Takeda, M., G. P. Leser, C. J. Russell, and R. A. Lamb.** 2003. Influenza virus hemagglutinin concentrates in lipid raft microdomains for efficient viral fusion. *Proc Natl Acad Sci USA* **100**:14610-14617.
140. **Tamm, L. K., J. Crane, and V. Kiessling.** 2003. Membrane fusion: a structural perspective on the interplay of lipids and proteins. *Curr Opin Struct Biol* **13**:453-466.
141. **Tatulian, S. A., and L. K. Tamm.** 2000. Secondary structure, orientation, oligomerization, and lipid interactions of the transmembrane domain of influenza hemagglutinin. *Biochemistry* **39**:496-507.
142. **Thomas, S. M., R. A. Lamb, and R. G. Paterson.** 1988. Two mRNAs that differ by two nontemplated nucleotides encode the amino coterminal proteins P and V of the paramyxovirus SV5. *Cell* **54**:891-902.
143. **Tong, S., M. Li, A. Vincent, R. W. Compans, E. Fritsch, R. Beier, C. Klenk, M. Ohuchi, and H. D. Klenk.** 2002. Regulation of fusion activity by the cytoplasmic domain of a paramyxovirus F protein. *Virology* **301**:322-333.
144. **Tsurudome, M., M. Ito, M. Nishio, M. Kawano, H. Komada, and Y. Ito.** 2001. Hemagglutinin-neuraminidase-independent fusion activity of simian virus 5 fusion (F) protein: difference in conformation between fusogenic and nonfusogenic F proteins on the cell surface. *J Virol* **75**:8999-9009.
145. **von Heijne, G.** 2007. The membrane protein universe: what's out there and why bother? *J Intern Med* **261**:543-557.
146. **Waning, D. L., C. J. Russell, T. S. Jardetzky, and R. A. Lamb.** 2004. Activation of a paramyxovirus fusion protein is modulated by inside-out signaling from the cytoplasmic tail. *Proc Natl Acad Sci USA* **101**:9217-9222.

147. **West, J. T., P. B. Johnston, S. R. Dubay, and E. Hunter.** 2001. Mutations within the putative membrane-spanning domain in the simian immunodeficiency virus transmembrane glycoprotein define the minimal requirements for fusion, incorporation, and infectivity. *J Virol* **75**:9601-9612.
148. **White, J. M., S. E. Delos, M. Brecher, and K. Schornberg.** 2008. Structures and mechanisms of viral membrane fusion proteins: multiple variations on a common theme. *Crit Rev Biochem Mol Biol* **43**:189-219.
149. **Wickner, W., and R. Schekman.** 2008. Membrane fusion. *Nat Struct Mol Biol* **15**:658-664.
150. **Wittels, M., and P. G. Spears.** 1990. Penetration of cells by herpes simplex virus does not require a low pH-dependent endocytic pathway. *Virus Res.* **18**:271-290.
151. **Yang, L., and H. W. Huang.** 2002. Observation of a membrane fusion intermediate structure. *Science* **297**:1817-1818.
152. **Yang, X., S. Kurteva, X. Ren, S. Lee, and J. Sodroski.** 2006. Subunit stoichiometry of human immunodeficiency virus type 1 envelope glycoprotein trimers during virus entry into host cells. *J Virol* **80**:4388-4395.
153. **Yao, Q., X. Hu, and R. W. Compans.** 1997. Association of the parainfluenza virus fusion and hemagglutinin-neuraminidase glycoproteins on cell surfaces. *J Virol* **71**:650-656.
154. **Yin, H.-S., R. G. Paterson, X. Wen, R. A. Lamb, and T. S. Jardetzky.** 2005. Structure of the uncleaved ectodomain of the paramyxovirus (hPIV3) fusion protein. *Proc Natl Acad Sci. USA* **102**:9288-9293.
155. **Yin, H. S., X. Wen, R. G. Paterson, R. A. Lamb, and T. S. Jardetzky.** 2006. Structure of the parainfluenza virus 5 F protein in its metastable, prefusion conformation. *Nature* **439**:38-44.
156. **Yuan, P., T. Thompson, B. A. Wurzburg, R. G. Paterson, R. A. Lamb, and T. S. Jardetzky.** 2005. Structural studies of the parainfluenza virus 5 hemagglutinin-neuraminidase tetramer in complex with its receptor, sialyllactose. *Structure* **13**:1-13.
157. **Zanetti, G., J. A. G. Briggs, K. Grunewald, Q. J. Sattentau, and S. D. Fuller.** 2006. Cryo-electron tomographic structure of an immunodeficiency virus envelope complex in situ. *PLOS Pathogens* **2**:790-797.

158. **Zebedee, S. L., and R. A. Lamb.** 1988. Influenza A virus M₂ protein: monoclonal antibody restriction of virus growth and detection of M₂ in virions. *J Virol* **62**:2762-2772.
159. **Zhang, Y., J. Corver, P. R. Chipman, W. Zhang, S. V. Pletnev, D. Sedlak, T. S. Baker, J. H. Strauss, R. J. Kuhn, and M. G. Rossmann.** 2003. Structures of immature flavivirus particles. *EMBO J.* **22**:2604-2613.
160. **Zhao, X., M. Singh, V. N. Malashkevich, and P. S. Kim.** 2000. Structural characterization of the human respiratory syncytial virus fusion protein core. *Proc Natl Acad Sci USA* **97**:14172-14177.
161. **Zhou, T., L. Xu, B. Dey, A. J. Hessel, D. Van Ryk, S. H. Xiang, X. Yang, M. Y. Zhang, M. B. Zwick, J. Arthos, D. R. Burton, D. S. Dimitrov, J. Sodroski, R. Wyatt, G. J. Nabel, and P. D. Kwong.** 2007. Structural definition of a conserved neutralization epitope on HIV-1 gp120. *Nature* **445**:732-737.

APPENDIX A: MONOCLONAL ANTIBODIES THAT RECOGNIZE THE PRE- AND POSTFUSION CONFORMATIONS OF THE F PROTEIN

The crystal structures of the prefusion and postfusion forms of paramyxovirus fusion (F) proteins have been solved (154, 155). The conformational changes in the F protein as it transitions from the prefusion to the postfusion form can be divided into several intermediates based on biochemical data (24, 125). F₀ is proteolytically cleaved by the host cell protease furin into the F₁ and F₂ segments, which exposes the fusion peptide at the newly formed N-terminus (69). Upon receptor binding to sialic acid on target cells, the hemagglutinin-neuraminidase (HN) attachment protein causes a conformational change in F. This change allows binding of the N1 inhibitory peptide (derived from HRA) to the corresponding HRB region, similar to forming the six-helix bundle (6HB) (125). Fusion can be inhibited by the addition of N1 peptide during the binding of target cells at 4°C prior to inducing fusion at 37°C, and F can be immunoprecipitated with tagged versions of this peptide (125). HRB forms a three-helix bundle (3HB) in the prefusion crystal structure, and based on peptide binding studies, this 3HB separates after receptor binding to form the open-stalk intermediate (125, 155). The C1 inhibitory peptide derived from HRB does not inhibit fusion under these conditions (125). The conformation of the head domain in the open-stalk intermediate is not known, but based on the inability of C1 to inhibit fusion during target cell binding, HRA is not accessible as an extended helix at the open-stalk intermediate (155). When added during the 37°C shift to trigger fusion, both HRA and HRB regions can bind inhibitory peptides. The data suggest C1 peptide inhibits fusion by

binding to HRA after HRA has formed the extended α -helix and the fusion peptide has inserted into the target cell membrane and has formed the pre-hairpin intermediate (24, 125, 155).

Although biochemical studies have elucidated some of the structural and conformational changes of the F protein during the intermediate stages of fusion, not all the conformational rearrangements are known. Initial studies suggest there is little conformational change after cleavage that exposes the fusion peptide (24). Upon heating to 60°C, F-GCNt converts to the postfusion form even if uncleaved, as shown by its morphology in electron microscopy and conformational antibody reactivity (24).

However, the conformational changes in the head of F, particularly in domain III that contains HRA, after receptor binding, in the open stalk, or in the pre-hairpin intermediate are not known. Currently our lab has two conformational monoclonal antibodies (MAb) to the F protein, F1a and 6-7. The MAb F1a (Randall 1987) recognizes cleaved F protein (F1+F2) better than uncleaved protein (F0) (32), and recognition decreases when the F protein is heated to 53°C (24), suggesting F1a recognizes the prefusion conformation of F. The epitope of F1a is unknown. MAb F1a is a neutralizing antibody, but attempts to map the epitope by sequencing escape mutants have proven unsuccessful (32).

The MAb 6-7 was raised against the PIV5 strain W3A F mutant F S443P (144). F S443P has previously been shown to demonstrate a lower temperature requirement for fusion, faster fusion kinetics, reduced requirement for HN triggering (111). F S443P forms extensive syncytium at

room temperature in the absence of HN and has been labeled hyperfusogenic. Residue 443 is located in the HRB-linker region of prefusion F, and it is thought that the S443P mutation destabilizes the interactions between the top of the HRB 3HB and the HRB-linker to the IgG-like Domain II to lower the energy barrier to convert to the open-stalk conformation (155). MAb 6-7 recognizes F S443P better than W3A F, but MAb 6-7 reactivity to wt W3A F increases after heating F (24, 144, 146), suggesting 6-7 recognizes the postfusion form of wt W3A F. The epitope of MAb 6-7 is unknown, but the data support that the unknown epitope is not exposed on native F protein but does become exposed when heated or destabilized (24, 144, 146). From analysis of W3A F and SV41 F chimeras, residues 227-320 and 20-47 are thought to be involved in the MAb 6-7 epitope (144). However, these residues cover a large portion of Domain I in the pre- and postfusion structures of the F protein. There is compacting of the head between the pre- and postfusion conformations and the Domain I regions of the trimer pivot slightly inwards and shear intersubunit contacts to allow the Domain II regions to swing across and contact neighboring subunits (155). However, individual Domain I regions remain similar between the pre- and postfusion structures (155). The structural data suggest the epitope of MAb 6-7 may be complex. The two MAbs F1a and 6-7 alone are not enough to determine the conformational changes in F as it proceeds through the intermediates of fusion. In this study, a panel of MAb against uncleaved soluble F protein or heated uncleaved soluble F protein were made in order to obtain conformational antibodies to the pre- and postfusion form of F, respectively.

Uncleaved F-GCNt (prefusion conformation) and uncleaved F-GCNt heated to 60°C for 10 min (postfusion conformation) were injected into five mice a piece to generate antibodies at the

Monoclonal Antibody Facility of Northwestern University and the Robert H Lurie Comprehensive Cancer Center (Chicago, IL). The soluble F-GCNt was produced from stable insect S2 cell lines generated by Dr. Reay G. Paterson using standard methods (77). Soluble protein produced from the S2 system show similar “ball-and-stem” (prefusion) and “golf tee”-like (postfusion) shapes in electron microscopy as the F-GCNt produced in the baculovirus system (24) (Fig. A-1).

Five mice were inoculated with 50 µg of soluble uncleaved F-GCNt protein to generate prefusion antibodies, and five mice were inoculated with 50 µg of heated soluble uncleaved F-GCNt to generate postfusion

antibodies. Booster

immunizations of 50 µg of protein were given on days 21 and 45 after the initial immunization. Test bleeds were drawn after each

immunization boost, and the

mouse immune response was

determined by ELISA using

pre- or postfusion protein

immobilized on nickel-coated

plates. All mice showed strong

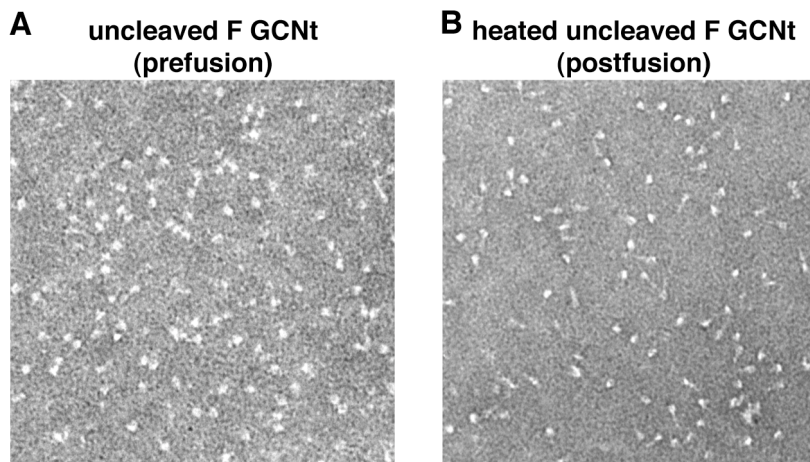


Figure A-1. Shape of pre- and postfusion F-GCNt in electron microscopy.

(A) Uncleaved F-GCNt soluble protein grown in the S2 cell system in electron microscopy. Protein demonstrates the “ball-and-stem” prefusion shape. (B) uncleaved F-GCNt soluble protein heated to 50°C for 10 min. Protein has “golf-tee” postfusion shape. All pre- and postproteins grown in the S2 cells have similar morphology as the pre- and postfusion proteins from the baculovirus system.

immune responses at 1:10000 dilution (data not shown). Hybridoma cells were cultured from the fusion of murine myeloma cells and splenocytes from the pre- and postfusion inoculated mice with the strongest immune response.

The resulting hybridomas were initially screened by ELISA using purified soluble pre- or postfusion F-GCNt protein immobilized on nickel-coated plates. The protein was bound via the 6-His tag on its C-terminal end to increase the likelihood that F would remain properly folded in the assay and decrease the potential for antibodies to linear epitopes. The initial ELISA screen generated 53 pre-fusion and 59 postfusion candidate conformational MAbs (Table A-1).

Further screening was performed by flow cytometry. PIV5 W3A virus was bound to CV-1 cells (multiplicity of infection of 10 plaque forming units, MOI=10 pfu) at 4°C for 1 h, and cells were then shifted to 37°C for 1 h. The media was replaced with Dulbecco's modified Eagle's medium (DMEM) supplemented with 2% fetal bovine serum (FBS), and the pre-fusion samples were treated with 100 mU/ml of neuraminidase (*Vibrio cholera*) (Sigma Aldrich, St. Louis, MO) overnight to inhibit syncytium formation. Flow cytometry was performed as previously described (146). Prior to the addition of the MAbs, warmed PBS was added to the postfusion samples and the plates were incubated at 50°C for 10 min and washed with cold PBS. The pre-fusion samples remained at 4°C. MAb F1a was used at 1:100 dilution, and MAb 6-7 and the MAb supernatants undergoing screening were added undiluted. The mean fluorescence intensity (MFI) was expected to decrease upon heating for conformational antibodies that recognize the

prefusion form of F. This decrease is seen with F1a due to the loss of the prefusion conformation upon driving F to the postfusion conformation (24). The opposite was expected

Table A-1: Mean fluorescence intensity of all candidate MAb to wt W3A F

	MFI		%total			MFI		%total	
	unheated	heated	unheated	heated		unheated	heated	unheated	heated
F1a	1388.46	636.73	92.98	94.58	1E1	36.76	33.48	1.59	0.89
6-7	109.26	144.87	73.51	92.75	1E3	31.91	62.18	27.49	5.72
1C3	73.41	177.26	18.52	4.26	1F5	76.29	14.19	1.81	15.46
1C6	30.56	30.79	49.42	70.81	1D7	57.43	11.15	1.41	1.48
1B7	98.37	12.2	2.17	7.8	1E7	69.43	38.68	1.25	2.36
1A8	81.01	4.77	1.91	3.57	1B9	34.43	41.15	14.56	72.22
1F10	85.61	67.98	71.3	51.1	1E10	97.22	206.85	63.64	94.85
1A11	59.89	15.66	1.72	1.65	1D11	148.05	32.73	1.99	0.49
1H11	56.64	9.88	2.17	1.68	2H1	220.34	203.66	1.68	2.8
1C12	47.93	66.18	9.64	2.48	2D3	43.77	82.61	13.22	29.44
2E5	49.68	38.35	54.53	43.06	2H5	37.5	19.67	7.48	36.1
2C7	79.77	26.04	1.64	1.59	2B5	21.22	11.87	1.78	7.24
2C10	108.92	12.96	1.59	2.24	2G5	86.48	12.48	1.84	9.44
2D10	46.54	10.84	1.12	3.15	2C7	110.6	174.95	67.11	95.54
2H10	29.4	25.18	2.49	1.93	2D8	61.23	34.55	2.38	3.37
2D12	122.95	40	1.98	1.32	2F8	112.17	77.04	77.48	67.4
3D2	33.08	53.66	40.46	5.75	2C9	129.54	21.12	1.93	4.69
3F3	61.78	39.37	1.84	0.83	2B10	20.38	24.28	1.85	1.96
3F4	68.81	13.51	1.33	1.1	2C10	181.59	202.51	1.64	2.89
3F8	26.74	25.81	34.63	20.74	2F11	69.45	116.04	47.85	92.84
3G8	57.87	6.23	1.09	1.87	2D12	74.56	157.51	52.22	94.11
3F9	95.09	18.3	1.74	1.77	3G1	35.28	12.64	1.02	1.86
3B11	39.69	23.01	1.23	0.98	3H2	39.86	16.01	1.83	4.23
3G11	29.71	19.37	1.54	2.35	3H4	100.74	149.16	60.18	94.45
3E12	49.28	42.29	1.97	1.51	3D6	81.38	15.92	2.63	28.24
4G2	46.66	5.51	1.7	62.69	3A8	89.94	6.48	1.55	1.36
4B6	42.61	5.63	1.51	5.62	3D9	66.39	11.73	1.17	1.52
4E9	75.27	12.38	1.51	1.9	3D11	16.23	17.77	7.51	1.96
4H10	58.72	39.37	1.75	2.09	3F9	17.37	3.83	3.98	4.6
4B11	46.98	44.26	2.7	2.68	4A3	34.07	42.79	31.41	17.23
4C6	74.38	21.42	1.7	1.53	4C3	14.59	13.9	10.86	11.27
4E8	28.09	9.27	1.6	1.79	4C6	189.54	16.38	1.29	2.71
5D2	65.22	63.18	39.48	38.8	4H7	44.52	3.13	1.72	9.4
5B3	28.93	31.19	2.2	1.5	4E7	45.66	8.66	1.69	2.38
5C4	16.83	13.76	1.49	2.45	4F8	38.1	17.22	6.79	13.21
5B7	41.9	11.71	0.99	2.25	4F10	374.08	85.41	89.89	88.7
5D7	99.06	6.99	1.55	4.27	4B12	118.34	7.15	2.45	5.3
5H7	39.89	12.17	1.12	3.2	4E12	30.66	19.02	34.94	47.98
5E9	60.85	21.17	3.22	2.25	4F12	26.93	19.94	23.77	47.23
5A11	81.58	23.03	1.51	1.89	4D6	151.92	74.16	69.15	86.69
5E11	32.95	27.49	1.58	2.37	5G2	113.73	5.69	2.35	6.15
5B12	91.37	34.03	1.42	1.07	5A3	23.91	4.53	1.91	8.21
5E12	38.73	14.62	2.73	1.62	5B3	141.42	8.07	2.07	7.51
5H12	98.45	37.75	1.25	1.24	5C3	67.84	6.34	2.64	3.04
5F2	63.93	9.76	1.4	1.91	5A4	81	6.06	3.56	5.57
6B2	90.31	44.13	1.88	0.61	5D6	82.16	20.44	11.22	8.23
6C2	41.35	19.53	13.6	29.25	5G6	106.3	19.7	4.2	3.19
6H4	57.38	55.86	10.49	7.77	5D12	60.3	17.56	0.97	1.78
6B9	66.75	19.81	1.29	1.36	5G12	91.29	18.16	1.99	0.74
6E9	36.69	15.17	1.55	1.21	5A9	85.24	144.42	43.62	2.78
6E10	85.09	20.87	1.78	1.35	6D1	45.41	2.54	1.83	10.06
6B11	48.73	12.9	1.9	1.28	6D6	170.41	50.22	70.92	83.88
6F11	52.97	15.99	2.44	1.36	6F6	170.51	51.08	68.26	73.95
6G11	49.69	12.68	1.38	9.78	6E6	159.51	46.65	67.86	77.33
6A12	42.41	57.44	37.09	11.45	6C7	33.73	4.66	6.49	4.37
					6E7	27.85	23.33	2.94	1.56
					6F9	26.11	10.03	8.63	1.17
					6E10	47.02	13.14	2.09	3.06
					6A4	30.52	5.19	1.76	5.13

for conformational antibodies to the postfusion form, where the MFI would increase upon heating, as is seen for MAb 6-7 (24, 144, 146). The majority of the candidate antibody supernatants showed either a decrease (red) or an increase (blue) in MFI (Table A-1). No supernatant produced a MFI as high as MAb F1a, due to it being derived from ascites fluid rather than hybridoma tissue culture supernatant like MAb 6-7 and the candidate antibodies. The majority of the candidate antibodies recognized the F protein on a few percent of the total cells counted (percent total). Only 29 of the 112 candidate antibody supernatants recognized F on more than 20% of total cells counted (green). Near 100% of cells bound MAbs F1a and 6-7, but percent totals for the candidate antibodies ranged from 20% (prefusion 3F8) to 95% (postfusion 2C7) (Table A-1). The low recognition may be due to the antibody binding to a partially exposed epitope, an epitope that is exposed in a conformational intermediate of F, or a linear epitope that is not exposed in properly folded F and is only present on a small percentage of misfolded F on the surface. Some candidate antibodies demonstrated a very high MFI but a percent total of only a few percent, such as postfusion 4C6. If an antibody had a strong reactivity to F to give a high MFI, it would be expected that the majority of cells would demonstrate this reactivity. The high MFI with low percentage total may be due to aggregation of the secondary antibody.

A smaller scale screen to clarify the high MFI/low percent total flow cytometry data was performed by fluorescence microscopy. Based on the initial flow cytometry screen, 68 candidate antibody supernatants, including antibodies with high and low percent totals, were selected for screening (Table A-2). CV-1 monolayers were grown on 16-well Lab-Tek Chamber Slides

Table A-2

Prefusion	Postfusion
1C3	1E3
1C6	1F5
1B7	1E7
1A8	1B9
1F10	1E10
1A11	1D11
1H11	2H1
1C12	2D3
2E5	2G5
2C7	2C7
2C10	2D8
2D12	2F8
3D2	2C9
3F3	2C10
3F4	2F11
3F8	2D12
3F9	3H4
4G2	3D6
4E9	3A8
4C6	4A3
5D2	4C6
5D7	4F10
5A11	4B12
5B12	4E12
5H12	4F12
5F2	5G2
6B2	5B3
6C2	5C3
6B9	5A4
6E10	5D6
6A12	5G6
	5D12
	5G12
	5A9
	6D6
	6F6
	6E6

(Thermo Fisher Scientific, Rochester, NY), and cells were either mock infected or infected with PIV5 W3A virus (MOI= 10 pfu). At 16 h post infection (p.i.), the postfusion samples were heated to 50°C for 10 min, and MAb F1a was used at 1:100 dilution, and MAb 6-7 (144) and the MAb candidate supernatant were added to all samples undiluted for 1 h at 4°C. Cells were washed with cold PBS and incubated for 1 h with FITC-conjugated goat anti-mouse IgG secondary antibody. Cells were washed again and fixed with 2% formaldehyde for 15 min. Samples were viewed by fluorescence microscopy (LSM 5 Pascal, Carl Zeis MicroImaging, Inc., Thornwood, NY). Antibodies that bound well to the F protein corresponded to antibodies that demonstrated F binding with a higher percent total in flow cytometry, shown in bold (Table A-2, data not shown).

The ability of all 112 candidate antibodies to immunoprecipitate the F protein was tested.

Monolayers of CV-1 cells were grown and either mock infected or infected with PIV5 W3A virus (MOI=10 pfu). The cells were labeled with 300 μ Ci of 35 S-Promix (GE Healthcare Bio-Sciences, Piscataway, NJ) in Cys- and Met-deficient DMEM for 1 h and then chased with cold DMEM for 1 h. Immunoprecipitations require detergent to disrupt cell membranes; detergent can potentially unfold the F protein and reveal linear epitopes that may not be completely exposed under biological conditions. To maintain the fold of the F protein and select for conformational antibodies, cells were lysed in NP40 lysate buffer (1% NP40, 0.1% SDS, 150 mM NaCl, and 20

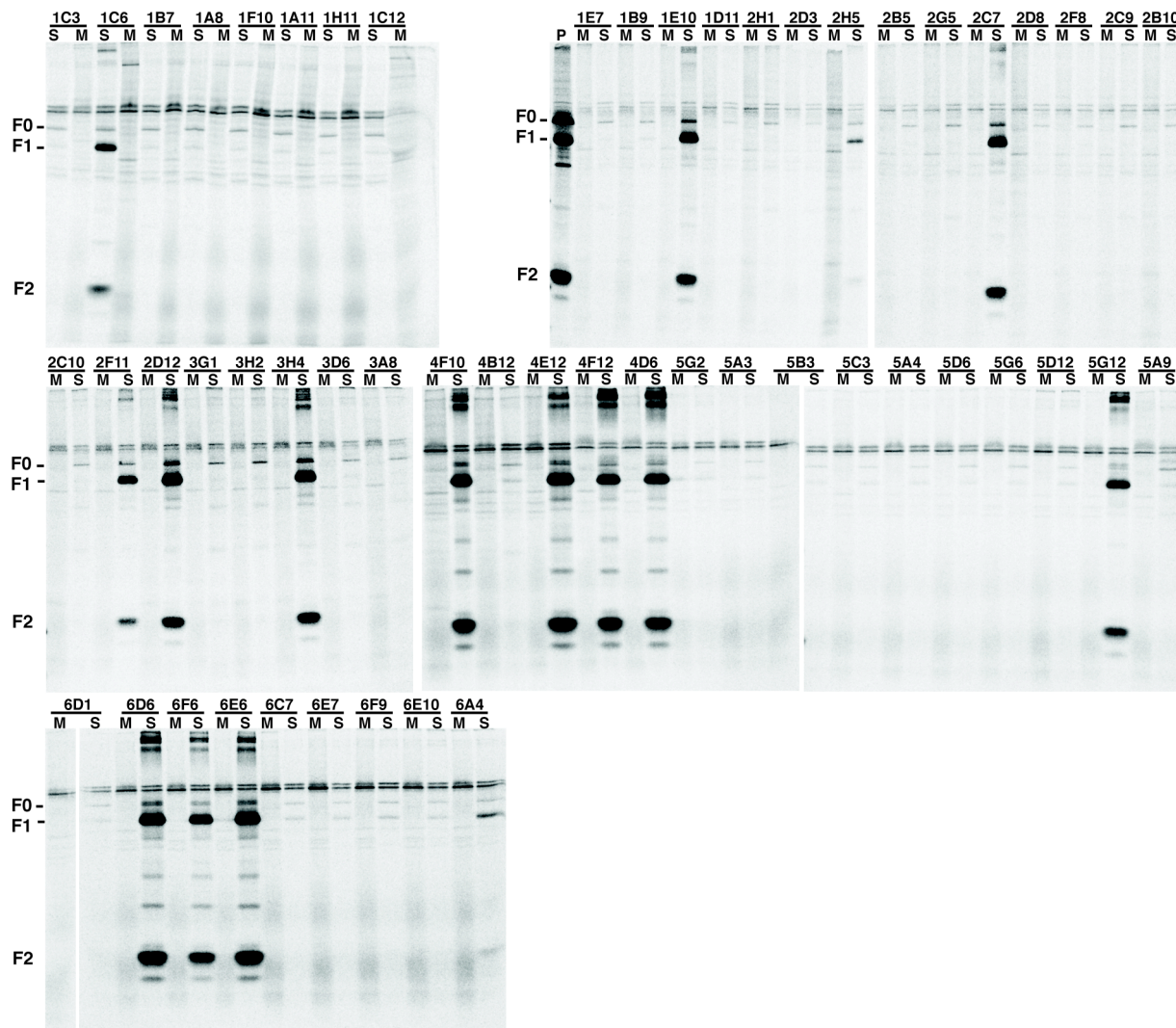


Figure A-2. Immunoprecipitation of wt W3A F by select MAb.

W3A F protein immunoprecipitations of selected candidate prefusion (first gel) or postfusion (remaining gels) MAb supernatant. To maintain the F protein in its biological conformation, cells were lysed in NP40 buffer, a mild detergent. Antibodies were added to mock infected (M) or W3A infected cells (S). The PAb anti-F sol R9176 was added to W3A infected cells (P). All antibodies recognized F0 to with varying strengths. Prefusion 1C6 and postfusion 1E10, 2C7, 2F11, 2D12, 3H4, 4F10, 4E12, 4F12, 4D6, 5G12, 6D6, 6F6, and 6E6 all reacted more strongly to cleaved F, F1 and F2, than uncleaved F, F0, even though the antibodies were raised against uncleaved soluble protein.

mM Tris, pH 7.4), and 40 μ l of undiluted antibody supernatant was added and incubated for 2 h at 4°C. Samples were incubated with 40 μ l of protein G-Sepharose beads for 1 h at 4°C, washed three times with NP40 wash buffer (0.5% NP40, 150 mM NaCl, 20 mM Tris, pH 7.4), and analyzed by SDS-PAGE on 15% acrylamide gels under reducing conditions (113). All 112 candidate antibody supernatants immunoprecipitated F, but most only recognized F₀. The binding to F was generally weak, but F₀ is present in the infected sample lane (S) and not in the mock infected lane (M) (Fig. A-2). Recognition of uncleaved F was expected because the antibodies were raised against an uncleaved F protein antigen. However, 16 antibodies, one pre-fusion (1C6) and 15 post-fusion (1E10, 2H5, 2C7, 2F11, 2D12, 3H4, 4F10, 4E12, 4F12, 4D6, 5G12, 6D6, 6F6, 6E6, 6A4) recognized cleaved F (F₁+F₂) better than uncleaved F (F₀) and demonstrated a stronger response comparable to the anti-F sol R9176 polyclonal antibody (P) (Fig. A-2). The majority of the candidate antibodies that recognized cleaved F better than uncleaved F also demonstrated a larger percentage total in flow cytometry, with the exceptions of 5G12 and 6A4, likely due to the majority of F on the surface of the infected cells being cleaved rather than uncleaved.

To determine if antibody supernatants that showed potential as conformational antibodies in the fluorescence and immunoprecipitation screens recognize various conformations of the F protein, six antibodies were further examined for their reactivity to different conformations of the F protein. HeLa CD4 LTR β gal cells were transfected with 1 μ g pCAGGS PIV5 FR3 F DNA using the Lipofectamine Plus expression system (Invitrogen, Carlsbad, CA) and tested in flow

cytometry. The FR3 F cleavage mutant contains only three arginine residues at the cleavage site rather than five and is not cleaved intracellularly by host cell furin but can be cleaved at the cell surface by exogenous trypsin (112). FR3 F either remained uncleaved, remained uncleaved

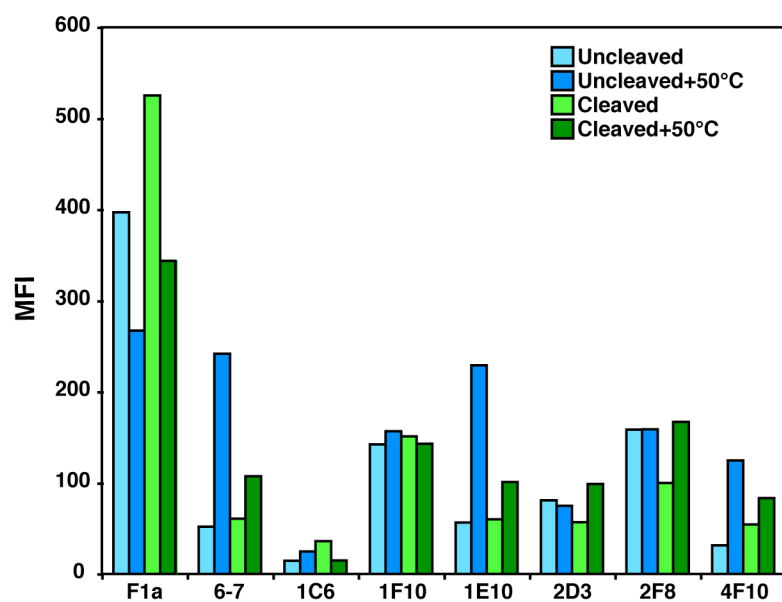


Figure A-3. Mean fluorescent intensity of several MAb to the cleavage mutant FR3 F.

To determine the ability of the MAbs to recognize different conformations of the F protein, HeLa CD4 LTR β gal cells were transfected with the F cleavage mutant FR3. The F mutant FR3 can be cleaved to expose the fusion peptide with exogenous trypsin. Samples were either uncleaved (light blue), uncleaved and heated to 50°C for 10 min (blue), cleaved with TPCK trypsin (light green), or cleaved and heated to 50°C for 10 min (green). 50°C for 10 min converts F to the postfusion form. 1C6, 1E10, and 4F10 all recognize cleaved F more than uncleaved F, consistent with the immunoprecipitation. 1C6 lost reactivity similar to F1a, suggesting it may be a conformational prefusion antibody. 1E10 and 4F10 lost activity similar to 6-7, suggesting it may be a conformational postfusion antibody.

and heated to 50°C for 10 min, was cleaved by exogenous trypsin, or was cleaved and heated to 50°C for 10 min. While cleavage alone does not trigger fusion, cleavage can affect antibody recognition, where the MAb F1a recognizes the F protein better after cleavage

(24, 32). Heat has also been shown to affect antibody reactivity, where MAb 6-7 recognition of F increases after heating to 50°C (144, 146) but MAb F1a loses reactivity (24), suggesting MAb 6-7 recognizes a postfusion conformation of F while MAb F1a recognizes a prefusion conformation. Prefusion antibodies 1C6 and 1F10 and

postfusion antibodies 1E10, 2D3, 2F8, and 4F10 were tested in the above conditions in flow cytometry (Fig. A-3). Similar to MAb F1a, 1C6 showed an increase in reactivity upon cleavage and a decrease upon heating, suggesting this antibody is a good conformational candidate antibody. All postfusion antibodies increased reactivity to F upon heating similar to MAb 6-7, and 1E10 and 4F10 also showed increased reactivity upon heating uncleaved F, suggesting the antibodies 1C6, 1E10, 2D3, 2F8, and 4F10 show promise as conformational antibodies.

Two of the antibodies that recognized cleaved F better than uncleaved F by immunoprecipitation (prefusion 1C6 and postfusion 4F10) also showed a stronger reaction to cleaved over uncleaved FR3 F by flow cytometry. However, the postfusion antibody 1E10, which immunoprecipitated cleaved F better than uncleaved, showed equal reactivity. This may be because the postfusion 1E10 epitope is not exposed after cleavage, and conversion to the postfusion form by heat or mild detergent such as NP40 is necessary to expose its binding site on F. The antibodies 1C6, 1F10, 2F8, and 4F10 showed different changes reactivity to FR3 F and heat than the large-scale flow cytometry screen. This difference may be due to error in the large-scale screen or may be due to the presence of HN altering the antibody epitope in the infected cells in the large-scale screen.

Out of 112 candidate pre- and postfusion antibodies, 31 demonstrated strong reactivity in either flow cytometry or in immunoprecipitating F under mild detergent conditions. Of these 31 antibodies, the reactivity of six antibodies, two prefusion and four postfusion, were further tested against several conformations of F: uncleaved, uncleaved and heated, cleaved, and cleaved and

heated. While prefusion 1C6 showed a change in reactivity under the four conditions, prefusion 1F10 did not recognize conformational differences. This is in contrast to the initial flow cytometry screen (Table A-1). The high MFI of prefusion 1F10 in the initial flow cytometry screen may be due to FITC secondary antibody aggregation, which is also the likely explanation for the high MFI but low percent of total samples, or may be due to error in having a large sample number to run on the flow cytometer. In contrast, all candidate postfusion antibodies exhibited differences upon cleavage and heating in all flow cytometry screens.

The next step for these antibodies is cloning the hybridomas. Based on the screenings performed to date, six antibodies have been chosen for cloning, the prefusion antibodies 1C6, 1F10, and 4G2 and the postfusion antibodies 1E10, 2F8, and 4F10. While the results are inconclusive for 1F10, it does have a higher reactivity and MFI to F than other antibodies. Although it may not be conformational, 1F10 will be cloned because the lab only possesses two mouse MAb to the F protein and an additional antibody would be useful. The reactivity of candidate prefusion antibody 4G2 was not tested with FR3 F. However, 4G2 showed a decrease in reactivity upon heating in the initial flow cytometry screen (Table A-1) and may also have promise as a prefusion conformational antibody. As more experiments are done, such as the above experiment with other antibody supernatants, the nature of 1F10 and 4G2 will be clearer, and more antibodies will also be cloned.

To further determine what domains are exposed or structural rearrangements occur at the intermediates of fusion, such as the open-stalk or pre-hairpin intermediates, the epitopes on F of

these antibodies will be mapped. PIV5 W3A virus will be grown in the presence of the antibodies to determine if any are neutralizing. By maintaining the antibody presence as a selective pressure and looking for escape mutants, the epitope on F can be mapped by sequencing these mutants. If the antibodies are not neutralizing or no escape mutants emerge, the antibodies can be divided into groups based on binding in competition assays. Whether the epitopes can or cannot be mapped, changes in conformation can be determined by antibody reactivity to fusion intermediates. Antibody binding to fusion intermediates can be determined by trapping the open-stalk and pre-hairpin intermediates with the inhibitory peptides N1 and C1, respectively and by testing antibody reactivity in flow cytometry or immunoprecipitation under mild detergent conditions. This data could be combined with structural data to develop a comprehensive of the conformational changes in the F protein during fusion.

APPENDIX B: A THREE-HELIX BUNDLE ON THE CYTOPLASMIC TAIL OF THE PIV5 FUSION PROTEIN TRAPS THE PRE-HAIRPIN INTERMEDIATE IN FUSION

The cytoplasmic tail (CT) of many class I viral fusion proteins is thought to play an important role in membrane fusion. Several retroviruses require proteolytic cleavage of their fusion protein to activate fusion activity (10, 99). Truncation of the HIV fusion protein gp41 CT increases fusion activity, and HIV virions deficient in protease activity have an uncleaved gp41 CT and show impaired fusion activity (99). The length of the CT of PIV5 F varies depending on the isolate. Isolates W3A and WR cause extensive cell-cell fusion and have CTs that are 20 residues long whereas the canine isolate T1 and porcine isolate SER cause reduced or no detectable cell-cell fusion and have CT that are 42 residues long (61, 143). The overall sequences of these isolates are very similar, but the translational stop codon of the wild type (wt) W3A F protein is replaced by a serine in isolates T1 and SER, and protein synthesis is terminated at a subsequent downstream stop codon (143) (Fig. B-1A). Although T1 and SER do not cause visible syncytium formation, the viruses are infectious (61, 133). Replacing the wt W3A F CT with the CT of T1 F to form the F 551 mutant (Fig. B-1A) did not affect surface expression of the F 551 mutant but did reduce cell-cell fusion (146). By scrambling the sequence of the CT on F 551, fusion was restored to wt W3A F levels (146). It has been suggested that the extended tail reduces visible cell-cell fusion by inside-out signaling, where the longer tail may form a structure that inhibits

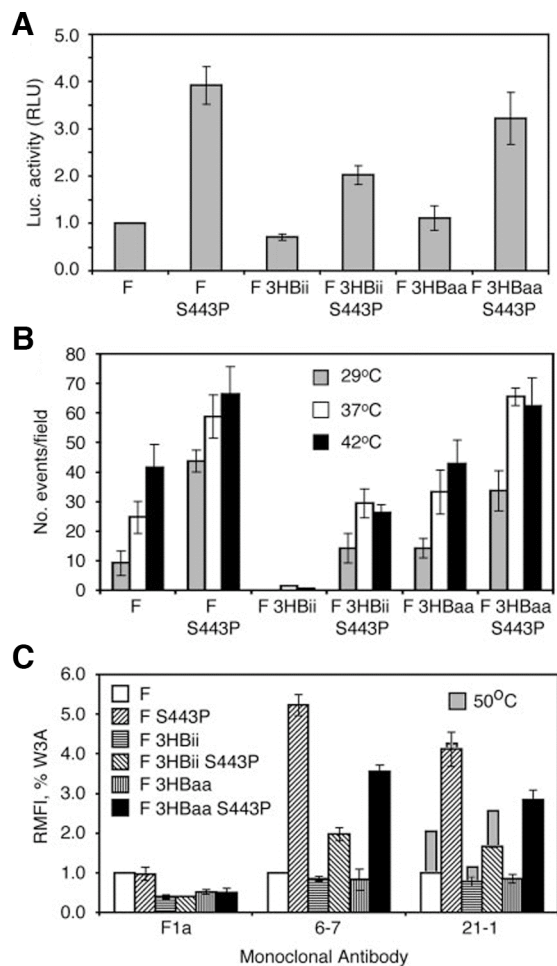


Figure B-2. Fusion of F3HBii and F 3HBaa.

(A) Cell-cell fusion of wt F, F3HBii, F 3HBaa, and these constructs with the hyperfusogenic mutation F S443P. The fusion of wt F and F S443P was reduced with the addition of the 3HB but restored with 3HBaa. (B) Dye transfer assay for fusion of the wt F and mutant F proteins at 29°C, 37°C, and 42°C. Shown is the quantification of fusion events from 7-10 microscopic fields. The fusion of F 3HBii cannot be driven with increased temperature. (C) MAb reactivity (RMFI) of transfected cells expressing wt F and mutant F proteins. MAb 6-7 and 21-1 are postfusion antibodies, and heating the wt F protein to 50°C increased MAb 21-1 reactivity. MAb 21-1 reactivity to F 3HBii did not increase with heating, suggesting F 3HBii does not refold to the postfusion form. (146)

as a surrogate for receptor binding with wt W3A F, and increasing temperature increases fusion (125); however, heat cannot drive F 3HBii fusion (Fig. B-2B) (146). The double mutant F 3HBii S443P that contains the hyperfusogenic mutation S443P in addition to the C-terminal 3HB also showed reduced fusion (Fig. B-2A) (146). The monoclonal antibodies (MAbs) 21-1 and 6-7 are similar conformational antibodies that bind to similar regions and recognize the postfusion conformation of the F protein (144). The reactivity of wt W3A F to MAbs 21-1 and 6-7 increases upon heating to 50°C for 10 min (126). Liposome binding studies and electron microscopy have confirmed that increased temperature converts F to the postfusion form (24). Heating F 3HBii and F 3HBii S443P to 50°C for 10 min did not increase MAb 21-1 reactivity

compared to wt W3A F (Fig. B-2C) (146). In aggregate, the data suggest the 3HB forms a protein structure that suppresses fusion and traps F in an intermediate of fusion.

By adding a 3HB structure and presumptively stabilizing the CT, the conformation of the F protein is likely trapped at a step prior to hemifusion (146). Following receptor binding, the heptad repeat B (HRB) helices in the F protein separate to form the open stalk intermediate (125, 155). Heptad repeat A (HRA) then rearranges to form extended α -helices, and the fusion peptide is projected toward and inserted into the target cell membrane to form the pre-hairpin intermediate. At this stage, HRA is accessible to C1 peptide inhibition. The C1 peptide is derived from the HRB region in wt W3A F (63) and binds in the grooves formed by the HRA coiled-coil (4) to block fusion and trap the pre-hairpin intermediate (125). CV1 cells coexpressing the wt W3A attachment protein hemagglutinin-neuraminidase (HN) and wt W3A F, F 3HBii, or F 3HBaa proteins were labeled with the dye STYO 17 and incubated with target red blood cells (RBCs) labeled with 6-carboxyfluorescein (6-CF, Invitrogen, Carlsbad, CA) at 4°C for 1 h (Fig. B-3). The HN protein will bind rather than release RBCs at 4°C when conditions are not optimal for its neuraminidase activity. When the temperature is shifted to 37°C for 15 min, the majority of RBCs either fuse via the F protein or are released due to the neuraminidase activity of HN that is present at 37°C but not at 4°C (116, 125). If the F protein expressed is unable to refold to the postfusion conformation after inserting its fusion peptide into the target cell membrane, then more RBCs remain bound to cells after the temperature shift to 37°C. The remaining RBCs are

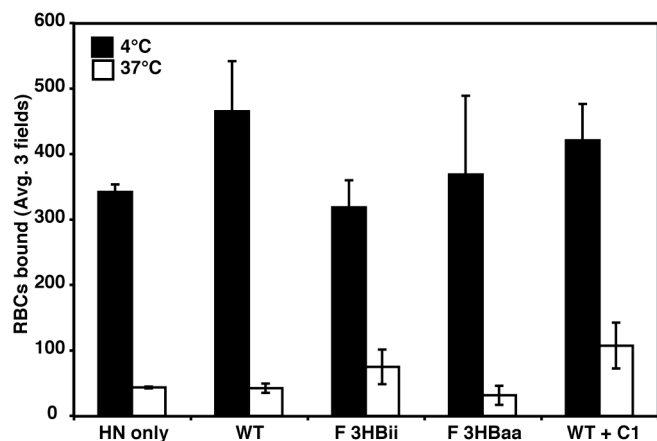


Figure B-3. Analysis of the pre-hairpin intermediate.

RBC binding for HN only or HN plus wt F, F 3HBii, and F 3HBaa expressing CV-1 cells was quantified. C1 peptide was added to wt F during the 15 min 37°C incubation to capture the pre-hairpin intermediate. Black bars represent number of RBCs bound at 4°C, and white bars represent the number of RBCs bound after the 15 min 37°C incubation. More RBCs remained bound to F 3HBii expressing cells than wt F or F3HBaa expressing cells. The RBCs bound to F 3HBii cells was similar to that of the wt F+C1 cells which are trapped at the pre-hairpin intermediate. Means and error bars shown are from three microscopic fields.

tethered to the CV1 cells via the F protein.

The formation of the pre-hairpin intermediate under these conditions is confirmed by adding the C1 peptide to wt W3A F to block fusion at this stage. The black bars represent the RBCs bound at 4°C

and the white bars show the number of RBCs remaining after increasing the temperature to 37°C (Fig. B-3). The number of RBCs remaining bound via F 3HBaa is similar to the number bound via wt W3A F. However, F 3HBii retains more RBCs similar to the wt W3A F + C1 peptide positive control, suggesting F 3HBii is trapped at the pre-hairpin intermediate (Fig. B-3).

To verify F 3HBii is trapped at the pre-hairpin intermediate, the F 3HBii protein can be captured by binding a commercially generated HA tagged C1 peptide (HAt-C1) with the 11 residue HA tag (YPYDVPDYASL) (Genemed Synthesis, Inc., San Francisco, CA) to the pre-hairpin intermediate and immunoprecipitating with an antibody that recognizes the HA tag (12CA5). It has been shown previously that the HAt-C1 peptide only immunoprecipitates F under conditions

in which the C1 peptide inhibits fusion (Russell 2001). The HAt-C1 peptide only immunoprecipitated F if it was added after target cell binding during the 37°C incubation when HRA is accessible. When added after fusion was triggered by the 37°C incubation, the HAt-C1 peptide did not capture the F protein (Russell 2001). HeLa CD4 LTR βgal cells were co-transfected with pCAGGS HN and pCAGGS wt F, F 3HBii, or F 3HBaa expressing plasmids with the Lipofectamine Plus system (Invitrogen) and labeled with 250 μCi of ³⁵S-Promix (GE Healthcare Bio-Sciences, Piscataway, NJ) in Cys- and Met-deficient Dulbecco's modified Eagle's Medium (DMEM) for 1 h and then incubated with cold DMEM for 2 h (chase). Cells were incubated with 0.1% RBCs for 1 h at 4°C (Fig. B-4). All samples were shifted to 37°C for 45 min to trigger fusion. One set of samples was incubated at 50°C for an additional 10 min to drive fusion to completion. After heating, all samples were incubated at 4°C for an additional 45 min. Samples were incubated with 15 μg of HAt-C1 peptide either during the 37°C incubation, during the 4°C incubation after the 37°C treatment, or during the 4°C incubation after the 50°C treatment (Fig. B-4). The wt and mutant F proteins were then immunoprecipitated with 30 μg of the monoclonal antibody 12CA5 in serum-free media for 3 h at 4°C, lysed in 1 ml of RIPA buffer, and visualized by SDS-PAGE on 15% acrylamide gels (109). The HAt-C1 peptide was predicted to immunoprecipitate the F protein during fusion at 37°C when HRA is exposed but not at 4°C after extensive heating when F should be in the postfusion conformation and HRA has formed the 6HB with HRB (125). However, the HAt-C1 peptide immunoprecipitated wt F, F 3HBii, and F 3HBaa under all conditions (Fig. B-4). This may be because samples were metabolically labeled rather than visualized by Western blot (125) and the sensitivity of radiolabeling for detecting F may be greater than the polyclonal F antibody used to detect the F

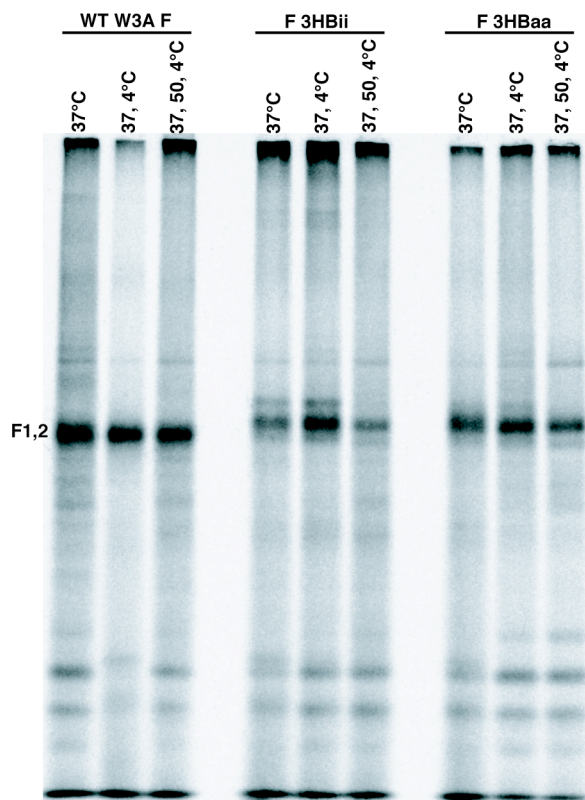


Figure B-4. Capture of the pre-hairpin intermediate.

HA-tagged C1 peptide binds to the pre-hairpin intermediate of wt F in the presence of HN and target red blood cells. HeLa CD4 LTR β gal cells expressing HN and wt F, F 3HBii, or F 3HBaa were metabolically labeled with 250 μ Ci of 35 S-Promix. Lanes 1, 4, and 7: cells were incubated 45 min at 37°C in the presence of 15 μ g HAt-C1 peptide. Lanes 2, 5, 8: cells were incubated 45 min at 37°C followed by a 45 min 4°C incubation in the presence of HAt-C1 peptide. Lanes 3, 6, 9: cells were incubated 45 min at 37°C, then 10 min at 50°C, followed by 45 min at 4°C in the presence of HAt-C1 peptide. All F proteins were co-immunoprecipitated by the HA tag specific MAb 12CA5.

protein in Western blot analysis. The immunoprecipitation of the pre-hairpin intermediate for all F proteins confirms that F 3HBii does form the pre-hairpin intermediate, and suggests that the kinetics of fusion may be slowed and a portion of the F protein population on the cell surface has not converted to the postfusion form after 45 min at 37°C or an additional 10 min at 50°C.

The F 3HBii mutant can form the pre-hairpin intermediate but cannot convert to the postfusion form or cause fusion. The 3HB may constrict movement of a monomer in the F trimer and hinder the refolding necessary to form the postfusion 6HB and in turn slow fusion at the pre-hairpin intermediate. The 3HB may also alter the conformation of the ectodomain, which slows fusion and affects the conformational changes necessary for fusion. To determine potential differences in pre- and postfusion ectodomain structure between the F proteins, HeLa CD4 LTR

β gal cells expressing HN and either wt W3A F, F 3HBii, or F 3HBaa were incubated with 0.1% RBCs for 1 h at 4°C. Half the samples were heated to 37°C for 1 h to trigger fusion while the other half remained at 4°C. All samples were subsequently incubated with the polyclonal antibodies 244 and anti-F2 for 3 h at 4°C. Samples were lysed in a mild detergent (50 mM tris pH 7.4, 0.1% SDS, 1.0% NP40) to maintain the conformation of the F proteins. The samples

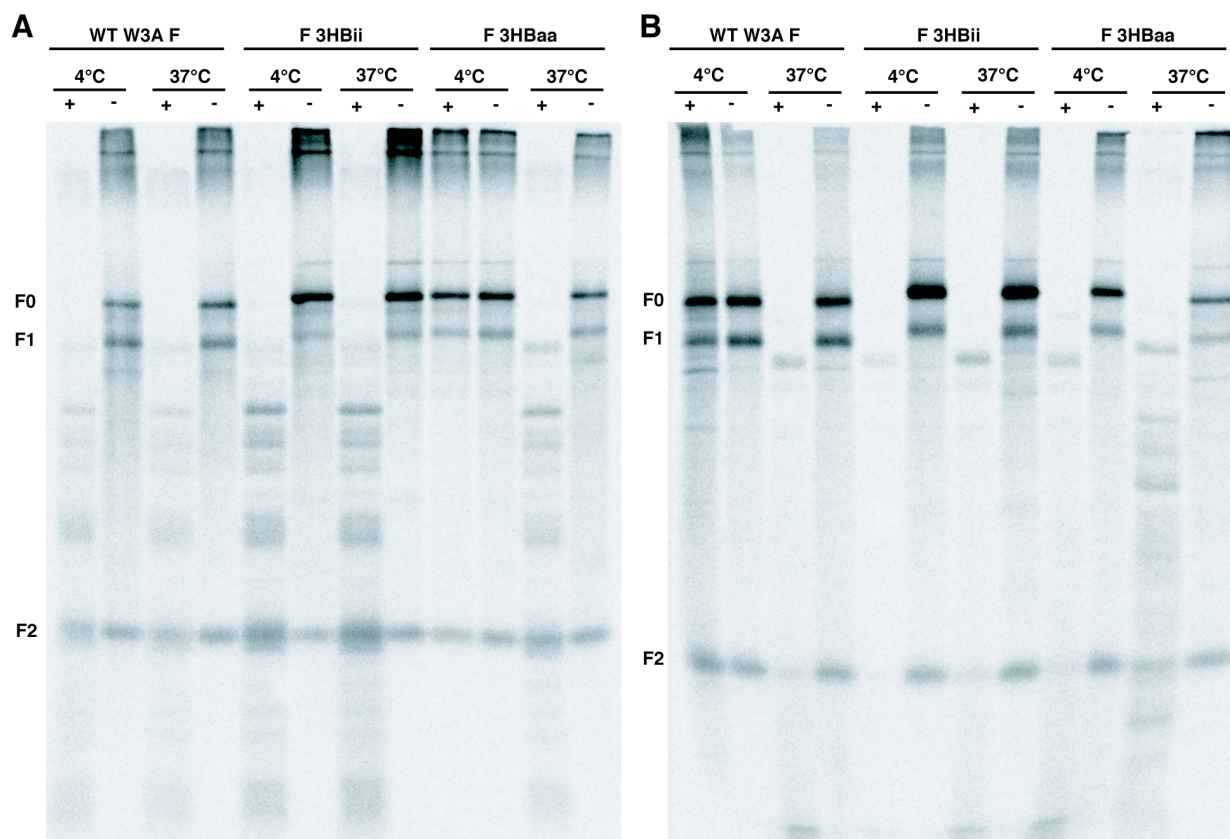


Figure B-5. Protease digestions of wt F, F 3HBii, and F 3HBaa proteins.

HeLa CD4 LTR β gal cells expressing HN and wt F, F 3HBii, or F 3HBaa were incubated with target red blood cells for 1 h at 4°C. Samples either remained at 4°C or were incubated at 37°C for 1 h to trigger fusion, and samples were either untreated or digested with (A) 50 μ g/ml proteinase K or (B) 50 μ g/ml TPCK trypsin for 1 h at room temperature. The proteinase K and TPCK trypsin digestions of all F proteins show similar digestion patterns. All F proteins were immunoprecipitated with the PAbs 244 and anti-F2.

were then incubated with or without 50 µg/ml of proteinase K or TPCK trypsin for 1 h at room temperature. Digestion was stopped with 2X RIPA, 200 µg/ml soybean trypsin inhibitor, 1 mM phenylmethanesulfonyl fluoride (PMSF). Samples were incubated with 40 µl protein A-Sepharose and visualized by SDS-PAGE on 15% acrylamide gels. After heating to 37°C, all F proteins showed similar digestion to both proteases (Fig. B-5), although proteinase K did not digest wt W3A F at 4°C (Fig. B-5A) and TPCK trypsin did not digest F 3HBaa at 4°C (Fig. B-5B).

There are no conformational differences between wt W3A F and F 3HBii based on these two protease digestions, but more digestions with other proteases, such as chymotrypsin, are necessary. In addition to more digestions, conformational MAb could also determine conformational differences. The reactivity of postfusion antibodies MAb 21-1 (146) and MAb 6-7 (M.L.B., unpublished observation) did not increase when F 3HBii was heated to 50°C, suggesting F 3HBii does not form the postfusion conformation and the MAb 6-7 epitope is not fully accessible (146). While the postfusion MAb 6-7 gains reactivity to wt W3A F after heating, prefusion antibodies are predicted to lose reactivity upon heating. Comparing the reactivity to potential prefusion-specific antibodies (Appendix A) of F 3HBii and wt W3A F could determine what epitopes are exposed on F 3HBii and any difference in conformation of the ectodomain compared to wt W3A F that may be due to the stabilizing 3HB structure.

CURRICULUM VITA

Mei Lin Z. Bissonnette

Home Address

1606 W. Grace St.
Chicago, IL 60613
Tel: (312) 375-6150
E-mail: mzimmerman005@md.northwestern.edu

Personal Information

Born December 8, 1978, Grand Haven, MI

Education

- 2001 - 2010 Northwestern University Feinberg School of Medicine, Medical Scientist Training Program (MSTP), Chicago, IL.
- 1997 – 2001 The Johns Hopkins University, Baltimore, MD. B.A. Biophysics.
- 1993 – 1997 Grand Haven High School, Grand Haven, MI.

Scientific Experience

- 1998-2001 Undergraduate Student, Department of Biophysics, The Johns Hopkins University, Baltimore, MD.
Advisor: Bertrand Garcia-Moreno E., Ph.D. Professor.
Molecular mechanism of acid denaturation of staphylococcal nuclease
- 2003-Present Graduate Student, Department of Biochemistry, Molecular Biology, and Cellular Biology, Northwestern University, Chicago IL
Advisor: Robert A. Lamb, Ph.D., Sc.D. Investigator, Howard Hughes Medical Institute.
Structural and conformational requirements of membrane fusion mediated by the parainfluenza virus 5 fusion protein

Publications

Bissonnette, M.Z., S.A. Connolly, D.F. Young, R.E. Randall, R.G. Paterson, and R.A. Lamb. 2006. Analysis of the pH requirement for membrane fusion of different isolates of the paramyxovirus parainfluenza virus 5. *J. Virol.* 80:3071-3077.

Bissonnette, M.Z., J.E. Donald, W.F. DeGrado, T.S. Jardetzky, and R.A. Lamb. 2008. Functional analysis of the transmembrane domain in paramyxovirus F protein-mediated membrane fusion. *JMB* (submitted).

Abstracts

Bissonnette, M.Z., R.G. Paterson, D.F. Young, R.E. Randall, and R.A. Lamb. 2005. Analysis of the different fusion activity of two isolates of parainfluenza virus 5 (SV5), a monkey isolate W3A and a porcine isolate SER. American Society for Virology 24th Annual Meeting. Abstract W51-5

Bissonnette, M.Z., T.S. Jardetzky, and R.A. Lamb. 2006. A three-helix bundle on the cytoplasmic tail of parainfluenza virus 5 traps the pre-hairpin intermediate in fusion. Keystone Symposia Cell Biology of Virus Entry, Replication and Pathogenesis. Abstract 111

Bissonnette, M.Z., T.S. Jardetzky, and R.A. Lamb. 2006. A three-helix bundle on the cytoplasmic tail of parainfluenza virus 5 traps the pre-hairpin intermediate in fusion. American Society for Virology 25th Annual Meeting. Abstract W26-8

Bissonnette, M.Z., T.S. Jardetzky, and R.A. Lamb. 2007. Residues in the outer leaflet of the transmembrane domain of the parainfluenza virus 5 fusion protein are critical for membrane fusion. American Society for Virology 26th Annual Meeting. Abstract W14-3

Bissonnette, M.Z., T.S. Jardetzky, and R.A. Lamb. 2008. Residues in the outer leaflet of the transmembrane domain of the parainfluenza virus 5 fusion protein are critical for membrane fusion. Keystone Symposia Cell Biology of Virus Entry, Replication and Pathogenesis. Abstract 110

Presentations

Professional Conferences

April 2008 Residues in the outer leaflet of the transmembrane domain of the parainfluenza virus 5 fusion protein are critical for membrane fusion. Keystone Symposia Cell Biology of Virus Entry, Replication and Pathogenesis, Victoria, British Columbia

- September 2007 Residues in the outer leaflet of the transmembrane domain of the parainfluenza virus 5 fusion protein are critical for membrane fusion. Poster, Workshop on Replication and Cell Biology of Negative Strand RNA viruses, Evanston, IL.
- July 2007 Residues in the outer leaflet of the transmembrane domain of the parainfluenza virus 5 fusion protein are critical for membrane fusion. American Society for Virology 26th Annual Meeting, Corvallis, Oregon
- July 2006 A three-helix bundle on the cytoplasmic tail of parainfluenza virus 5 traps the pre-hairpin intermediate in fusion. American Society for Virology 25th Annual Meeting, Madison, Wisconsin
- February 2006 A three-helix bundle on the cytoplasmic tail of parainfluenza virus 5 traps the pre-hairpin intermediate in fusion. Poster, Keystone Symposia Cell Biology of Virus Entry, Replication and Pathogenesis. Santa Fe, New Mexico
- June 2005 Analysis of the different fusion activity of two isolates of parainfluenza virus 5 (SV5), a monkey isolate W3A and a porcine isolate SER. American Society for Virology 24th Annual Meeting. University Park, Pennsylvania (presentation)
- June 2004 Is There a Role for Low pH in the Activation of Fusion of the SER Isolate of the Paramyxovirus Simian Virus 5? Poster, Workshop on Replication and Cell Biology of Negative Strand RNA Viruses. Evanston, Illinois

Internal Meetings and Conferences

- July 2008 Residues in the outer leaflet of the transmembrane domain of the parainfluenza virus 5 fusion protein are critical for membrane fusion. Poster, MSTP Student-Faculty Retreat, Chicago, IL.
- May 2008 Residues in the outer leaflet of the transmembrane domain of the parainfluenza virus 5 fusion protein are critical for membrane fusion. Poster, BMBCB Department Retreat, Zion, IL.
- April 2008 Residues in the outer leaflet of the transmembrane domain of the parainfluenza virus 5 fusion protein are critical for membrane fusion. Presentation, Molecular Biology Club, BMBCB Departmental Seminar.
- October 2006 The role of the transmembrane domain in parainfluenza virus 5 fusion. Presentation, IBiS Student Organization, Student Seminar.

- August 2006 A three-helix bundle on the cytoplasmic tail of parainfluenza virus 5 traps the pre-hairpin intermediate in fusion. Presentation, MSTP Student-Faculty Retreat, New Buffalo, MI.
- April 2006 A three-helix bundle on the cytoplasmic tail of parainfluenza virus 5 traps the pre-hairpin intermediate in fusion. Poster, BMBCB Department Retreat, Lake Bluff, IL.
- March 2006 A three-helix bundle on the cytoplasmic tail of parainfluenza virus 5 traps the pre-hairpin intermediate in fusion. Poster, CMBD 2006 Symposium: Host-Pathogen Signal Transduction, Evanston, Illinois.
- August 2005 A three-helix bundle on the cytoplasmic tail of parainfluenza virus 5 traps the pre-hairpin intermediate in fusion. Poster, MSTP Student-Faculty Retreat, Zion, IL.
- October 2004 Is There a Role for Low pH in the Activation of Fusion of the SER Isolate of the Paramyxovirus Simian Virus 5? Presentation, IBiS Student Organization, Student Seminar.
- October 2004 Is There a Role for Low pH in the Activation of Fusion of the SER Isolate of the Paramyxovirus Simian Virus 5? Poster, MSTP Student-Faculty Retreat, Lakeside, MI.
- September 2004 Is There a Role for Low pH in the Activation of Fusion of the SER Isolate of the Paramyxovirus Simian Virus 5? Poster, IBiS Graduate Program Retreat, Lake Delevan, WI.

Scientific Meetings

- 2008 Keystone Symposia Cell Biology of Virus Entry, Replication and Pathogenesis, Victoria, British Columbia
- 2008 Workshop on Replication and Cell Biology of Negative Strand RNA Viruses, Evanston, Illinois
- 2007 American Society for Virology 26th Annual Meeting, Corvallis, Oregon
- 2006 American Society for Virology 25th Annual Meeting, Madison, Wisconsin
- 2006 Keystone Symposia Cell Biology of Virus Entry, Replication and Pathogenesis, Santa Fe, New Mexico
- 2005 American Society for Virology 24th Annual Meeting, University Park, Pennsylvania
- 2004 Workshop on Replication and Cell Biology of Negative Strand RNA Viruses, Evanston, Illinois.

Professional Service

- 2003-2004 Evanston Representative, MSTP Student Council, Northwestern University
Feinberg School of Medicine.
- 2002-2003 M2 Student Curriculum Committee, Northwestern University Feinberg School
of Medicine.
- 2002-2003 Community Health Clinic M2 volunteer
- 2001-2002 Community Health Clinic M1 volunteer

Teaching

- Winter 2008 Teaching Assistant, Animal Viruses, Northwestern University, Evanston, IL.
- Winter 2005 Teaching Assistant, Biochemistry and Molecular Biology, Northwestern
Univeristy, Evanston, IL.

Awards and Honors

- Interdepartmental Biological Sciences Program (IBiS) travel award, 2008
American Society for Virology student travel award, 2007
Keystone Symposia Travel Scholarship, 2006
American Society for Virology student travel award, 2006
Northwestern University Conference Travel Grant, 2006
General honors, The Johns Hopkins University, 2001
Departmental honors in Biophysics, The Johns Hopkins University, 2001
Phi Beta Kappa, The Johns Hopkins University, 2001

Societies and Memberships

- American Medical Association
American Medical Student Association
Chicago Medical Society
Illinois State Medical Society
American Society of Virology